

Electronic Thesis and Dissertation Repository

6-26-2018 1:00 PM

The role of TGF β type III receptor in lung cancer cell migration and invasion

Anthony Zicarelli, *The University of Western Ontario*

Supervisor: Di Guglielmo, John, *The University of Western Ontario*

A thesis submitted in partial fulfillment of the requirements for the Master of Science degree in Physiology and Pharmacology

© Anthony Zicarelli 2018

Follow this and additional works at: <https://ir.lib.uwo.ca/etd>

Recommended Citation

Zicarelli, Anthony, "The role of TGF β type III receptor in lung cancer cell migration and invasion" (2018). *Electronic Thesis and Dissertation Repository*. 5454.
<https://ir.lib.uwo.ca/etd/5454>

This Dissertation/Thesis is brought to you for free and open access by Scholarship@Western. It has been accepted for inclusion in Electronic Thesis and Dissertation Repository by an authorized administrator of Scholarship@Western. For more information, please contact wlsadmin@uwo.ca.

Abstract

Metastasis is responsible for 90% of cancer-related deaths. An important early step in the metastatic process is epithelial-to-mesenchymal transition (EMT) of tumor cells. Stimulated by TGF β signaling, cells that undergo EMT have increased migratory and invasive potential, resulting in metastasis and the development of tumors at a secondary site. The TGF β type 3 receptor (T β R3) has been implicated in modulating TGF β signaling, yet its functional outcomes remain unclear. My findings demonstrated that T β R3 silencing does not alter TGF β -dependent Smad2 phosphorylation in neither H1299, nor A549 non-small cell lung carcinoma cells but reduces Smad2 expression in H1299 cells. Interestingly, although T β R3 knockdown did not alter mRNA expression of EMT markers, it resulted in the reduction of TGF β -dependent EMT protein markers. Finally, inhibition of EMT attenuated cellular invasion while enhancing chemotactic migration. Together, these results suggest that T β R3 has a distinct role in modulating EMT and cellular motility in a Smad-independent manner.

Keywords

Transforming growth factor beta (TGF β), Smad signaling, transforming growth factor beta type III receptor (T β R3), betaglycan, epithelial-to-mesenchymal transition (EMT), migration, invasion

Co-Authorship Statement

All experiments were conducted and analyzed by Anthony Zicarelli. For the microarray analysis, RNA was extracted by Anthony Zicarelli, processed and loaded onto Affymetrix Human GeneChip 2.0 by David Carter (London Regional Genomics Center), and analyzed by Anthony Zicarelli.

Acknowledgments

Firstly, I'd like to thank Dr. John Di Guglielmo for taking me on as a student on short notice and putting great faith in me right from the start of my project. Your constant positivity, optimism, and encouragement helped me get through those tough times when experiments weren't progressing as smoothly as I hoped. Trusting my independence, while addressing any question, comment, or concern I had, allowed me to think critically and come up with solutions on my own. You welcomed me into your lab with open arms and made every day enjoyable. Your Netflix recommendations, Bill Burr jokes, and interesting facts kept the mood around the lab fun and light. Thank you for welcoming us into your home for holiday dinners, while celebrating our birthdays and accomplishments with lunches, donuts, and snacks. These subtleties made the lab feel much less like a work environment, and much more like a family. Also, thank you for letting me act as a teaching assistant in my first semester, even though there was a lot on my research plate to learn. It helped me appreciate the intricacies and effort that goes into undergraduate courses.

Thank you to my advisory committee members – Dr. Peter Chidiac, Dr. Lina Dagnino, and Dr. Ruud Veldhuizen – for your advice and suggestions. Your tough questions during our meetings have compelled me to think critically when developing experiments and analyzing data, allowing me to become a better researcher.

I want to thank Dr. Nicole Campbell and Dr. Sarah McLean for giving me the opportunity to develop my teaching skills through TAing your IMS lab courses. As a graduate from that program, it was an incredible feeling to give back to the program that helped me get to where I am now. Also, teaching students how to perform techniques that I perform daily forced me to know them inside and out, which helped troubleshooting whenever I had technical issues in my own experiments.

To my fellow grad students, Charles, Eddie, Sam, and Evelyn. Thanks for teaching me how to perform the techniques I needed to conduct my research, and for showing me the ropes on the entire graduate school process. I can only imagine how difficult it would've been to figure everything out on my own. Having you around while we were going through similar

difficulties really helped convince me there was a light at the end of the tunnel. I'm confident your advice regarding what to do, and what not to do, saved me from many headaches. I know how tough presentations can be, but thanks for allowing me to sit in on your talks. It always gave me thoughts and ideas that I could incorporate into my own presentations. Many apologies for not giving in to your attempts at making me more cultured.

A big thank you to Colleen and Craig for helping with any reagent, kit, or piece of equipment that I was having trouble with. All your experimental tips and tricks made my research more clear, complete, and successful. Thanks for letting me pick your brain and lean on you for wisdom whenever I hit roadblocks in my research or my life, it's really meant a lot. Get ready for a Leafs/Oilers 2019 Stanley Cup Final, Craig.

To my roommates, friends from the Soo, and friends from school: I know I can be irritable sometimes, especially when stressed, but I'm thankful you understood and put up with me. You collectively helped me overcome pessimism, frustration, and a lack of confidence when times were tough. Despite my hesitation, your convincing me to take breaks and enjoy myself helped maintain a work-life balance and kept me sane. The sports, concerts, board game nights, and day trips always put a smile on my face and gave my brain a rest. With all the ups and downs, the last two years have been some of the best of my life.

Finally, thank you to my family for the unending support over the years. Being so far from home hasn't been easy, but no matter how short or infrequent my visits were, every day was special (except that time I crushed my hand). Even though none of you are scientists, you've done your best to try and understand what I've been doing for the last two years.

The next 100 or so pages are dedicated to you.

Table of Contents

Abstract.....	i
Co-Authorship Statement.....	ii
Acknowledgments.....	iii
Table of Contents.....	v
List of Tables.....	viii
List of Figures.....	ix
Abbreviations List.....	xi
Chapter 1: Introduction.....	1
1.1 Lung Cancer.....	1
1.1.1 Disease Process.....	1
1.1.2 Lung Cancer Metastasis.....	2
1.1.3 Epithelial to Mesenchymal Transition and Metastasis.....	3
1.2 TGF β Signaling.....	7
1.2.1 TGF β in Cancer.....	7
1.2.2 TGF β Family of Ligands and Receptors.....	7
1.2.3 SMAD Function and Regulation.....	11
1.2.4 Canonical and Non-Canonical TGF β Signaling.....	13
1.2.5 Regulation of EMT.....	17
1.2.6 TGF β , EMT, and Autophagy.....	19
1.2.7 Matrix Metalloproteinases.....	21
1.3 Transforming Growth Factor β Type 3 Receptor.....	23
1.3.1 T β R3 in Cancer.....	23
1.3.2 Structure of T β R3.....	24
1.3.3 Modulation of TGF β Signaling.....	27

1.3.4 T β R3 Modulation of Other Signaling Pathways	30
1.4 Rationale, Objectives, and Hypothesis	31
Chapter 2: Materials and Methods	33
2.1 Antibodies, Primers and Reagents	33
2.2 Cell Culture and Transfection	36
2.2.1 Cell Culture	36
2.2.2 Cell Transfection	36
2.3 TGF β Administration	37
2.4 Cell Lysis and Protein Assay	38
2.5 SDS-PAGE and Western Blotting	38
2.6 RNA Isolation and cDNA Synthesis	39
2.7 Quantitative Polymerase Chain Reactions	40
2.8 Transwell Assays	40
2.8.1 Cell Migration	40
2.8.2 Cell Invasion	42
2.9 Microarray Analysis	42
2.10 Statistical Analyses	43
Chapter 3: Results	44
3.1 The effect of T β R3 on TGF β -dependent Smad2 phosphorylation in A549 and H1299 cells	44
3.2 The effect of T β R3 silencing on TGF β -dependent EMT markers	53
3.3 Cell migration and invasion in the absence of T β R3	63
3.4 Changes in mRNA expression	66
3.4.1 Microarray Analysis	66
3.4.2 Gene Ontology Analysis	66
Chapter 4: Discussion	74

4.1 TGF β -dependent Smad2 signaling in the absences of T β R3	74
4.2 TGF β -dependent EMT marker analysis.....	75
4.3 Interplay between cell migration and invasion	81
4.4 Summary of Observations.....	85
4.5 Limitations and Future Directions	86
References.....	91
Appendix.....	104
Curriculum Vitae	123

List of Tables

Table 2.1 Primary and secondary antibodies used for western blotting	33
Table 2.2 Primer sequences used for qPCR	34
Table 2.3 Reagents used for cell processing and data collection.....	35
Table 3.1 Regulation of Chemotaxis	73
Table 3.2 Regulation of Locomotion	73

List of Figures

Figure 1.1 Characterization of cellular epithelial-to-mesenchymal transition (EMT): an early metastatic process	4
Figure 1.2 Processes involved in tumor metastasis	6
Figure 1.3 Structure of membrane bound TGF β receptors I, II, and III	9
Figure 1.4 Schematic displaying the canonical TGF β signaling pathway	14
Figure 1.5 Complex role of T β R3 in TGF β signaling	28
Figure 3.1 Knockdown of T β R3 in H1299 cells by siRNA.....	45
Figure 3.2 Knockdown of T β R3 in A549 cells by siRNA.....	46
Figure 3.3 The effect of T β R3 knockdown on TGF β -dependent Smad2 phosphorylation in H1299 cells	48
Figure 3.4 The effect of T β R3 knockdown on TGF β -dependent Smad2 phosphorylation in A549 cells	49
Figure 3.5 Time course of Smad2 phosphorylation in H1299 cells following T β R3 knockdown.....	50
Figure 3.6 Time course of Smad2 phosphorylation in A549 cells following T β R3 knockdown.....	51
Figure 3.7 TGF β -dependent transcription in response to T β R3 knockdown	54
Figure 3.8 Expression of cadherin mRNA in the absence of T β R3	56
Figure 3.9 T β R3 knockdown on TGF β -dependent cadherin shift in H1299 cells.....	58
Figure 3.10 T β R3 knockdown on TGF β -dependent cadherin shift in A549 cells.....	59
Figure 3.11 LC3B expression in H1299 cells following T β R3 knockdown	61

Figure 3.12 LC3B expression in A549 cells following T β R3 knockdown	62
Figure 3.13 The number of H1299 cells that invaded through Matrigel following T β R3 knockdown.....	64
Figure 3.14 The number of A549 and H1299 cells that migrated following T β R3 knockdown.....	65
Figure 3.15 mRNA expression of selected genes from H1299 microarray analysis	67
Figure 3.16 MMP1 and MMP14 mRNA expression following T β R3 knockdown.....	69
Figure 3.17 Gene ontology analysis of microarray mRNA expression.....	70
Figure 3.18 Specific upregulated genes that regulate locomotion and chemotaxis.....	72
Figure 4.1 Proposed mechanism of T β R3 influence on cell migration and invasion.....	90

Abbreviations List

°C	Degrees Celsius
αSMA	Alpha-smooth muscle actin
A549	A549 non-small cell lung carcinoma cell
Akt	Alias: protein kinase B
ANOVA	Analysis of variance
Atg	Autophagy-related
BMP	Bone morphogenetic protein
C-	Carboxy
CCN	Cyclin
CDC	Cell division cycle
CDK	Cyclin-dependent kinase
CO ₂	Carbon dioxide
Co-Smad	Common-Smad
CRISPR	Clustered Regularly Interspaced Short Palindromic Repeats
DAPI	4',6-diamidino-2-phenylindole
DNA	Deoxyribonucleic Acid
DNMT	DNA methyltransferase
E-cadherin	Epithelial cadherin
ECM	Extracellular matrix
EDTA	Ethylenediaminetetraacetic acid
EMT	Epithelial-to-mesenchymal transition
Erk	Extracellular signal-regulated kinase
F12K	Ham's F-12k (Kaighn's) medium
FBS	Fetal bovine serum

bFGF2	basic Fibroblast growth factor 2
FKBP12	FK506 binding protein 12
GAG	Glycosaminoglycan
GAPDH	Glyceraldehyde 3-phosphate dehydrogenase
GPI	Glycosylphosphatidylinositol
Grb2	Growth factor receptor-bound protein 2
GS	Glycine-serine rich
H1299	NCI-H1299 non-small cell lung carcinoma cell
HGF	Hepatocyte growth factor
HGFR	Hepatocyte growth factor receptor
HPRT	Hypoxanthine-guanine phosphoribosultransferase
HRP	Horseradish peroxidase
ILK	Integrin-linked kinase
LC3B	Microtubule-associated proteins 1A/1B light chain 3B
kbp	Kilobase pair
kDa	Kilodalton
MAPK	Mitogen-activated protein kinase
MET	Alias: Hepatocyte growth factor receptor
MH1	MAD homology domain 1
MH2	MAD homology domain 2
MMP	Matrix metalloproteinase
mTOR	Mammalian target of rapamycin
N-	Amino
N-cadherin	Neural-cadherin
NF- κ B cells	Nuclear factor kappa-light-chain-enhancer of activated B

nM	Nanomolar
NSCLC	Non-small cell lung carcinoma
PBS	Phosphate buffered saline
PCP	Planar cell polarity
PDZ	Initialism for PSD95, Dlg1, ZO-1
PI3K	Phosphoinositide 3-kinase
PKC ζ	Protein kinase C-zeta
pM	picomolar
PMSF	Phenylmethylsulfonyl fluoride
PRICKLE1	Prickle planar cell polarity protein 1
pSmad2	Phosphorylated Smad2
qPCR	Quantitative polymerase chain reaction
R-Smad	Receptor-regulated Smad
RNA	Ribonucleic Acid
ROCK	Rho-associated protein kinase
Rpm	Rotations per minute
RTK	Receptor tyrosine kinase
S	Serum
SF	Serum-free
S-	Serine
SARA	Smad anchor for receptor activation
SBE	Smad binding element
SD	Standard deviation
SDS-PAGE	Sodium dodecyl sulfate-polyacrylamide gel electrophoresis
SEM	Standard error of mean

Smurf2	Smad specific E3 ubiquitin protein ligase 2
Sos	Son of sevenless
SP-1	Specificity protein 1
TBST	Tris-buffered saline and tween
TIMP	Tissue inhibitor of metalloproteinases
T β R	Transforming growth factor-beta receptor
TGF β	Transforming growth factor-beta
X-	Any amino acid
ZEB	Zinc finger E-box-binding homeobox
ZO-1	Zona occludens-1

Introduction

1.1 Lung Cancer

1.1.1 Disease Process

Lung cancer is separated into two main categories based on cellular size: small cell lung carcinoma and non-small cell lung carcinoma (NSCLC). First characterized by Watson and Berg (1962), small cell lung carcinoma represents 15% of all lung cancer diagnoses and, despite being responsive to initial chemotherapeutic treatments, is more aggressive than non-small cell lung carcinoma. The remaining 85% of lung cancers are non-small cell lung carcinomas, which include histological subtypes such as adenocarcinoma, squamous cell carcinoma, and large cell carcinoma (Riihimaki, 2014). Since NSCLC is less responsive to chemotherapy and represents the majority of lung cancer diagnoses, this thesis will focus on investigating non-small cell lung carcinomas.

Riihimaki et al. (2014) observed that the most prevalent histological subtype of cancer in its cohort was adenocarcinoma, representing 43% of all lung cancer diagnoses. While no significant sex difference was found, 80% of all lung cancer diagnoses were made in patients who were 60 years of age or older. This year, only 750 Canadians under the age of 50 are expected to be diagnosed with NSCLC, whereas 28,000 diagnoses are expected among those who are 50 years of age or older (Canadian Cancer Society, 2017). Survival is also reduced as the age of diagnosis increases. Patients diagnosed under the age of 40 have the highest five-year survival rate of 45%, while patients diagnosed at 80+ have the lowest at 10% (Canadian Cancer Society, 2017).

Smoking tobacco is associated with 85% of all cases of lung cancer in Canadian patients (Canadian Cancer Society, 2017). Other risk factors include inhalation of radon, asbestos or air pollution, in addition to genetic predisposition. Despite the associated health concerns, approximately 15% of Canadian men and women remain daily smokers (Statistics Canada, 2015).

Epithelial in origin, lung cancer is responsible for approximately 20,000 deaths in Canada annually, accounting for 26% of cancer-related deaths and 8% of all deaths (Canadian Cancer Society, 2017). Behind prostate cancer in males, breast cancer in females, and nonmelanoma skin cancer, lung cancers account for one of the most prevalent cancer subtypes (Canadian Cancer Society, 2017). The discrepancy between incidence and mortality rate of lung cancer reinforces its severity and aggressiveness. Furthermore, survival rates of patients diagnosed with lung cancer are poor, with more than 50% of patients dying within 1 year of initial diagnosis (U.S. National Institutes of Health, 2016). The five-year survival rate of lung cancer is 55% when diagnosis shows a localized tumor (U.S. National Institutes of Health, 2016).

1.1.2 Lung Cancer Metastasis

Metastasis involves the migration of tumor cells away from the primary tumor, local invasion, transport through the bloodstream and/or lymphatic system, and relocation into the secondary location. Metastatic processes are an important target for cancer research, as the prevention of metastasis drastically improves prognoses and treatment outcomes. The seed and soil hypothesis, first described by Paget (1889), expressed the idea that cancer cells migrated throughout the body, and would only form a secondary tumor after reaching a fertile tissue that promotes development. However, the advancement of recent genetic

technologies has led to studies that counter this view by suggesting cancer cells are pre-programmed to target specific regions of the body as secondary tumor sites (Bloom et al., 2004). Common locations of secondary tumors arising from primary lung carcinomas include brain (39%), bone (34%), and liver (20%), although metastasis to the liver or bone yields worse prognoses than to nervous system tissue. Riihimaki et al. (2014) showed that various types of lung cancer have different preferred locations of secondary tumor development. For example, adenocarcinomas tend to metastasize to bone or liver tissue, while squamous cell lung cancers develop secondary tumors primarily in the nervous system and liver. Tumor metastasis occurs prior to diagnosis in 84% of cases, reducing a patient's five-year survival rate to 4% (U.S. National Institutes of Health, 2016). Additionally, the average survival rate of patients exhibiting metastatic lesions is reduced from 13 to 5 months when compared to patients with localized lung tumors (U.S. National Institutes of Health, 2016; Riihimaki et al., 2014).

1.1.3 Epithelial to Mesenchymal Transition and Metastasis

In response to the TGF β signaling cascade, epithelial-to-mesenchymal transition (EMT) involves the transition of adherent epithelial cells to mesenchymal cells, which possess an enhanced ability to migrate, invade, and resist apoptosis (Gunaratne & Di Guglielmo, 2013; Kalluri & Neilson, 2003). Although EMT is necessary during normal embryogenesis, fibrotic wound healing, and organ development, it is commandeered by epithelial tumor cells to metastasize to secondary sites in the body (Kalluri & Weinberg, 2009).

Epithelial-to-mesenchymal transition (**Figure 1.1**) involves the reduced expression of epithelial markers including E-cadherin, claudins, and occludins, which are necessary in establishing cell-to-cell junctions (Kalluri & Weinberg, 2009). Alterations in epithelial

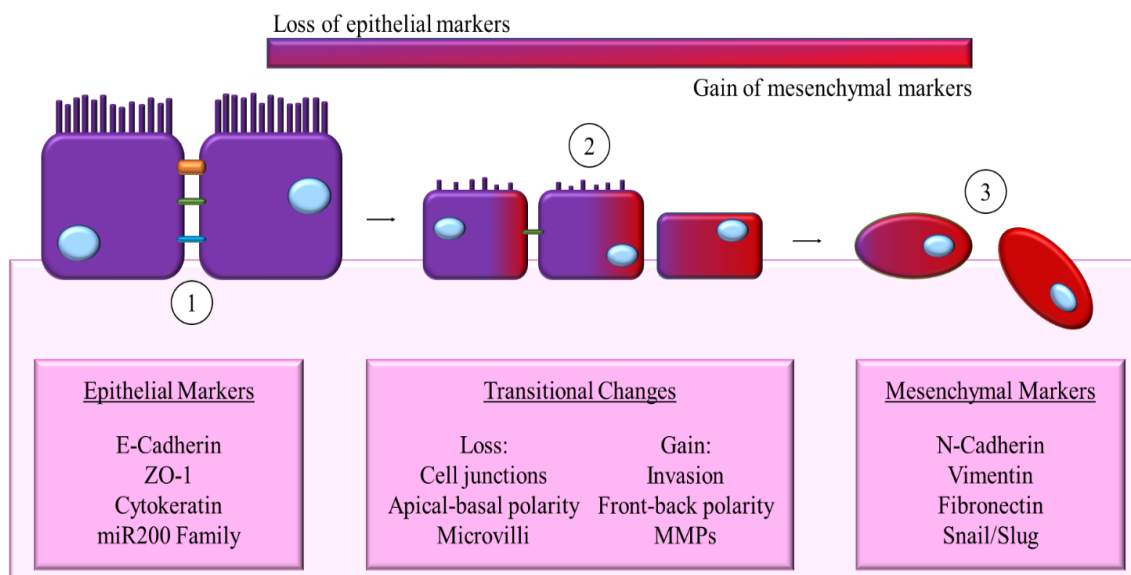


Figure 1.1 Characterization of cellular epithelial-to-mesenchymal transition (EMT): an early metastatic process.

Epithelial cells express several cell-cell adhesions, including E-cadherin and ZO-1 to form tight junctions (orange), adherens junctions (green), and desmosomes (blue) which limit a cells migratory potential (1). Facilitated by transcription factors Snail, Slug, Zeb1, Zeb2, and Twist, epithelial cells lose cellular contacts, undergo changes in polarity, and develop an enhanced ability to migrate and invade (2). A reduction in epithelial markers is matched by an upregulation of mesenchymal markers, which include N-cadherin and vimentin. It is important to note that EMT is a reversible process, and mesenchymal cells can reacquire epithelial phenotype through a mesenchymal-to-epithelial transition (MET).

protein expression results in morphological changes such as the dissociation of tight-junctions, adherens-junctions, desmosomes, and the loss of apical-basal polarity (Zhang et al., 2016; Angadi & Kale, 2015). Complementarily to the loss of epithelial markers is the increased expression of mesenchymal markers, including N-cadherin, vimentin, and α -smooth muscle actin (Angadi & Kale, 2015). Cellular transformation into a more mesenchymal phenotype promotes front-back polarity and cytoskeletal reorganization. In epithelial cells, actin is primarily cortical but it is rearranged through EMT to create stress fibers, thus bolstering migratory and invasive potential (Thiery, 2002). This invasive potential is exacerbated by the upregulation of matrix metalloproteinases, with their ability to degrade components of the extracellular matrix (Angadi & Kale, 2015).

E-cadherin is a traditional marker of epithelial cells, as its high expression level is indicative of established cell-cell junctions (Baum & Georgiou, 2011). These cellular connections are modulated via the cytoplasmic domain of E-cadherin, which interacts with various components of adherens junctions including p120 and β -catenin (Harris & Tepass, 2010). The maintenance of epithelial integrity is important in preventing metastatic dispersion of cancer cells.

Epithelial-to-mesenchymal shift is an early process involved in tumor metastasis (**Figure 1.2**). Cells undergoing EMT develop increased migratory and invasive potential, leading to local invasion of their surrounding stroma and intravasation into the bloodstream. Bodily dissemination occurs, followed by extravasation of cancer cells into secondary sites of micrometastasis. It is important to note that EMT is a reversible process, and cells undergo mesenchymal-to-epithelial transition (MET) to reacquire epithelial characteristics after reaching a targeted body region. Supplementary to distant metastasis, cells that have locally

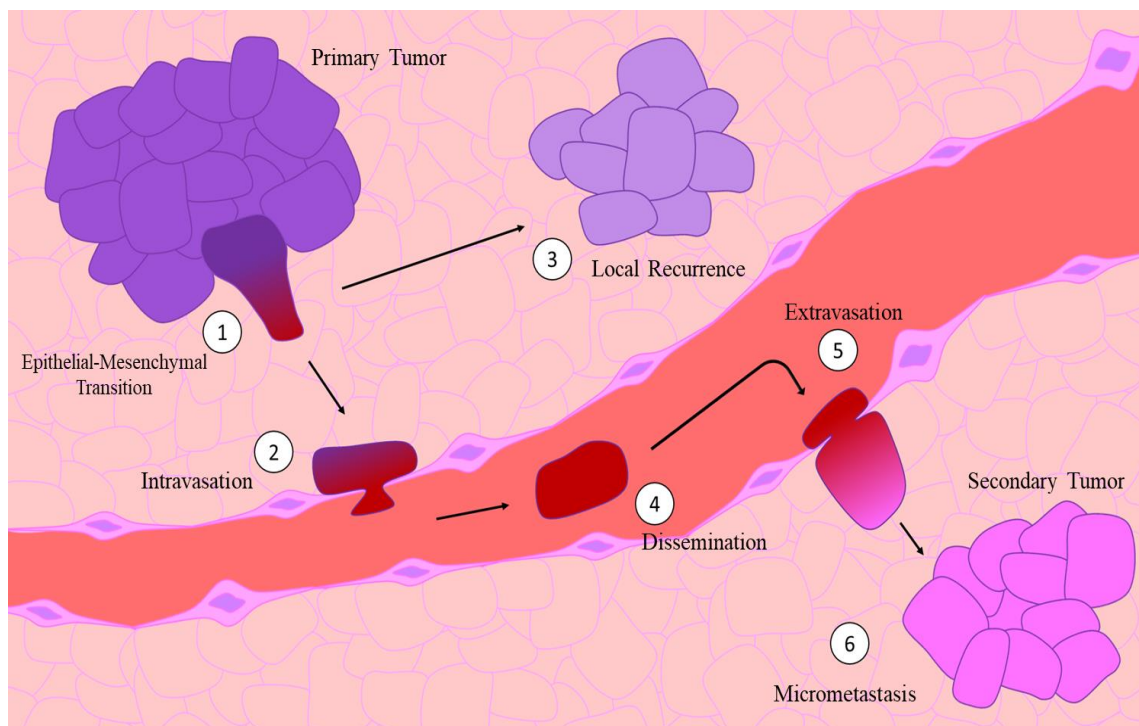


Figure 1.2 Processes involved in tumor metastasis.

Cancerous cells dissociate from a primary tumor and locally invade after undergoing EMT (1; EMT is denoted by the colour shift). Cells can then intravasate into the bloodstream (2) or reacquire an epithelial phenotype to locally recur (3). Once in the bloodstream, tumor cells disseminate (4) to a secondary location, where they adhere to endothelial cells and extravasate into surrounding tissues (5). Finally, cellular phenotype is reversed via mesenchymal-to-epithelial transition (demonstrated by a change in colour) and a secondary, micrometastatic tumor is developed (6).

invaded have the potential to reversibly shift back from a mesenchymal to an epithelial state. Thus, the initiation of EMT promotes both metastasis to a secondary location, as well as local recurrence after treatment (Kalluri & Weinberg, 2009; Thompson & Haviv, 2011).

1.2 TGF β Signaling

1.2.1 TGF β in Cancer

Under normal physiological conditions, transforming growth factor-beta (TGF β) signaling acts as a tumor suppressor by controlling cell growth, proliferation, and differentiation (Kalluri & Weinberg, 2009). However, dysregulation of the TGF β signaling pathway in tumor cells results in the promotion of cancerous characteristics. Late stage tumors often upregulate the expression of TGF β ligands, which possess context-specific tumor promoting effects such as angiogenesis, evasion of immune defenses, and epithelial-to-mesenchymal transition (Elliot & Blobe, 2005; Rahimi & Leof, 2007; Xu et al., 2009). Activity of the TGF β signaling pathway is elevated in tumor cells, establishing a target for chemotherapeutic treatments.

1.2.2 TGF β Family of Ligands and Receptors

Pathway activation is initiated via ligand binding to TGF β receptors, which triggers a downstream signaling cascade. TGF β 1, TGF β 2, and TGF β 3 are tightly regulated cytokines that are synthesized and secreted as precursor proteins that remain in a latent state until pro-peptide N-terminal regions are cleaved by MMP2, MMP9, or thrombospondin (Flanders et al., 2016; Konrad et al., 2007; Yu & Stamenkovic, 2000; Schultz-Cherry & Murphy-Ullrich, 1993). All three forms of TGF β are highly conserved, with 80% amino acid sequence homology (Robertson & Rifkin, 2013). Despite genetic similarity, structural

variation influences ligand function. For example, TGF β 3 possesses a more flexible structural conformation than the rigid TGF β 1, resulting in difference in binding affinity for different receptors (Huang et al., 2014; Konrad et al., 2007).

There are three main receptors involved in the TGF β signaling pathway, termed TGF β type 1 (T β R1), type 2 (T β R2), and type 3 (T β R3) receptors. The genes that encode T β R1 and T β R2 contain multiple splice variants with different exons in sequences corresponding to the extracellular domain. However, alternative splicing does not occur during T β R3 mRNA maturation, resulting in a single protein isoform (Konrad et al., 2007). Each of these three receptors possesses an extracellular, transmembrane, and cytoplasmic domain, yet the functionality of each region varies among receptor types (**Figure 1.3**). Since T β R1 lacks a canonical extracellular ligand binding site, TGF β signaling relies on ligand association with T β R2 to transform external stimuli into intracellular communication. While both T β R1 and T β R2 transduce signaling via intracellular serine/threonine kinase domains, that of T β R2 is constitutively active and phosphorylated. The cytoplasmic region of T β R1 also incorporates a 20-amino acid glycine-serine rich (GS) pocket which, when unphosphorylated, is occupied by FKBP12. This binding pocket is phosphorylated by T β R2 and undergoes a conformational change to dissociate from FKBP12 and open the domain to R-Smad interactions (Wrana et al., 1994).

T β R1 and T β R2 are internalized via clathrin-dependent and clathrin-independent mechanisms. Following ligand binding, the T β R1/2 heteromeric complex is internalized via clathrin-coated pits to facilitate TGF β signaling from the early endosome. However, cell surface receptor levels are also regulated by clathrin-independent endocytosis. When present in lipid-raft membranes, clathrin-independent internalization of T β R1/2 into

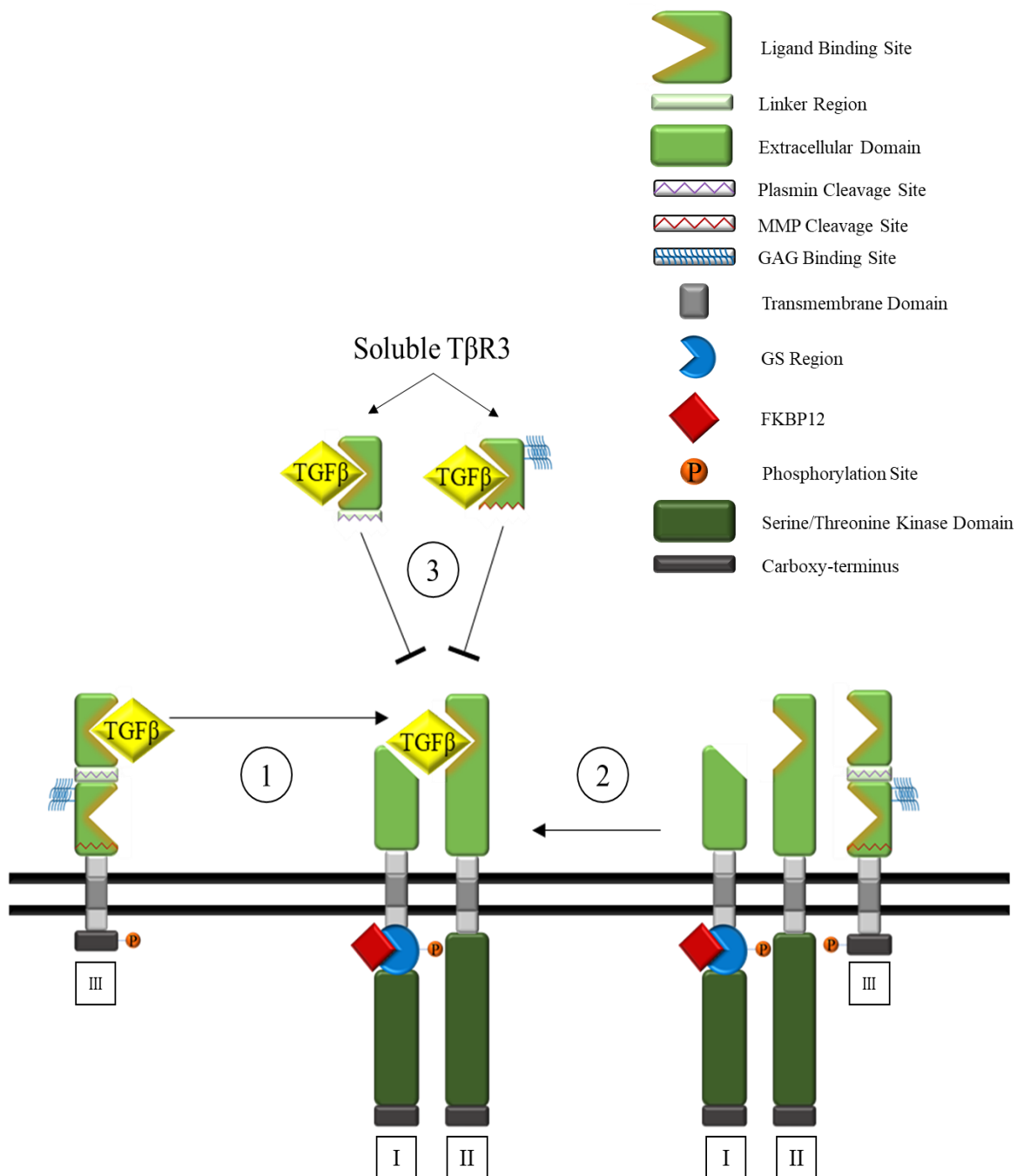


Figure 1.3 Structure of membrane bound TGFβ receptors I, II, and III.

The type III TGFβ receptor (TβR3) facilitates TGFβ signaling by binding and presenting TGFβ ligand to the type II TGFβ receptor (TβR2) (1), and by binding and relocating TβR1/2 receptors in membrane domains (2). Additionally, membrane bound TβR3 can be cleaved at sites recognized by plasmin and matrix metalloproteinases into soluble factors, which bind and sequester TGFβ ligand from interacting with TβR1/2 (3).

caveolin-1 positive vesicles causing Smurf2-mediated ubiquitination and proteasomal/lysosomal degradation (Di Guglielmo et al., 2003).

Mutations in T β R1 or T β R2 often arise in epithelial tissues, interfering with TGF β -dependent apoptosis. Furthermore, inactivating mutations in T β R2 occur more frequently than T β R1, primarily in the cytoplasmic kinase domain responsible for phosphorylating T β R1 (de Caestecker et al., 2000).

TGF β receptor level is regulated through mechanisms that involve post-translational changes. An inhibitory-Smad, Smad7, recruits an E3-ubiquitin ligase, Smurf2, to associate with T β R1 and T β R2, inducing ubiquitin-dependent proteolysis (Kavsak et al., 2000). Like T β R1 and T β R2, T β R3 internalization is a ligand-independent process. Furthermore, modifications to the glycosaminoglycan region of T β R3 has no effect on receptor internalization or degradation (Finger et al., 2008a). In addition, the short cytoplasmic tail of T β R3 is critical for docking of β -arrestin2, which initiates receptor endocytosis through intracellular processes (Finger et al., 2008a). T β R3 endocytosis is important for both Smad-dependent and Smad-independent signaling. A decrease in the phosphorylation of Smad2 and p38 MAP kinase, following blockade of T β R3 internalization by nystatin, suggests that T β R3 has specific functions dependent on endocytosis (Finger et al., 2008a).

While T β R2 is restricted to binding TGF β 1 and TGF β 3, T β R3 is able to bind all three forms of TGF β ligand (Finger et al., 2008a). Thus, T β R3 possesses the unique ability to induce TGF β signaling of TGF β 2. In addition to T β R3 uniquely binding TGF β 2, it also binds with greater affinity than either TGF β 1 or TGF β 3 (Mendoza et al., 2009). T β R1 is unable to bind any TGF β ligand isoform as it does not possess an extracellular ligand

binding domain (Finger et al., 2008a). Notably, regardless of ligand subtype, T β R2 binds more strongly to TGF β that is being presented by T β R3 than it does to free ligand (Lopez-Casillas et al., 1993). Binding affinity of certain ligands is also dependent on receptor interactions. When T β R1 is not physically associated with T β R2, T β R2 possesses low affinity for TGF β 1 (Lopez-Casillas et al., 1994). However, formation of a receptor complex with T β R1 increases T β R2 binding affinity for TGF β 1, while the affinity for TGF β 2 remains low. Additionally, cells become more responsive to TGF β stimulation following expression of exogenous T β R3 (Lopez-Casillas, 1993).

Although the TGF β 1, TGF β 2, and TGF β 3 have similar functions *in vitro*, genetic inactivation of individual ligands in mice reveals distinctly different phenotypical outcomes. Further *in vivo* research has revealed unique roles that are performed by specific TGF β subtypes. For example, wound healing during embryogenesis is associated with high levels of TGF β 3, but not TGF β 1 or TGF β 2 (Whitby & Ferguson, 1991).

1.2.3 SMAD Function and Regulation

Smad proteins, named after shared similar genetic sequences with Sma and Mad proteins, function as downstream effectors of TGF β signaling by acting as receptor substrates (Liu et al., 1996). Of the eight Smad proteins involved in TGF β signaling, only five, Smad-1, -2, -3, -5, and -8, act as substrates for type 1 receptor activation, and are therefore referred to as receptor-regulated Smads (R-Smads). Smad4, a common-Smad (Co-Smad), is not a substrate for type 1 receptor phosphorylation, and instead forms complexes with R-Smads prior to nuclear localization. Finally, inhibitory-Smads (I-Smads), Smad6 and Smad7, repress TGF β signaling by interfering with R-Smad interactions with Co-Smad or activated receptors (Massague, 1998).

Approximately 500 amino acids long, R- and Co-Smad proteins are comprised of an N-terminal Mad-homology 1 domain (MH1), a central linker region, and a C-terminal MH2 domain. Interestingly, the MH1 domain is absent in I-Smads. Additionally, although a C-terminal MH2 domain is conserved among all Smad proteins, functionality of this domain differs between Smad subtypes. When unphosphorylated, Smad2 and Smad4 exist as homotrimers (Wu et al., 2001b). However, upon Smad2 phosphorylation, Smad2/4 form a heterodimer, or a heterotrimer (2 R-Smads, 1 Co-Smad) via binding of MH2 domains (Wu et al., 2001a). R-Smad interaction with receptor kinases is dependent on the connection between loop 3 domain in the carboxy-terminal region of R-Smads with a loop 1 domain of the receptor. Co-Smads do not possess a loop 3 domain, and are therefore unable to bind to, or be phosphorylated by, activated type 1 receptors (Massague, 1998). Receptor kinases are responsible for phosphorylation of R-Smad C-terminal S-S-X-S domain (Wrana, 2000). Specifically, T β R1 and activin type 1 receptors target Smad2 and Smad3 for phosphorylation, while BMP type 1 receptors are primarily associated with Smad1, Smad5, and Smad8.

MH1 and MH2 domains are separated by a proline rich central linker region, which in Smad1, Smad2, and Smad3 is phosphorylated by serine/threonine MAP kinases Erk1 and Erk2 to impede Smad nuclear localization and TGF β signaling (Wrana, 2000; Kretzschmar et al., 1999).

Ski and Sno are oncogenes without catalytic function. However, interactions with the Smad2/4 complex negatively regulates canonical TGF β signaling. Ski and Sno have been shown to simultaneously bind to Smad2 and Smad4, hindering their ability to modulate gene transcription. Specifically, Ski has been shown to competitively bind Smad4 MH2

domain, preventing its association with phosphorylated Smad2 (Wu et al., 2002). Additionally, when interacting with Smad2/4 complexes, Ski and Sno act as corepressors by binding promoter regions and inhibiting gene transcription (Akiyoshi et al., 1999; Stroschein et al., 1999).

Inactivating mutations in the MH2 domains inhibit Smad2/4 complex formation and are evident in cancer cells (Wu et al., 2001b). Mutations can occur in the MH2 domain of Smad2, Smad3, and Smad4, most frequently in the binding sites responsible for heteromeric complex formation (Fleming et al., 2012). Missense mutations are more common than nonsense, and Smad4 is generally more prone to genetic mutations than R-Smads (Fleming et al., 2012; de Caestecker et al., 2000).

Hairpin loops of Smad4 MH1 domains bind to Smad binding elements (SBE) in the promoter regions of target genes (Shi et al., 1998). Smad2/4 weakly binds to DNA on its own and relies on interactions with other co-activators, co-repressors, or transcription factors to induce transcriptional change (Wrana, 2000).

1.2.4 Canonical and Non-Canonical TGF β Signaling

Canonical Transforming Growth Factor-beta (TGF β) signaling (**Figure 1.4**) is responsible for the regulation of many cellular processes, including cellular apoptosis, differentiation, and growth (Kalluri & Weinberg, 2009). Two ubiquitously expressed, membrane bound serine/threonine kinase receptors initiate TGF β signaling upon ligand binding: TGF β Type 1 Receptor and TGF β Type 2 Receptor. Upon ligand binding, two constitutively

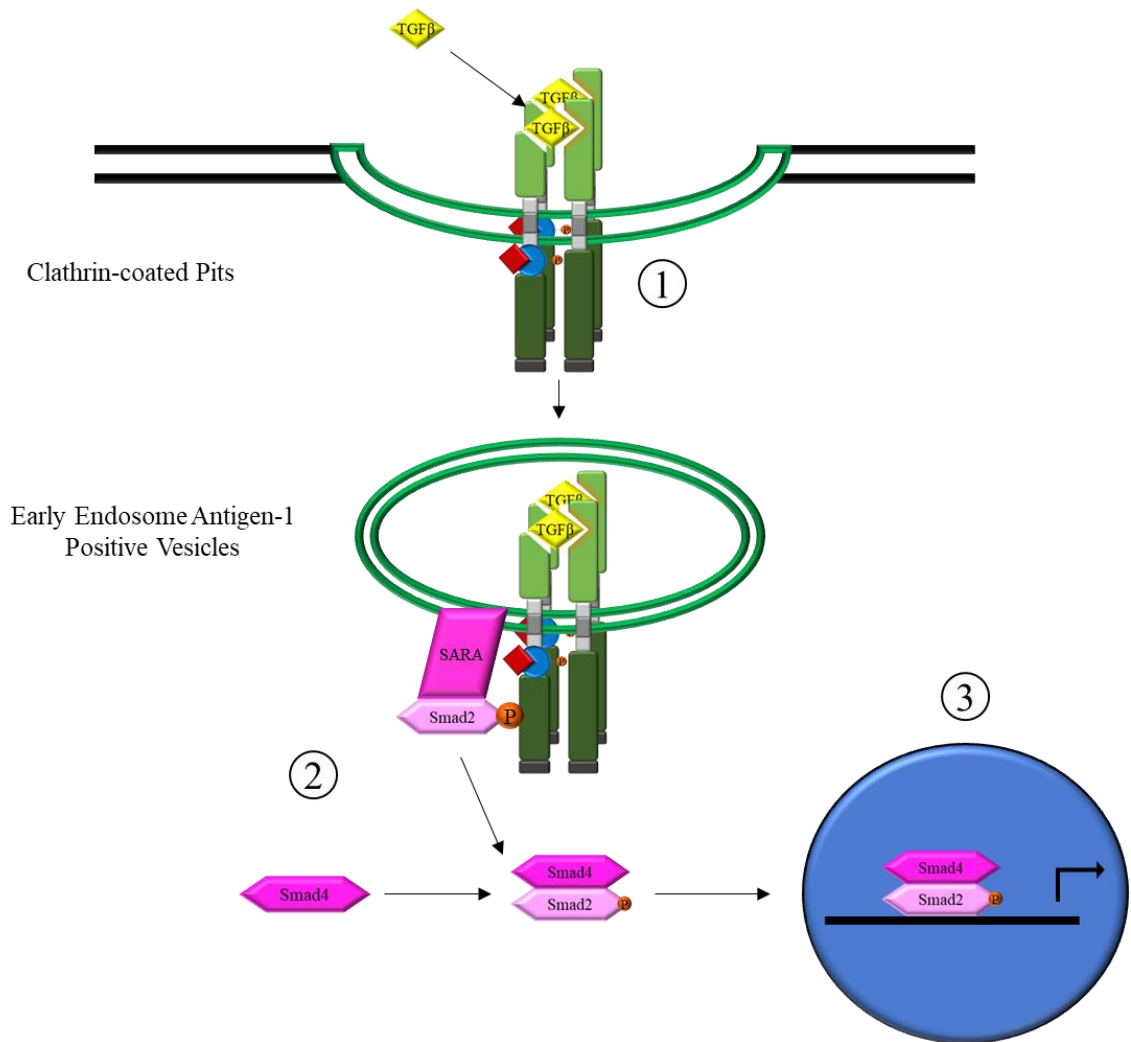


Figure 1.4 Schematic displaying the canonical TGFβ signaling pathway.

TGFβ ligand binding to the serine/threonine kinase TGFβ type II receptor (TβR2) induces the transphosphorylation of the TGFβ type I receptor (TβR1) (1). After the TβR1/2 complex is internalized into an early endosome, Smad anchor for receptor activation (SARA) recruits intracellular signaling protein to be phosphorylated by TβR1 (2). After phosphorylation, Smad2 dissociates from the TβR1, forms a complex with Smad4 to translocate into the nucleus, and facilitates gene transcription (3).

phosphorylated type 2 receptors interact with two type 1 receptors. This heterotetrameric complex is internalized into the early endosome, where downstream signaling processes are initiated. Following endocytosis, constitutively phosphorylated T β R2 transphosphorylates T β R1. T β R1 then phosphorylates intracellular proteins Smad2 and Smad3 at C-terminal residues. Smad2/3 are referred to as receptor-activated Smads (R-Smad) since they are responsive to external stimuli (Siegel & Massague, 2003; Finger et al., 2008b; Zhang et al., 2016). This association of T β R1 and Smad2 is mediated by Smad anchor for receptor activation (SARA) (Di Guglielmo et al., 2003). SARA has been shown to enhance Smad2 interaction with activated T β R1 by retaining Smad2 localization near the plasma membrane and increasing its proximity to the receptor (Tsukazaki et al., 1998). Once phosphorylated, Smad2 is released from the T β R1/2 complex into the cytoplasm and forms a complex with a common-mediated Smad, Smad4 (Massague, 1998; Wrana, 2000). Smad2/4 complexes undergo constant shuffling between the cytoplasm and the nucleus, which is dependent on the phosphorylation of Smad2 (Xu & Massague, 2004). The accumulation of Smad2/Smad4 complex in the nucleus facilitates transcription factor binding to DNA, initiating the transcription of genes that inhibit cell growth and proliferation in non-cancerous cells (Massague, 1998).

However, while TGF β signaling acts as a tumor suppression in healthy cells, TGF β activity in tumor cells is tumor promoting. An intact TGF β signaling pathway crosstalks with other signaling pathways including the MAPK, receptor tyrosine kinase (RTK), Wnt, and Notch pathways, exacerbating tumorigenic processes (Terai et al., 2011; Principe et al., 2014; Zavadil et al., 2004). Previous research has investigated the role of Type I and II receptors

on metastatic potential, yet the contributions of a third type of TGF β receptor, the TGF β Type III receptor remain unclear (Docea et al., 2012; Zhang et al., 2014).

In an atypical fashion, TGF β signaling has been linked to integrin-linked kinase (ILK) expression. Studies have demonstrated that ILK forms complexes with T β R2 and protects the receptor from ubiquitination and degradation (Vi et al., 2015). Furthermore, ILK expression may be necessary for Smad2 phosphorylation and for the facilitation of downstream TGF β -dependent transcriptional responses (Vi et al., 2011). Li et al. (2003) have shown that ILK expression is involved in EMT processes including cadherin shift, migration, and invasion, which can be abrogated by ILK inhibition via HGF.

TGF β 1-induced signaling can occur independent of both Smad2 phosphorylation and ILK. Non-canonical, or Smad-independent, TGF β signaling through RhoA (a small GTPase) and its downstream kinase, ROCK, has been implicated in actin reorganization and cell migration, two necessary characteristics of epithelial-to-mesenchymal transition (Masszi et al., 2003; Bhowmick et al., 2001). However, RhoA activation was not observed to disturb cell-cell adherens junctions (Kaartinen et al., 2002). While both pathways are dependent upon TGF β ligand for activation, their parallel function influence EMT separately.

Furthermore, TGF β ligand triggers T β R1 phosphorylation of ShcA, which, after forming a complex with Grb2 and Sos, induces Ras activation and the downstream activation of Erk1/2 via tyrosine phosphorylation (Roskoski, 2012). Increased Erk activation through the MAP kinase signaling pathway has been shown to enhance EMT in a TGF β dependent

manner, through a reduction in E-cadherin and an increase in N-cadherin expression (Grande et al., 2002).

1.2.5 Regulation of EMT

The expression of epithelial and mesenchymal markers during EMT is regulated at both a transcriptional and post-translational level. Regulation of E-cadherin expression at a transcriptional level is repressed by several E-box binding transcription factors, including Snail, Slug, ZEB1, and ZEB2 (Peinado et al., 2007). Through a separate means of interaction, the helix-loop-helix transcription factor Twist also represses E-cadherin expression, facilitating EMT (Peinado et al., 2007). Once translated, these proteins are translocated to the nucleus, where the 5' promoter region E-cadherin is bound, and transcription is repressed (Peinado et al., 2007). However, the action of these EMT regulating molecules may be dependent on cell-context. For instance, while it is well established that transcription factor Snail is necessary for mediation of E-cadherin expression, EMT in renal cells is Snail-independent (Li et al., 2003).

E-cadherin expression is also regulated post-translationally via tyrosine phosphorylation or ubiquitination, promoting protein endocytosis and weakening cellular adhesions (Fujita et al., 2002). In addition to transcriptional and post-translational methods of modulating E-cadherin expression, the degradative powers of matrix metalloproteinases (MMPs) have also been linked to E-cadherin repression. While MMPs have classically been characterized as tools used to remodel the extracellular matrix, recent studies have shown E- and N-cadherin to be alternative substrates for MMP proteolytic cleavage. Furthermore, cadherin cleavage by MMPs appears to be dependent on the makeup of surrounding extracellular matrix, with collagen I and IV providing a microenvironment that was more

prone to degradation of both E- and N-cadherin by MMP14 when compared to fibronectin (Covington et al., 2005).

microRNAs are single-stranded, non-coding oligomeric nucleotides, 20-25 nucleotides in length, that bind to transcribed mRNA (Esquela-Kerscher & Slack, 2006). Once bound, microRNAs have two separate regulatory functions: reduce mRNA stability or inhibit protein translation (Esquela-Kerscher & Slack, 2006). Recently, microRNAs have been investigated with regards to their ability to alter EMT. The downregulation of two families of microRNA that share consensus seed sequences — miR-200 (miR-200a, -200b, -200c, -141, -429) and miR-30 (miR-30a-5p, -30a-3p, -30e, -30e-3p) — have been linked to enhanced epithelial-to mesenchymal transition and tumor metastasis (Schliekelman & Liu, 2014). Furthermore, a reduction in miR-200 family members has been correlated with shortened survival of cancer patients (Mlcochova et al., 2016; Tang & Xu, 2015). Specifically, miR-200 family microRNAs target and repress the translation of mRNA encoding E-cadherin repressors ZEB1/2 (Mlcochova et al., 2016). In essence, these microRNAs act as repressors of E-cadherin transcriptional repressors. Furthermore, a double-negative feedback loop exists between expression of ZEB1 and the miR-200 family, as ZEB1 is able to bind to the promoter region of miR-200 genes and inhibit transcription (Schliekelman & Liu, 2014). Treatment with miR-200 family members has been shown rescue TGF β -dependent E-cadherin repression, and the suppression of EMT (Mlcochova et al., 2016; Zhang et al., 2012). Correspondingly, it is suggested that EMT may be suppressed in cancer patients via the upregulation of these microRNAs, or therapeutic treatment with exogenous oligomers that mimic microRNA sequences.

EMT can also be modulated independent of TGF β signaling. Expression of other ligands, including HGF and BMP-7, has been shown to inhibit EMT by preventing and even reversing TGF β 1-dependent cadherin shift both *in vitro* and *in vivo* (Yang & Liu, 2001; Zeisberg et al., 2003). In contrast, EMT processes can also be enhanced by the activation of other signaling cascades. EMT has been promoted by bFGF2 initiation of the FGF signaling pathway (Strutz et al., 2002). Additionally, phosphorylation of Erk1/2 via the MAP kinase cascade has been implicated in EMT progression (Schramek et al., 2003). Wnt and notch, and their ligands β -catenin and Jagged-1 respectively, have also been established as drivers of EMT (Ye & Weinberg 2016).

1.2.6 TGF β , EMT, and Autophagy

In addition to TGF β signaling, EMT progression has recently been linked to autophagic processes. Autophagy is a mechanism through which cells degrade and process cellular proteins in response to stress (Parzych & Klionski, 2014). Through the formation of protein complexes involving ULK1 kinase, Atg13, and Atg17, double-membraned vesicles called autophagosomes are employed to facilitate endocytosis (Degenhardt et al., 2006). Following autophagosome formation, autophagic proteins Atg5, Atg12, and Atg16 are responsible for the recruitment of LC3B1 (Matsushita et al., 2007), which undergoes proteolytic cleavage by Atg4 to generate LC3B2 and is incorporated into the autophagosomal membrane (Satoo et al., 2009). Next, fusion with lysosomes facilitates the degradation of cellular components. Since LC3B remains integrated in the autophagosome until lysosomal fusion is completed, LC3B is the gold-standard as a marker of autophagy. Recently published studies have demonstrated that chemical inhibition of autophagy by Bafilomycin-A1 or chloroquine-di-phosphate inhibits TGF β -induced EMT in cells from

retinal pigment epithelium, hepatocellular carcinoma, and NSCLC. (Alizadeh et al., 2018; Dash et al., 2018; Wu et al., 2018). Furthermore, knockdown of autophagic complex proteins Atg5 and Atg7 has been shown to inhibit EMT by reducing the protein expression of mesenchymal markers vimentin, Snail, and Slug (Jiang et al., 2018, Dash et al., 2018). Additionally, an increase in TGF β - or rapamycin-induced autophagy simultaneously exacerbated epithelial-to-mesenchymal transition in both a time- and concentration-dependent manner (Wu et al., 2018).

In 2014, Nitta et al. found that TGF β -induced cellular invasion was significantly hindered by autophagy inhibition, establishing a functional link between autophagy, EMT, and metastasis to supplement previously studied changes in cellular morphology.

A study by Pang et al. (2016) demonstrated that autophagosome formation was necessary to induce E-cadherin degradation via the autophagosome-lysosomal degradation pathway. From their observations, an established mechanism displayed Src activation in response to autophagy, resulting in β -catenin phosphorylation and association with phosphorylated Smad2. This β -catenin/Smad2 complex translocates to the nucleus and initiates transcriptional upregulation of ILK, which has been implicated in EMT processes (Pang et al., 2016). In addition to its role as a structural component of adherens junctions by binding to the cytoplasmic domain of E-cadherin, β -catenin also regulates E-cadherin expression by stabilizing Smad2 DNA binding as a co-activator of gene transcription (Kim et al., 2009). As such, the relationship between the expression of LC3B, an autophagic marker, and ILK, an EMT facilitator, is positive.

1.2.7 Matrix Metalloproteinases

Matrix metalloproteinases (MMPs) are a group of 23 enzymes that carry out several functions, one of which is to degrade and remodel specific components of the extracellular matrix (ECM) and are classified into different groups based on structure or substrate. MMP1, MMP13, and MMP14 are collagenases, primarily responsible for degrading collagen I, II, and III, while MMP2 and MMP9 digest gelatin, collagen IV and collagen V (Lu et al., 2011). Under normal physiological conditions, MMPs play a vital role in embryogenesis and wound healing (Cepeda et al., 2017). However, their ability to degrade and remodel components of the extracellular matrix (ECM) promotes the migration and invasion of tumor cells.

The expression patterns of MMPs varies widely and are present in both tumor cells and the surrounding stroma (Okada et al., 1995; Sato et al., 1994). Membrane-bound MMP-14 has been characterized in cancer-associated fibroblasts, tumor-associated macrophages, and endothelial cells (Chun et al., 2004; Sakamoto & Seiki, 2009) However, MMP-15 and -16 are primarily expressed in endothelial cells. MMP14 expression is high in mesenchymal cancers and sarcomas, facilitating invasion of tumor cells through microenvironments that are rich in collagen (Apte et al., 1997).

MMP activity is tightly regulated. Translated as inactive zymogens, MMPs are only activated following N-terminal proteolytic cleavage (Cepeda et al., 2017). Plasmin is a common activator of collagenase MMPs, including MMP-1, -3, -8, -10, and -13 (Lu et al., 2011). However, MMPs that possess a transmembrane domain (MMP-14, -15, -16, -24) or have cytoplasmic C-termini anchored to glycosylphosphatidylinositol (GPI) (MMP-17, MMP-25), are activated only by furin (Lu et al., 2011; Sohail et al., 2008). Furin binds a

specific recognition site in the pro-peptide region, situated at the N-terminal end of the catalytic domain (Pei & Weiss, 1995). Interestingly, certain gelatinase pro-MMP zymogens must be activated by other MMPs. MMP-2 and MMP-9 are each activated by a plethora of MMPs that can specifically interact with one of the two gelatinases, but not both. Notably, all membrane-bound MMPs cleave pro-MMP-2, while pro-MMP-9 is activated by the secreted MMPs of MMP-3, -10, and -13. Once activated, MMP-2 also has the proteolytic potential to activate the zymogen of its fellow gelatinase MMP-9. (Lu et al., 2011).

Additionally, a group of four tissue inhibitors of metalloproteinases (TIMP-1, -2, -3, -4) can selectively restrict the functional capabilities of specific MMPs. Dysregulation of zymogen cleavage or TIMP expression by cancer cells can result in aberrant ECM degradation, facilitating tumor metastasis (Jackson et al., 2017). In a stoichiometric 1:1 ratio, TIMPs reversibly insert an intrinsic cysteine disulfide bridge into the active domain of MMPs, inhibiting their catalytic function (Jackson et al., 2017; Brew & Nagase, 2010).

The regulation of MMP activity by TIMPs in a stoichiometric fashion is important to control not only degradation of the extracellular membrane, but also downstream cell signaling (Cepeda et al., 2017; Frantz et al., 2010; Hynes & Naba, 2012). This is especially relevant to membrane-bound MMPs that possess a cytoplasmic C-terminus. Thus, these MMPs possess the intrinsic capability to modulate intercellular communication and intracellular signaling by acting as a scaffold to promote cytoplasmic protein association. Membrane-bound MMP14 can form a complex with TIMP-2 facilitating MAPK signaling and phosphorylating downstream effector Erk1/2 (Pahwa et al., 2014; Sounni et al., 2010) MMP14 has also been shown to induce NF- κ B transcription (Cepeda et al., 2017).

EMT transcription factors such as Snail, Zeb1/2, and Twist, have been shown to increase membrane-bound MMP transcription in addition to repressing E-cadherin (Ota et al., 2009; Huang et al., 2009; Liu et al., 2016). These EMT transcription factors influence metastasis on two separate levels: releasing cell-cell junctional connections and promoting the expression of proteolytic enzymes to degrade the extracellular matrix.

1.3 Transforming Growth Factor β Type 3 Receptor

1.3.1 T β R3 in Cancer

Transforming Growth Factor Type 3 receptor (T β R3), also referred to as betaglycan, is the most abundantly expressed TGF β receptor in normal epithelial cells and is ubiquitous (Zhang et al., 2016). However, many cancer types have abnormally low expression levels of T β R3, including breast, prostate, lung, and ovarian cancers, and reduction is further enhanced as cancers develop into more advanced grades and later stages (Finger et al., 2008a). These cancer types demonstrate that T β R3 expression is an active suppressor of tumorigenicity, invasiveness, and progression (Zhang et al., 2016; Dong et al., 2007; Turley et al., 2007; Finger et al., 2008b; Hempel et al., 2008). However, the reduction of T β R3 is not due to aberrations in transcriptional, translational, or degradational processes. Rather, loss of the chromosomal locus of T β R3, 1p31-32, has been demonstrated in cancerous tumors (Dong et al., 2007, Turley et al., 2007). In lung cancer specifically, T β R3 mRNA and protein expression are both reduced due to loss of heterozygosity (Finger et al., 2008b). Zhang et al. (2016) found that TGF β 1 stimulation suppresses both the mRNA and protein expression of T β R3, in a dose-dependent manner (Hempel et al., 2008). However, the mechanism by which this occurs is currently unclear.

Conflicting literature has suggested that overexpression or silencing of T β R3 in various cell types results in T β R3 acting as either a tumor promoter or suppressor (Criswell et al., 2008; Finger et al., 2008b). In colon cancer cells, T β R3 acts as a tumor promoter, and knockdown has been shown to inhibit cell viability, while reducing cell migration and invasion (Liu et al., 2013). On the contrary, overexpression of T β R3 has been shown to suppress migratory and invasive potential in non-small-cell lung carcinoma and hepatocellular carcinoma (Finger et al., 2008b; Zhang et al., 2016). Additionally, exogenous T β R3 following knockdown has been shown to inhibit invasion, and metastasis both in the presence and absence of TGF β (Dong et al., 2007; Turley et al., 2007, Sun et al., 1997). Abnormally repressed T β R3 expression in late stage malignant cancers suggests a possible involvement in suppressing cell migration, invasion, and *in vivo* tumorigenesis (McLean & Di Guglielmo, 2010; Zhang et al., 2016; Criswell et al., 2008; Finger et al., 2008b).

Additionally, the administration of TGF β increased the migratory potential of hepatocellular carcinoma cells. This suggests a link between the reduction in T β R3 and cellular migration (Zhang et al., 2016).

1.3.2 Structure of T β R3

Genetic coding for T β R3 is made of a 225 kbp sequence on chromosome 1p33-p32 (Zakrzewski et al., 2016). Divided into 18 exons, T β R3 transcription is primarily regulated by the more proximal of its two separate upstream promoter regions (Hempel et al., 2007; Zakrzewski et al., 2016). The core protein of T β R3 is 851 amino acids in length, comprised of a 766 amino acid extracellular region, transmembrane domain, and short, 42 amino acid cytoplasmic tail, and exhibits a molecular weight of 100 kDa (Lopez-Casillas et al., 1994).

The core molecular weight of T β R3 is 100 kDa, however specific composition of bound extracellular chondroitin sulfate glycosaminoglycans (GAGs) may increase the molecular weight to between 180 and 300 kDa (Zhang et al., 2016, Lopez-Casillas et al., 1994). However, while modifications to GAG does not alter T β R3 internalization, functional characteristics are impaired (Finger et al., 2008a). Importantly, ligand interaction with T β R3 is weakened, suppressing downstream TGF β signaling (Deng et al., 1999)

TGF β Type 3 Receptor (**Figure 1.3**) is a membrane-anchored, heparin sulfate proteoglycan that possesses a short cytoplasmic C-terminal tail (Finger et al., 2008a; Gatzka et al., 2010). The short cytoplasmic tail of T β R3 contains a PDZ binding motif, which is necessary for binding to the constitutively phosphorylated site of T β R2 (Blobe et al, 2001a; Lopez-Casillas et al., 1991; Blobel et al., 2001b). This interaction is released following the association of T β R1 to T β R2 (Blobe et al., 2001a). Tazat et al. (2015) also established that T β R3 can bind T β R1 or T β R2 independent of one another or form a heterotrimer containing all three TGF β receptors. This cytoplasmic tail can also be phosphorylated at its threonine 841 residue by T β R2, promoting the association of β -arrestin, and T β R3 endocytosis (Finger et al., 2008a). Independent of ligand, T β R3 can be internalized via clathrin-dependent or -independent mechanisms. Notably, endocytosis of a β -arrestin2/T β R2/T β R3 complex through a clathrin-independent sequence facilitates T β R3 degradation and suppresses both canonical and atypical routes of TGF β signaling (Finger et al., 2008a; Chen et al., 2003). Additionally, this tail may be responsible for anchoring T β R3 to clathrin-mediated membranes, or lipid-raft membranes through clathrin and flotillin, respectively (Finger et al., 2008a).

However, T β R3 lacks the Ser/Thr kinase abilities of TGF β Type 1 and 2 receptors, or any other intrinsic enzymatic capabilities (Finger et al., 2008a, Zhang et al., 2016). As such, it is unable to phosphorylate Smad2 and induce TGF β signaling on its own. The facilitation of TGF β signaling is reliant upon the T β R1/2 complex, to which T β R3 presents TGF β ligand.

T β R3 differs from its T β R1 and T β R2 counterparts in more ways than simply lacking an intracellular kinase domain. The extracellular domains of T β R1 and T β R2 are shorter than that of T β R3 and are primarily constructed of cysteine residues (Attisano et al., 1993). On the contrary, the N-terminal ectodomain of T β R3 is folded into two ligand binding regions, separated by a linker region (Wang et al., 1991; Lopez-Casillas et al., 1991; Lopez-Casillas et al., 1994; Mendoza et al., 2009). Together, these binding sites allow dual, independent action of the receptor which are modulated by receptor cleavage (Gatza et al., 2010).

In addition to membrane-bound T β R3, the receptor can undergo ectodomain shedding by proteolytic cleavage at two separate sites of the extracellular domain. This cleavage is mediated by two membrane-bound matrix metalloproteinases, MT1-MMP (MMP14) and MT3-MMP (MMP16), and plasmin (Velasco-Loyden et al., 2004; Zakrzewski et al., 2016). MMP cleavage occurs at an extracellular site proximal to the transmembrane domain, while plasmin cleavage is present in the more distal linker region that separate the two extracellular binding domains of T β R3 (**Figure 1.3**). Ectodomain shedding released a soluble form of T β R3, which can be detected in both the serum and the extracellular domain (Gatza et al., 2010). Interestingly, the two forms of T β R3 possess different and opposite actions with regards to TGF β signaling. Interestingly, the invasive capabilities of

NSCLC cells have been inhibited following culture in conditioned media containing soluble T β R3 (Finger et al., 2008a).

T β R3 resembles certain structural components of Endoglin in each of its distal extracellular, transmembrane, and intracellular domains (Lopez-Casillas et al., 1994). Like T β R3, endoglin is a glycoprotein coreceptor of TGF β , whose primary function is to induce angiogenesis among endothelial cells (Burrows et al., 1995; Cheifetz et al., 1992). Interestingly, despite these structural similarities, endoglin is only able to bind TGF β 1 and TGF β 3 ligands but is unable to mimic the ability of T β R3 to bind TGF β 2 (Cheifetz et al., 1992). Thus, T β R3 possesses unique binding capabilities that cannot be explained by structural similarities with other receptors.

1.3.3 Modulation of TGF β Signaling

T β R3 influences TGF β signaling in three distinct ways (**Figure 1.3**). Two of these functions act to promote TGF β stimulation and response, while the third acts as a protective neutralizer of excessive TGF β signaling. Firstly, T β R3 facilitates TGF β signaling by binding either TGF β 1, TGF β 2, or TGF β 3 and presenting the ligand to T β R2 (Lopez-Casillas et al., 1993). From there, the canonical TGF β signaling pathway can proceed as previously described. Since T β R3 has the ability to bind TGF β 2, unique among TGF β receptors, T β R3 can initiate TGF β -dependent processes that would otherwise not occur.

T β R3 further propagates TGF β signaling by extending the half-life of T β R1 and T β R2 (**Figure 1.5**). Normally, T β R1 and T β R2 can be internalized in either a clathrin-mediated

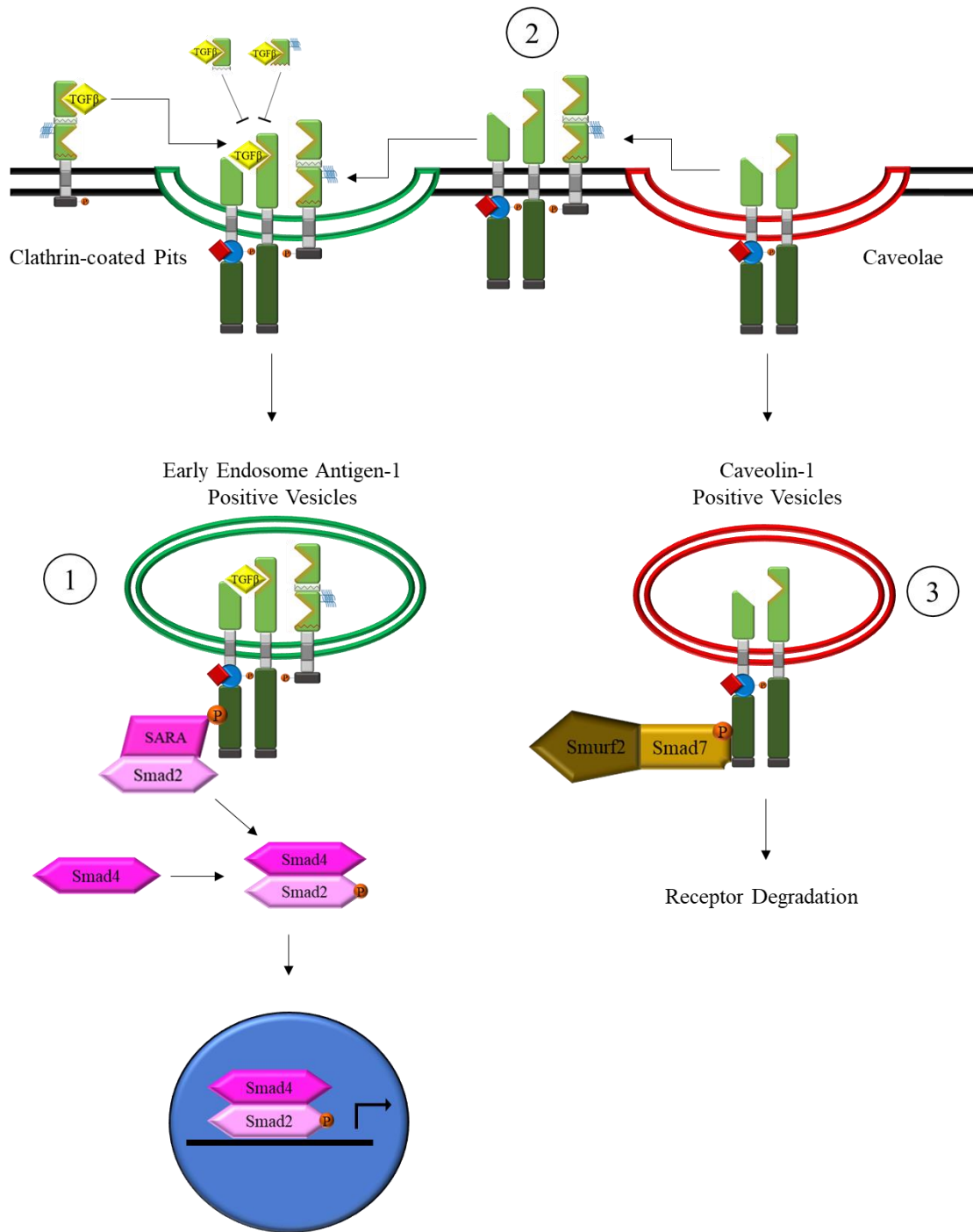


Figure 1.5 Complex role of TβR3 in TGFβ signaling.

In addition to facilitating or inhibiting TGFβ ligand association with the TβR1/2 complex, TβR3 extends the half-life of TβR1/2 receptors. Normally internalized into caveolin-1 positive vesicles and ubiquitinated by Smurf2 for degradation (3), TβR1/2 can be relocated out of lipid-raft membranes after binding to TβR3 (2). Thus, activation of the TGFβ signaling pathway is prolonged (1).

manner or through lipid-raft endocytosis (Finger et al., 2008a); distinct trafficking routes that serve opposing functions. T β R1/2 complexes found in lipid raft membranes are degraded through caveolae internalization and ubiquitination. Once endocytosed into caveolin-1 positive vesicles, Smurf2, an E3 ubiquitin ligase, is responsible for tagging T β R1 and T β R2 with ubiquitin, which targets the receptors for proteasomal/lysosomal degradation (McLean & Di Guglielmo, 2010; Kavsak et al., 2000). T β R3 has also been shown to bind and relocate T β R1/2 from lipid rafts to clathrin-coated pits, extending receptor complex half-life (McLean & Di Guglielmo, 2010). This relocation may occur by T β R3 binding T β R1 or T β R2 independently, in the absence or presence of TGF β ligand (McLean & Di Guglielmo, 2010). Furthermore, the relocation of these receptors has been shown to reduce trafficking of T β R2 into caveolin-1 positive vesicles, while increasing endocytosis into the early endosome. Extension of T β R1 and T β R2 half-life suggests that T β R3 expression heightens basal levels of TGF β signaling (McLean & Di Guglielmo, 2010)

Downstream signaling is propagated by the presentation of TGF β ligand by T β R3 to T β R1/2 complex, yet also reduced by inhibiting receptor complex formation by binding and sequestering ligand from binding to the T β R1/2 complex (Siegel & Massague, 2003; Zhang et al., 2016). Membrane-bound and soluble T β R3 possess different and opposite actions with regards to TGF β signaling. While membrane-bound T β R3 facilitates canonical TGF β signaling by increasing TGF β ligand affinity for T β R2, soluble T β R3 binds TGF β and interferes with ligand access to T β R2. Thus, ectodomain shedding of T β R3 acts as a negative feedback mechanism to neutralize excessive TGF β signaling, suppressing uncontrollable cell proliferation (Mendoza et al., 2009). Additionally, Tazat et

al. (2015) found that the ability of T β R3 to bind T β R1 or T β R2 competed with T β R1 and 2 from binding each other, thus reducing TGF β signaling.

1.3.4 T β R3 Modulation of Other Signaling Pathways

T β R3 is not limited to binding the three TGF β ligands. It also binds inhibin, and BMP-2, -4, and -7 through ligand binding sites. T β R3 also binds inhibin A, whose binding sites overlap with those of TGF β . Once bound, the T β R3/inhibin A complex interacts with, and inhibits activin and BMP type 2 receptor signaling (Mendoza et al., 2009, Finger et al., 2008a). T β R3 also interacts with basic fibroblast growth factor 2 (bFGF2), by way of GAG modifications (Finger et al., 2008a), thus implying that T β R3 is involved in a number of different signaling pathways, other than the one after which it was named.

Additionally, silencing of T β R3 has been shown to promote the phosphorylation of Akt kinase, facilitating downstream pro-tumorigenic influences (Zhang et al., 2016). Akt is an established anti-apoptotic factor, inactivating Bad and pro-caspase 9 through phosphorylation, downregulating p53, and activating NF- κ B (Downward, 2004; Pommier et al., 2004; Mayo & Donner, 2002; Zhou & Hung, 2002).

The overexpression of T β R3 has been shown to suppress the viability of nasopharyngeal carcinoma cells through the induction of apoptosis. T β R3 was demonstrated to increase the intracellular concentration of divalent calcium, a known inducer of apoptosis. As a mediator of apoptosis, T β R3 expression also activates apoptotic signaling through the protein upregulation of Bad and Bax, the downregulation of Bcl-2 expression, and inhibition of Bad phosphorylation. Together, these results suggest T β R3 acts as a tumour suppressor through the anti-proliferative effect of apoptosis (Zheng, 2013).

1.4 Rationale, Hypothesis, and Objectives

Previous studies have demonstrated that the tumor suppressive capabilities of T β R3 are lost in late stage tumors due to a reduction in receptor expression. Primarily, T β R3 modulates the TGF β signaling pathway by presenting TGF β ligand to, and extending the half-life of, the T β R1/2 receptor complex, in addition to soluble T β R3 sequestering overabundant TGF β to prevent excessive signaling. As such, it is of interest to investigate the sensitivity and longevity of TGF β -dependent signaling in the absence of T β R3. Furthermore, examining the transcriptional expression of TGF β -responsive genes could elucidate the multi-layered regulatory nature of T β R3 on TGF β signaling.

Although EMT is regulated through many pathways, an important driver of this pre-metastatic process is the TGF β signaling cascade. Exploring the effect of T β R3 silencing on EMT through alterations in epithelial and mesenchymal markers may reveal TGF-dependent and -independent influences on EMT.

TGF β signaling and EMT are established promoters of cell migration and invasion, which are both phenotypical characteristics of cancerous tumors. Thus, studying the migratory and invasive capabilities of T β R3 silenced non-small-cell lung cancer cells can reveal a functional process that is regulated by T β R3.

Based on these studies, since T β R3 is posited to facilitate TGF β signaling, thereby inducing EMT and enhancing cellular migratory and invasive potential, I **hypothesize** that silencing T β R3 will suppress TGF β signaling, shifting cells into a more epithelial phenotype and inhibiting migration and invasion.

Based on this hypothesis, my overall objectives are to:

- 1) Determine how T β R3 influences TGF β signaling in NSCLC cells.
- 2) Assess the role of T β R3 in regulating TGF β -dependent epithelial-to-mesenchymal transition of NSCLC cells.
- 3) Investigate the downstream functional implications of T β R3 on cell migration and invasion.

Materials and Methods

2 Materials and Methods

2.1 Antibodies, Primers, and Reagents

The following antibodies, primers, and reagents were used in applicable western blotting and qPCR analyses.

Table 2.1 Primary and secondary antibodies used for western blotting.

<u>Target</u>	<u>Supplier</u>	<u>Product Number</u>	<u>Dilution</u>
E-Cadherin (mouse)	BD Biosciences	610182	1:1000
GAPDH (rabbit)	Cell Signaling	2118S	1:2000
LC3B1/2 (rabbit)	Cell Signaling	2775S	1:1000
N-Cadherin (mouse)	BD Biosciences	610921	1:1000
Smad2 (mouse)	BD Biosciences	610843	1:1000
pSmad2 (rabbit)	Cell Signaling	3101	1:1000
TGFBR3 (goat)	R&D Systems	AF-242-PB	1:1000
Tubulin (mouse)	Sigma	T4026	1:2000
Goat HRP from donkey	Santa Cruz	Sc-2020	1:25 000
Mouse HRP from goat	Pierce	PI31430	1:25 000
Rabbit HRP from goat	Pierce	PI31460	1:25 000

Table 2.2 Primer sequences used for qPCR.

Primers were designed to correspond with human proteins using Integrated DNA Technologies Realtime PCR tool and supplied by Invitrogen. All sequences are 5' to 3'.

<u>Target Gene</u>	<u>Protein</u>	<u>Forward</u>	<u>Reverse</u>	<u>Coding Sequence</u>
TGFBR3	TβR3	CGGGAGATATGGATGAAGGAG	CATGTTGAAGGTGATGTTTCCG	CCDS55614.1
SNAI1	Snail	AATCGGAAGCCTAACTACAGCG	GTCCCAGATGAGCATTGGCA	CCDS13423.1
SNAI2	Slug	ATACCACAACCAGAGATCCTCA	GACTCACTCGCCCCAAAGATG	CCDS6146.1
SERPINE1	PAI-1	CATCCCCCATCCTACGTGG	CCCCATAGGGTGAGAAAACCA	CCDS5711.1
SMAD7	Smad7	GTGTTGCTGTGAATCTTACGG	TCGGGTATCTGGAGTAAGGAG	CCDS59317.1
CDH1	E-Cadherin	CCCACCACGTACAAGGGTC	CTGGGGTATTGGGGGCATC	CCDS82005.1
CDH2	N-Cadherin	CCCAAGACAAAGAGACCCAG	GCCACTGTGCTTACTGAATTG	CCDS11891.1
ARRB2	B-Arrestin2	AATCTTCCATGCTCCGTCAC	CGAATCTCAAAGTCTACGCCG	CCDS58504.1
MET	MET	GACTCCTACAACCCGAATACTG	ATAGTGCTCCCAATGAAAGTAG	CCDS47689.1
PRICKLE1	Prickle1	TGAGACCAGAGCAGATCCAG	AAAGACTGGCAATACCGTACC	CCDS8742.1
SMAD2	Smad2	GATCCTAACAGAACTTCCGCC	CACTTGTCTTCTCCATCTTCACTG	CCDS11934.1
TGFBR1	TβR1	ACATGATTCAGCCACAGATACC	GCATAGATGTCAGCACGTTTG	CCDS47998.1
TGFBR2	TβR2	GAGCTCCAATATCCTCGTGAAG	TATCTTGCAGTTCCACCTG	CCDS33727.1
MMP1	MMP1	GCACAAATCCCTTCTACCCG	AACAGCCCAGTACTTATTCCC	CCDS8322.1
MMP14	MMP14	TGCCTACCGACAAGATTGATG	ATCCCTTCCAGACTTTGATG	CCDS9577.1
HPRT	HPRT	TGGCGTCGTGATTAGTGATG	AACACCCTTTCCAAATCCTC	CCDS14641.1

Table 2.3 Reagents used for cell processing and data collection.

<u>Reagent</u>	<u>Supplier</u>	<u>Product Number</u>	<u>Application</u>
Clarity™ Western ECL Substrate	BioRad	170-5060	Western blotting
DC™ Protein Assay Reagent A Reagent B Reagent C	BioRad	500-0113 500-0114 500-0115	Protein Assay
E.N.Z.A.® Total RNA Kit I	OMEGA bio-tek	R6834-01	RNA Isolation
iScript™ Reverse Transcription Supermix for RT-qPCR	BioRad	1708841	Reverse Transcription
Lipofectamine® RNAiMAX	Invitrogen	13778-150	Transfection
Matrigel Matrix	BD Biosciences	356237	Transwell Invasion
BLUeye Prestained Protein Ladder	FroggaBio	PM007-0500	Western blotting
siRNA medium GC content Control	Ambion		Transfection
siRNA against TGFBR3	Ambion	439240	Transfection
SensiFAST™ SYBR No-ROX Kit	Bioline	BIO-98020	qPCR

2.2 Cell Culture and Transfection

2.2.1 Cell Culture

NCI-H1299 (hereafter termed H1299) non-small-cell lung carcinoma cells (ATCC® CRL-5803™) were cultured in RPMI-1640 medium with L-glutamine and sodium bicarbonate (Sigma R7858-500ML) and supplemented with 10% fetal bovine serum (FBS). A549 NSCLC cells (ATCC® CCL-185™) were cultured in Kaighn's modification of F-12 Ham nutrient mixture with L-glutamine and sodium bicarbonate (F12K; Sigma N3520-10X1L) medium containing 10% FBS. All cells were maintained at 37°C in a humidified atmosphere containing 5% CO₂.

2.2.2 Cell Transfection

H1299 and A549 cells were plated and transfected using Lipofectamine® RNAiMAX reagent (Invitrogen) as per manufacturer's recommendations. Specifically, 100 µL of OptiMEM medium was used as a diluent for appropriate volumes of each Lipofectamine® RNAiMAX and siRNA in separate 1.5 mL microcentrifuge tubes. The volumes of Lipofectamine® RNAiMAX and siRNA corresponded to a 3:1 ratio. After vortexing, solutions containing OptiMEM and siRNA were pipetted into their paired tube containing appropriate volumes of OptiMEM and Lipofectamine® RNAiMAX and mixed by pipetting. Solutions were incubated at room temperature for five minutes, then pipetted in a drop-wise fashion into their corresponding cell plates. Cells were incubated for 48 hours with the transfection agents prior to downstream applications.

2.3 TGF β Administration

For experiments that required TGF β 1 (hereby referred to as TGF β) administration, cells were rinsed three times with phosphate buffered saline (PBS) and serum-starved in growth media containing 0.2% FBS (low-serum) overnight. The following morning, TGF β ligand was diluted to a specific concentration (as indicated in individual experiments) in culture medium containing 0.2% FBS and vortexed. Spent media was aspirated, cells were washed with PBS, and fresh medium supplemented with TGF β was added. All control cells were cultured in low-serum medium lacking TGF β .

When investigating TGF β sensitivity and longevity, cells were incubated with a specific concentration of TGF β (dose response – 0 pM, 1 pM, 2.5 pM, 5 pM, and 10 pM; time course – 250 pM) at 37°C for 30 minutes. Experiments using a concentration gradient were then lysed. To assess a signaling time course, media containing 250 pM TGF β 1 was aspirated and one set of cell plates, one control and one T β R3 silenced, were lysed as a 30-minute timepoint. Remaining plates were rinsed three times with PBS. Culture media containing 0.2% FBS was added to cells, which were incubated at 37°C and lysed either 1 hour, or 4 hours later.

When investigating protein markers of EMT, following transfection and serum-starvation, cells were incubated with 250 pM TGF β in a reverse manner. In this regard, cells to be treated with TGF β for 48 hours were initially supplemented with TGF β , while remaining plates were cultured in media containing low-serum media without TGF β . Twenty-four hours later, fresh low-serum media including 250 pM TGF β was added to plates designated for 24- and 48-hour exposures to TGF β . After an additional 24 hours, all cells, including a 48-hour low-serum condition, were lysed.

All experiments examining transcriptional response to TGF β involved cells that were treated with 250 pM TGF β in low-serum media for 24 hours, after undergoing transfection and overnight serum-starvation.

2.4 Cell Lysis and Protein Assay

Following appropriate incubations, cells were rinsed with PBS. Next, a lysis buffer comprised of 50 mM Tris pH 7.5, 1 mM EDTA, 0.5% Triton X-100, 150 mM sodium chloride was used in conjunction with phosphatase and protease inhibitors 2.5 mM sodium fluoride, 10 mM sodium pyrophosphate, 50 μ M PMSF, and 1 mg/mL pepstatin A. This solution was pipetted onto the cells and rocked at 4°C for 20 minutes. Cells were scraped, and lysates were pipetted into individual 1.5 mL microcentrifuge tubes to be centrifuged at 4°C for 10 minutes at 15 000 rcf. Supernatants were transferred to separate tubes and sample prep buffer (30% glycerol, 10% 1.5M Tris pH 6.8, 1.2% sodium dodecyl sulfate, 0.018% bromophenol blue, 15% β -mercaptoethanol) and stored at -20°C.

Using the DC™ Protein Assay system (BioRad) as per manufacturer's instructions, concentrations of protein samples were determined prior to the addition of sample prep buffer. A Beckman Coulter DU® 730 Life Science UV/Vis Spectrophotometer was used to measure absorbance values relative to a standard curve and to calculate protein concentration.

2.5 SDS-PAGE and Western Blotting

For SDS-PAGE, separating gels containing 10% acrylamide (15% to separate LC3B1 from LC3B2) were used in conjunction with 5% acrylamide stacking gels. Following gel polymerization and the setup of a running apparatus, samples were heated at 90°C for 5

minutes. A BLUeye Prestained Protein Ladder (FroggaBio) was used as a reference in comparison to separation of total protein. Next, volumes corresponding to 50 μ g of protein sample were loaded and electrophoresed at 120 V. Following protein separation, a wet transfer technique was employed to transfer proteins from SDS-acrylamide gels onto nitrocellulose membranes at a constant amperage of 350 mA for 2 h. Nitrocellulose membranes were then stained using Ponceau S (15% acetic acid, 4 mg/mL Ponceau S) to visualize total protein. Membranes were then cut at appropriate protein sizes and Ponceau S was removed using tris-buffered saline-tween 20 (TBST; 50 mM Tris, 150 mM sodium chloride, 0.05% Tween-20, pH7.5).

As a method of blocking non-specific antibody binding, membranes were rocked at room temperature for 1 hour in 5% skim milk in TBST. After blocking, membranes were incubated overnight at 4°C on a rocker, in appropriate primary antibodies diluted in TBST. The next day, primary antibody solutions were removed, and membranes were washed with TBST three consecutive times for 10 minutes each. Next, membranes were incubated in appropriate secondary antibodies, conjugated to horseradish peroxidase, rocking at room temperature for 1 hour. An additional round of three 10-minute washes with TBST preceded membrane coating with Clarity™ Western ECL Substrate (BioRad) per manufacturer's instructions. A VersaDoc Imaging System (BioRad) was used to visualize luminescent proteins, and densitometry was completed via QuantityOne 1-D Analysis Software (BioRad).

2.6 RNA Isolation and cDNA Synthesis

Following TGF β incubations, an E.N.Z.A.® Total RNA Kit I (OMEGA bio-tek) was used per manufacturer's instructions to isolate total RNA, and eluted RNA was stored at -80°C.

Prior to reverse transcription, the concentration and purity of isolated RNA was assessed using a NanoDrop 2000 spectrophotometer (ThermoFisher Scientific). Next, 1 μg of RNA was mixed with iScript™ Reverse Transcription Supermix for RT-qPCR (BioRad) per manufacturer's instructions, and reverse transcription was performed in a DNA Engine (BioRad) with parameters of 25°C for 5 minutes, then 46°C for 20 minutes, and 95°C for 1 minute to generate cDNA. cDNA was then stored at -20°C.

2.7 Quantitative Polymerase Chain Reactions

For qPCR, master mixes comprised of 0.6 μL 10 mM forward primer, 0.6 μL 10 mM reverse primer, 4.3 μL nuclease-free water, and 7.5 μL SensiFAST™ SYBR (Bioline) were added to 2 μL of sample cDNA, per reaction, depending on the number of genes or samples being studied. Quantitative polymerase chain reactions were performed by a CFX96™ Real-Time System and C1000 Touch™ Thermal Cycler (BioRad), with PrimePCR parameters optimized for SYBR. Samples were initially denatured at 95°C for 2 minutes. Next, samples were cycled forty times through a denaturing step at 95°C for 5 seconds and primer annealing at 60°C for 30 seconds. After forty cycles, samples were incubated at 95°C for five seconds. The efficiency and amplification factor of each primer set was determined using a standard curve and calculated using ThermoFisher Scientific qPCR Efficiency Calculator.

2.8 Transwell Assays

2.8.1 Cell Migration

Following transfection, cells to be seeded in Transwell chambers were serum-starved using culture media with 0.2% FBS for 4 hours. Transwell® Permeable Supports (Corning; 6.5

mm Insert, 24 Well Plate, 8.0 μm Polycarbonate Membrane, REF#3422) were placed in 24-well plates with culture media containing either 0.2% or 10% FBS in the lower chamber. After serum starvation, cells were lifted following cleavage of adhesion proteins by Trypsin, counted, and diluted to a concentration of 250 000 cells/mL using low-serum media. Next, 200 μL of cell suspension (corresponding to 50 000 cells) was pipetted into the upper Transwell chamber and incubated for 24 hours at 37°C with 5% CO_2 .

The next day, cotton swabs soaked in PBS were inserted into the upper chamber and were used to gently remove any adherent cells from the upper side of the membrane. Washes with PBS removed any remaining non-adherent cells from the upper membrane and cleaned cells that were adherent to the lower side of the membrane. Cells were then fixed by 4% paraformaldehyde (PFA) for 10 minutes at room temperature, washed 5 times with PBS, and permeabilized with 0.25% Triton X-100. Following 3 additional PBS washes, a razorblade was used to precisely cut the Transwell membrane out of the supporting apparatus. Excised membranes were then incubated in DAPI (1 $\mu\text{g}/\text{mL}$) in the dark for 5 minutes. One final wash with PBS prepped the membranes for mounting between a glass slide and coverslip. When handling membranes, care was taken to not rub the underside of the membrane and accidentally remove migrated adherent cells.

Visualization of migrated cells (5 fields/experimental condition) was completed using an Olympus IX81 motorized inverted research microscope and InVivo software (MediaCybernetics; Version 3.2.2 Build 45, 2007). Finally, the number of migrated cells per field of view was quantified using ImageJ software (Version 1.51n).

2.8.2 Cell Invasion

Cellular invasion was investigated using the same procedure as Transwell migration above, with one addition: Prior to cell trypsinization and seeding, 50 μL of ice cold 1.02 mg/mL Matrigel Matrix (BD Biosciences) diluted in low-serum culture media was added to the upper chamber of each Transwell apparatus and incubated at 37°C. After allowing the matrix to gel for 30 minutes, cells were trypsinized and the protocol described above was performed.

2.9 Microarray Analysis

Following transfection of H1299 cells, total RNA was isolated using the E.N.Z.A. Total RNA Kit (OMEGA bio-tek) as per the manufacturer's instructions. Next, samples were diluted to a concentration of 100 ng/ μL and sent to the London Regional Genomics Center (Robarts Research Institute, London, Ontario, Canada) for processing. Once received, the use of an Agilent 2100 Bioanalyzer (Aligent Technologies) and an RNA 6000 Nano kit (Caliper Life Sciences) evaluated RNA quality. Upon validation, single-stranded complimentary DNA (sscDNA) was generated from 200 ng of total RNA via the Ambion WT Expression Kit for Affymetrix GeneChip Whole Transcript WT Expression Arrays (Applied Biosystems), and the Affymetrix GeneChip WT Terminal Labeling kit and Hybridization User Manual (Affymetrix). Total RNA was then converted to cDNA and *in vitro* transcription resulted in cRNA. Through this process, 5.5 μg of single stranded cDNA was synthesized, end-labeled, and hybridized to Human GeneChip 2.0 arrays for 16 hours at 45°C. To reduce human error, all steps involving liquid transfer were performed by a GeneChip Fluidics Station 450 (Affymetrix). Next, GeneChips were scanned using a GeneChip Scanner 3000 7G (Affymetrix) and probe level data was analyzed using

Affymetrix Command Console v1.1. Partek Genomics Suite v6.5 was used to convert probe data to gene level information, and an ANOVA was performed to determine significance. Gene fold-change represents the average of two separate experiments comparing gene expression in T β R3 silenced cells to control cells. A fold-change of ± 1.75 was considered the cutoff for further investigation. Microarray False Discovery Rate and multiple comparison tests were carried out using Partek Genomics Suite v6.5. Gene ontology analyses were performed using PANTHER v13.1.

2.10 Statistical Analyses

Statistical analysis for a minimum of three biological replicates was conducted using GraphPad Prism® 6 for Windows (Version 6.01). Unpaired t-tests, one-way ANOVA, or two-way ANOVA analyses were performed, followed by Tukey's post-hoc tests. Values were considered to be statistically significant when $p < 0.05$, which is denoted by asterisks as specified in the figures below.

Results

3 Results

3.1 The effect of T β R3 on TGF β -dependent Smad2 phosphorylation in A549 and H1299 cells

To determine how T β R3 influences TGF β signaling in NSCLC cells, I first assessed Smad2 phosphorylation. However, I first confirmed the expression of T β R3 in two NSCLC cell lines, H1299 and A549 cells, and the knockdown efficiency of siRNA-mediated T β R3 silencing. I observed that H1299 cells indeed expressed T β R3 and interestingly, significant T β R3 knockdown was observed even at the lowest concentrations of siT β R3 when compared to equivalent concentration of scrambled negative control siRNA (siControl) (**Figure 3.1**). Cells treated with 12.5 nM siT β R3 expressed 47% T β R3 when compared to siControl. However, since I observed that 25 and 37.5 nM of both siT β R3 and siControl resulted in approximately 25% of cell detachment from the culture dishes (data not shown), this suggested that increased volumes of Lipofectamine might be toxic to the cells. In contrast to H1299 cells, low basal expression of T β R3 in A549 cells prevented the quantification of knockdown of the western blots (**Figure 3.2a**). Therefore, qPCR was performed on mRNA extracted from both A549 and H1299 cells treated with 12.5 nM siT β R3 or 12.5 nM siControl using primers for T β R3 (**Table 2.2**). Consistent with H1299 cells, A549 cells had significantly reduced T β R3 mRNA levels (**Figure 3.2b**). Based on the western blotting and qPCR results, a concentration of 12.5 nM siT β R3 was used in all following experiments investigating T β R3 expression in H1299 or A549 cells.

I first investigated the impact of TBR3 knockdown on TGF β signaling by measuring Smad2 phosphorylation. First, sensitivity to different concentrations of TGF β was

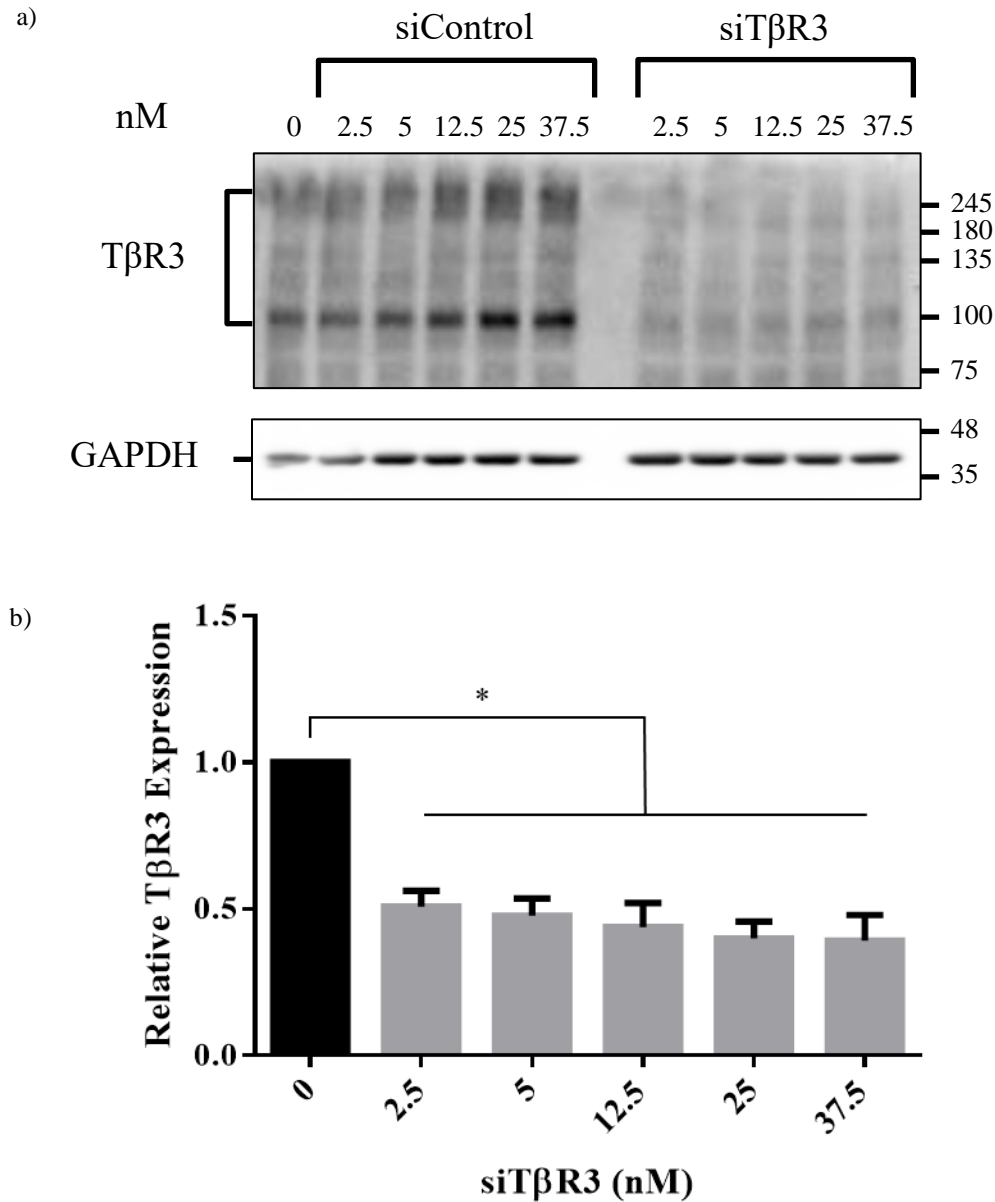


Figure 3.1 Knockdown of TβR3 in H1299 cells by siRNA

a) H1299 cells were transfected with increasing concentrations of either siTβR3 or siControl and incubated at 37°C for 48 hours. Cell lysates were then subjected to western blotting for TβR3 or GAPDH (loading control).

b) Three separate experiments were carried out as described in panel a, imaged and quantitated using the BioRad QuantityOne software. (Mean ± SD; One-way ANOVA with Tukey's post-hoc, *p<0.05)

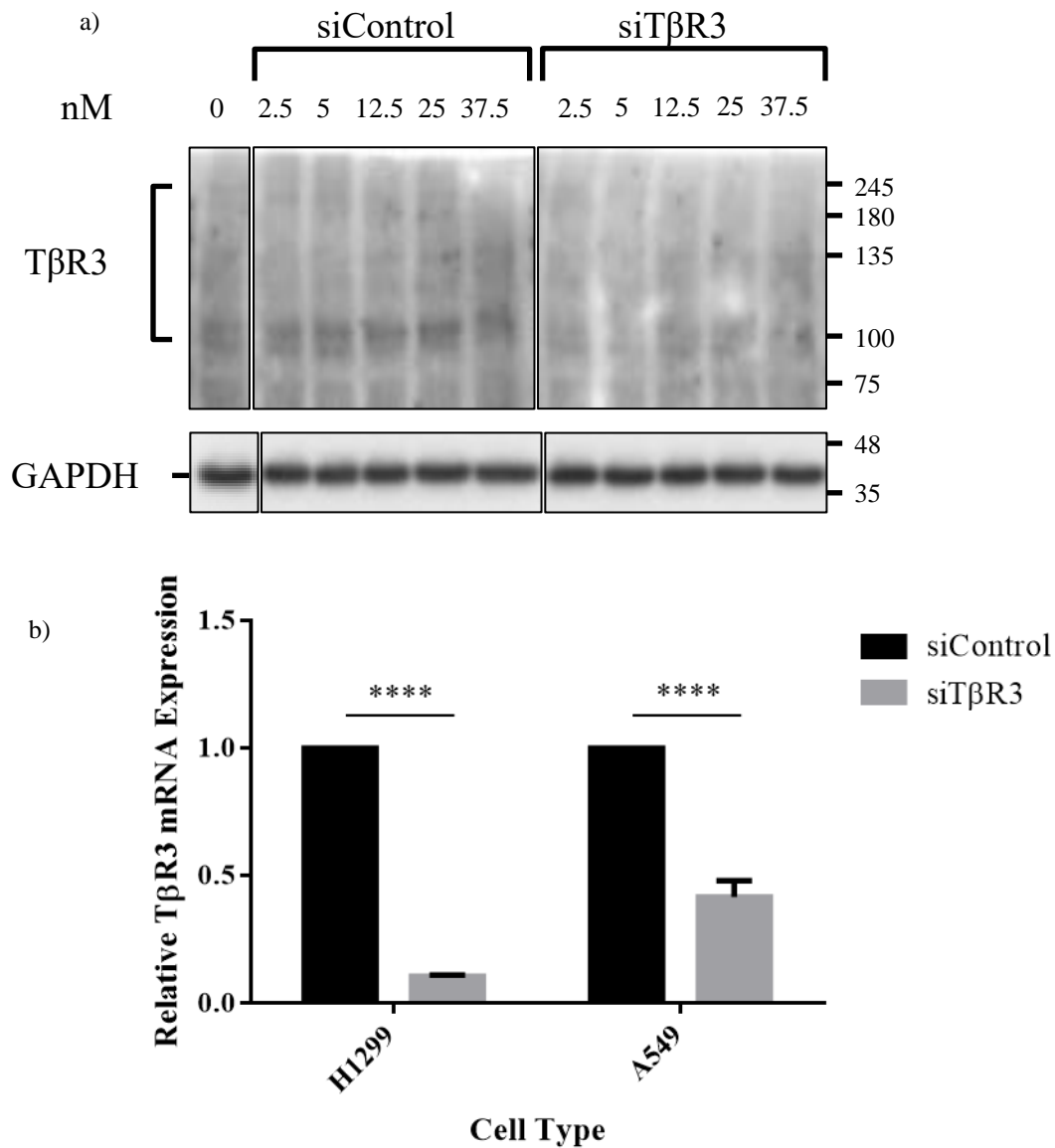


Figure 3.2 Knockdown of TβR3 in A549 cells by siRNA

a) A549 cells were transfected with increasing concentrations of either siTβR3 or siControl and cultured at 37°C for 48 hours. Cell lysates were then subjected to western blotting for TβR3 or GAPDH (loading control).

b) Relative mRNA expression of TβR3 in A549 and H1299 cells transfected with 12.5 nM siTβR3 or siControl and cultured at 37°C for 48 hours. RNA was isolated and subjected to reverse-transcription qPCR analysis to assess TβR3 transcript levels. (Two-way ANOVA; Mean ± SEM; N=3; Tukey's post-hoc ****p<0.0001)

measured by relative phosphorylation of Smad2. In both cell lines, T β R3 knockdown did not significantly alter the increase of Smad2 phosphorylation in response to an increase in TGF β concentration (**Figures 3.3, 3.4**). Second, the maintenance of Smad2 phosphorylation was assessed using a time-course protocol. Briefly, following administration of 250 pM TGF β for 30 minutes, TGF β was washed-out, replaced with TGF β free media, and lysed at various time points to determine the maintenance of signaling following ligand removal. Both H1299 and A549 cells responded to 250 pM TGF β following 30 minutes, demonstrated by increased Smad2 phosphorylation (**Figures 3.5, 3.6**). Both cell lines also displayed similar levels of TGF β signaling following TGF β washout, with Smad2 phosphorylation decreasing over time. Therefore, based on my results, I conclude that neither A549 nor H1299 cells displayed altered TGF β -dependent Smad2 signaling sensitivity (amplitude of signal), nor longevity (time course of signaling), following T β R3 knockdown. Interestingly, total Smad2 expression was insignificantly reduced following T β R3 knockdown in H1299 cells when compared to matched controls (**Figure 3.5**). However, a similar reduction in total Smad2 expression was not seen in A549 cells. Although the fraction of expressed Smad2 that had been phosphorylated was not altered following T β R3 knockdown, there was a reduction in Smad2 phosphorylation when compared to time- and concentration-matched controls. Thus, T β R3 knockdown may reduce TGF β signaling through suppressed Smad2 expression, rather than by regulating phosphorylation processes. To investigate this possibility, I assessed downstream effects of TGF β signaling, the E-to-N cadherin shift that is observed during TGF β -dependent EMT.

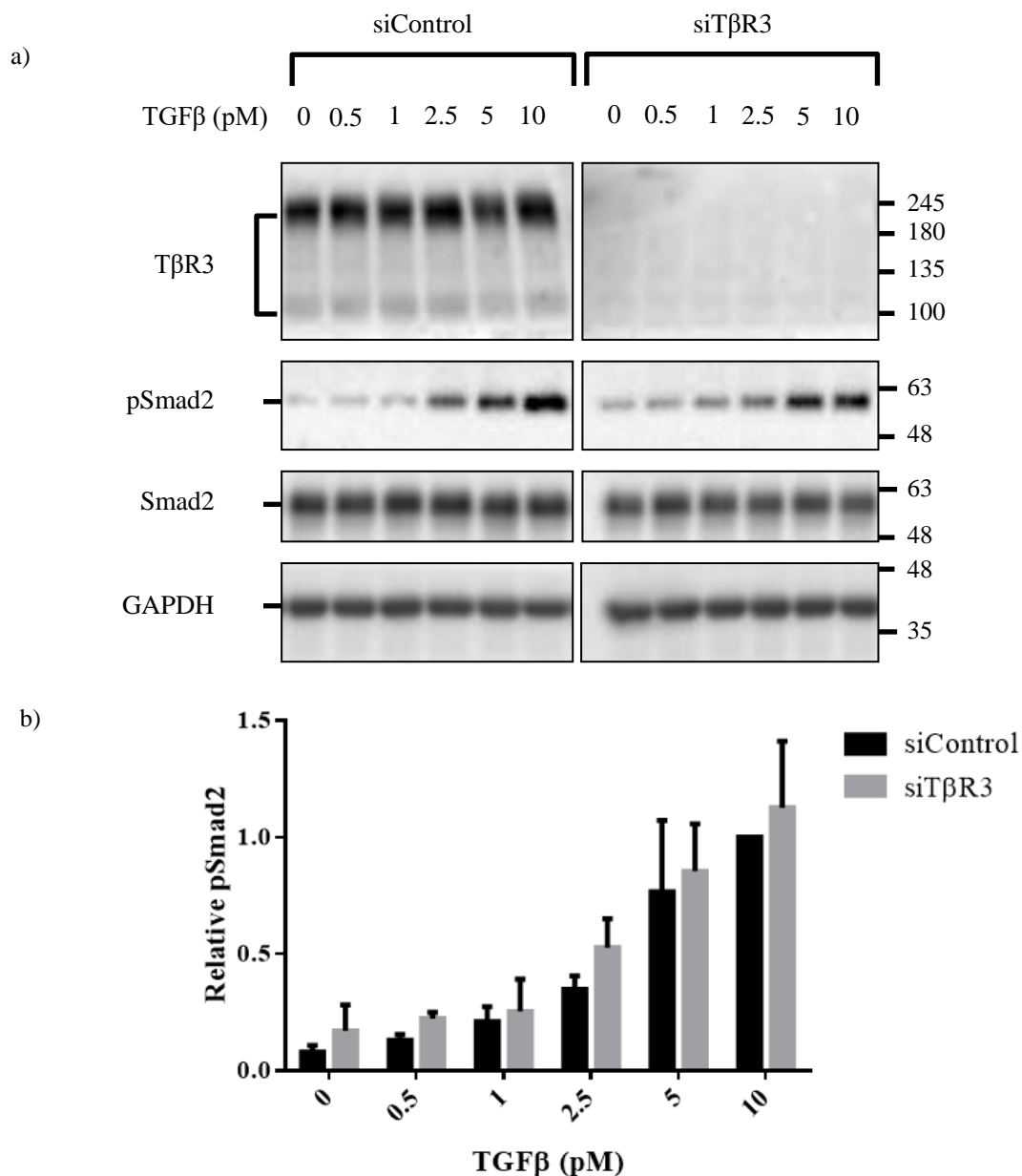


Figure 3.3 The effect of TβR3 knockdown on TGFβ-dependent Smad2 phosphorylation in H1299 cells

a) H1299 cells transfected with 12.5 nM siTβR3 or siControl were treated with the indicated concentrations of TGFβ in serum-free media for 30. Cell lysates were then subjected to western blotting for TβR3, phosphorylated Smad2 (pSmad2), Smad2 or GAPDH (loading control).

b) Three separate experiments were carried out as described in panel a, imaged and quantitated using the BioRad QuantityOne software, and expressed as phosphorylated Smad2/total Smad2 (Relative pSmad2). (Two-way ANOVA; Mean ± SD; N=3; Tukey's post-hoc)

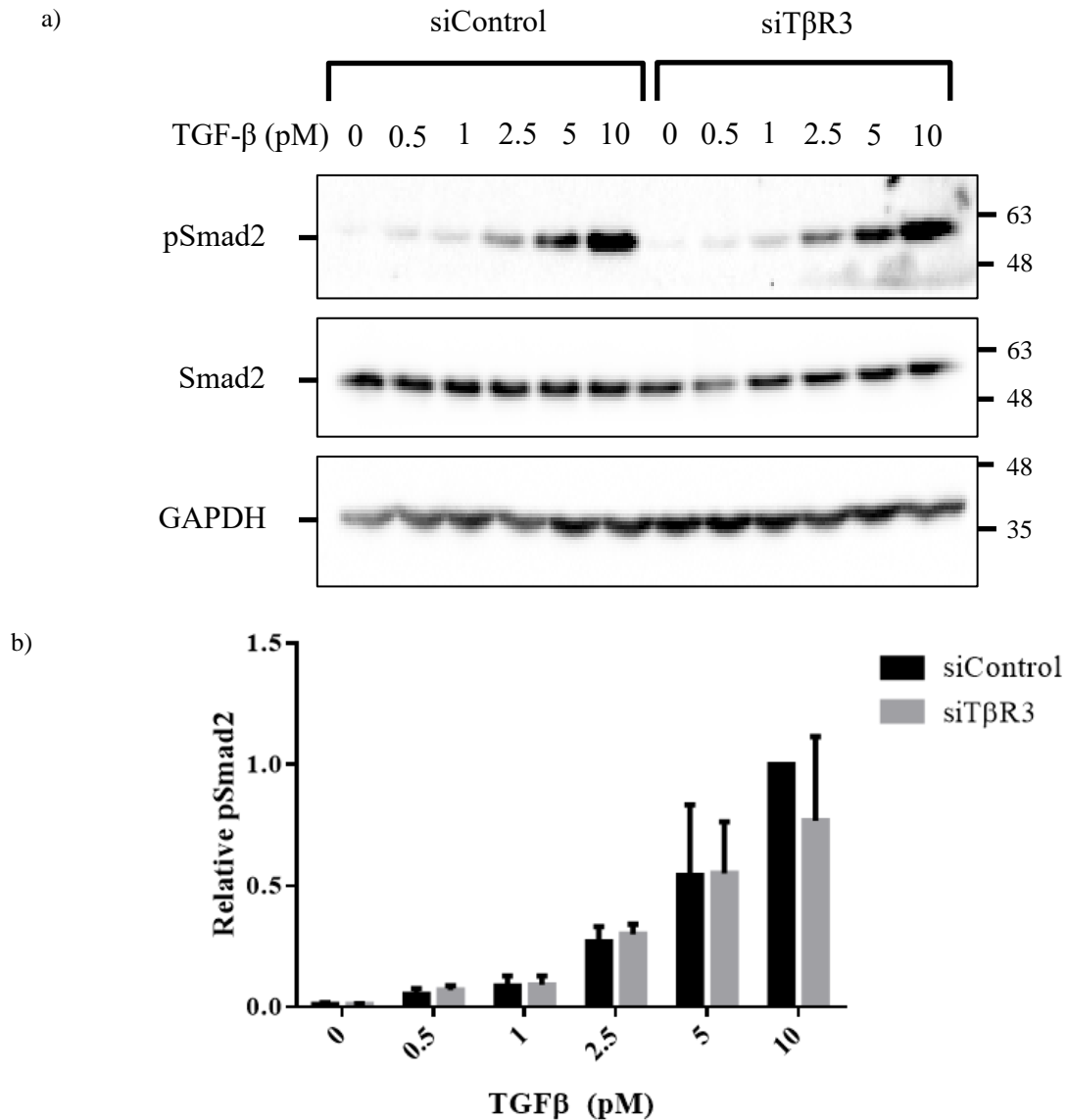


Figure 3.4 The effect of TβR3 knockdown on TGFβ-dependent Smad2 phosphorylation in A549 cells

a) A549 cells transfected with 12.5 nM siTβR3 or siControl were treated with the indicated concentrations of TGFβ in serum-free media for 30. Cell lysates were then subjected to western blotting for phosphorylated Smad2 (pSmad2), Smad2 or GAPDH (loading control).

b) Three separate experiments were carried out as described in panel a, imaged and quantitated using the BioRad QuantityOne software, and expressed as phosphorylated Smad2/total Smad2 (Relative pSmad2). (Two-way ANOVA; Mean ± SD; N=3; Tukey's post-hoc)

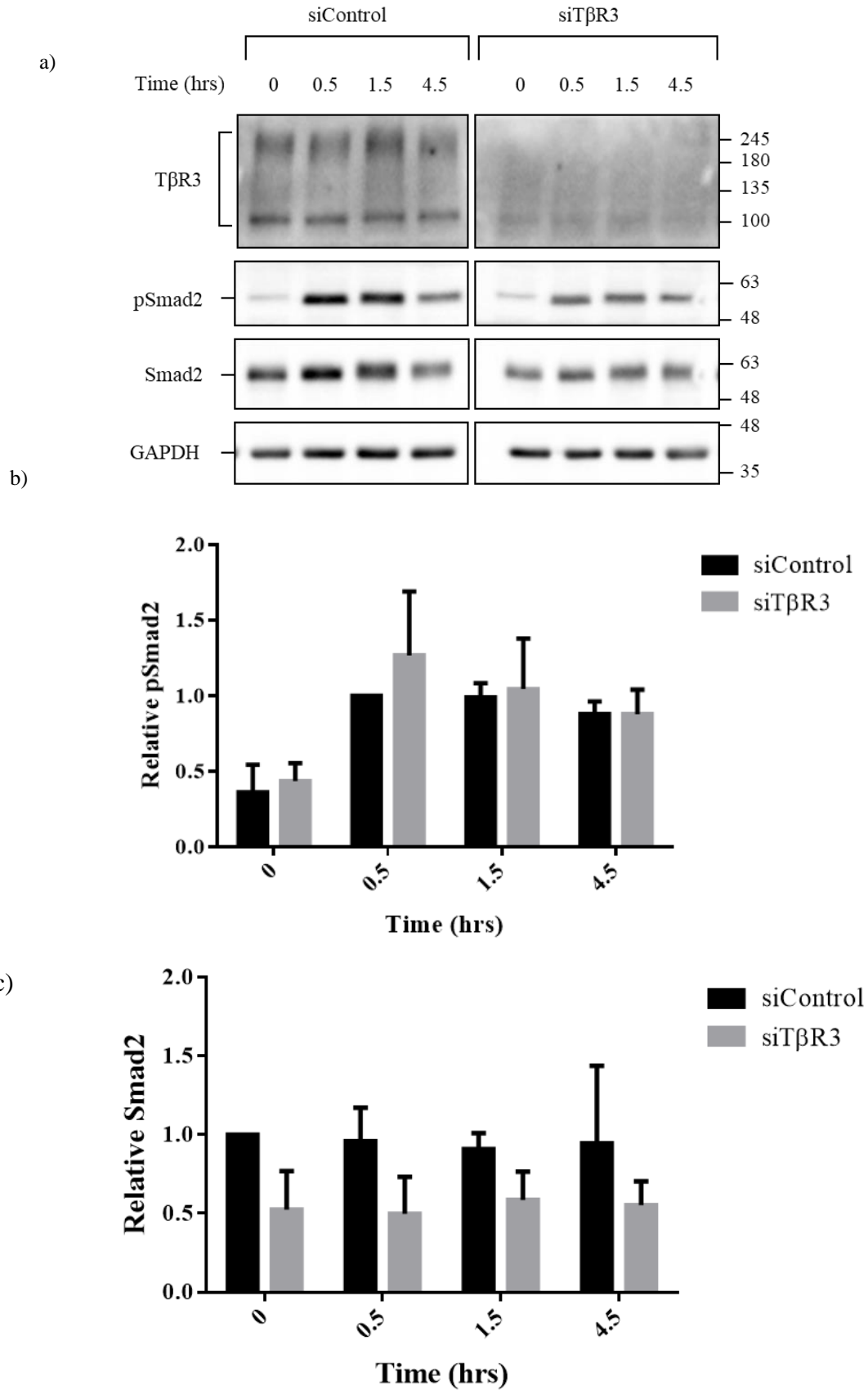


Figure 3.5 Time course of Smad2 phosphorylation in H1299 cells following T β R3 knockdown

a) H1299 cells were transfected with 12.5 nM siT β R3 or siControl, incubated for 48 hours at 37°C, and serum-starved overnight. Following incubation with 250 pM TGF β for 30 minutes, media was replaced with serum-free media and cells were lysed at various time points. Cell lysates were then subjected to western blotting for T β R3, phosphorylated Smad2 (pSmad2), Smad2 or GAPDH (loading control).

b) Three separate experiments were carried out as described in panel a, imaged and quantitated using the BioRad QuantityOne software, and expressed as phosphorylated Smad2/total Smad2 (Relative pSmad2). (Two-way ANOVA; Mean \pm SD; N=3; Tukey's post-hoc)

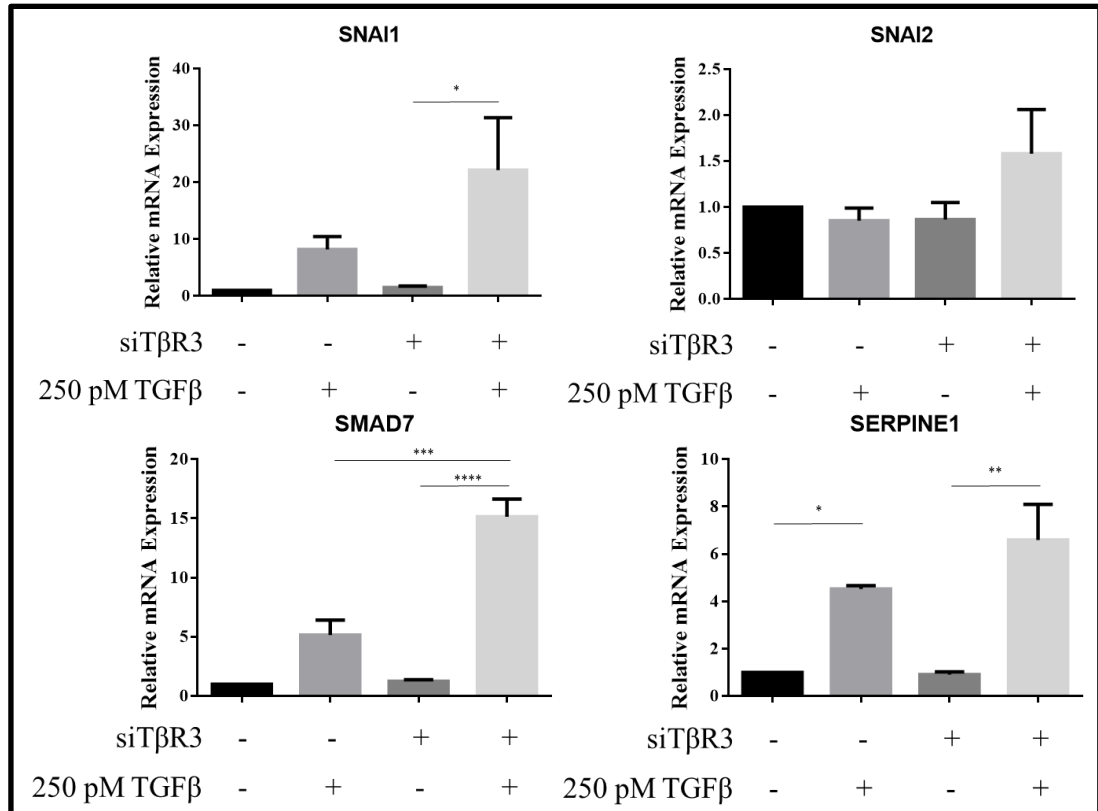
c) H1299 cells were transfected with 12.5 nM siT β R3 or siControl, incubated for 48 hours at 37°C, and serum-starved overnight. Following incubation with 250 pM TGF β for 30 minutes, media was replaced with serum-free media and cells were lysed at various time points. Cell lysates were then subjected to western blotting for Smad2 or GAPDH (loading control). The relative total Smad2 protein expression was normalized and graphed. (Two-way ANOVA; Mean \pm SD; N=3; Tukey's post-hoc)

3.2 The effect of T β R3 silencing on TGF β -dependent EMT markers

As described by Kalluri & Weinberg (2009), hallmarks of EMT include reduced E-cadherin and increased N-cadherin protein expression when treated with TGF β . Investigating genes such as SNAI1 (Snail), SNAI2 (Slug), SERPINE1 (PAI-1), and Smad7 would demonstrate a mechanism by which T β R3 expression influences gene transcription in a TGF β -dependent manner. Interestingly, T β R3 knockdown did not significantly alter gene transcription in the absence of TGF β , in either cell line (**Figure 3.7**). However, following TGF β stimulation, a significant increase in expression of Smad7 mRNA was found in the absence of T β R3 in both cell lines. This result was not demonstrated when TGF β was administered to control cells. Furthermore, the significant increase in SNAI1 in response to TGF β in control A549 cells was diminished when T β R3 was silenced. In contrast, SNAI1 mRNA expression did not significantly increase in H1299 control cells following TGF β administration but did in T β R3 silenced cells.

I next carried out qPCR analysis to investigate E-cadherin and N-cadherin mRNA levels in both cell lines. Following T β R3 knockdown, a significant increase in CDH1 (E-cadherin) expression was observed in A549 cells, but not in H1299 cells, regardless of TGF β administration (**Figure 3.8**), suggesting that the altered E-cadherin levels might be post-translational. In contrast, A549 N-cadherin expression was significantly increased in the presence of TGF β (**Figure 3.8b**), yet no difference was seen between control and knockdown conditions. Interestingly, I observed an additive effect between T β R3 knockdown and TGF β administration in H1299 N-cadherin expression (**Figure 3.8a**).

a)



b)

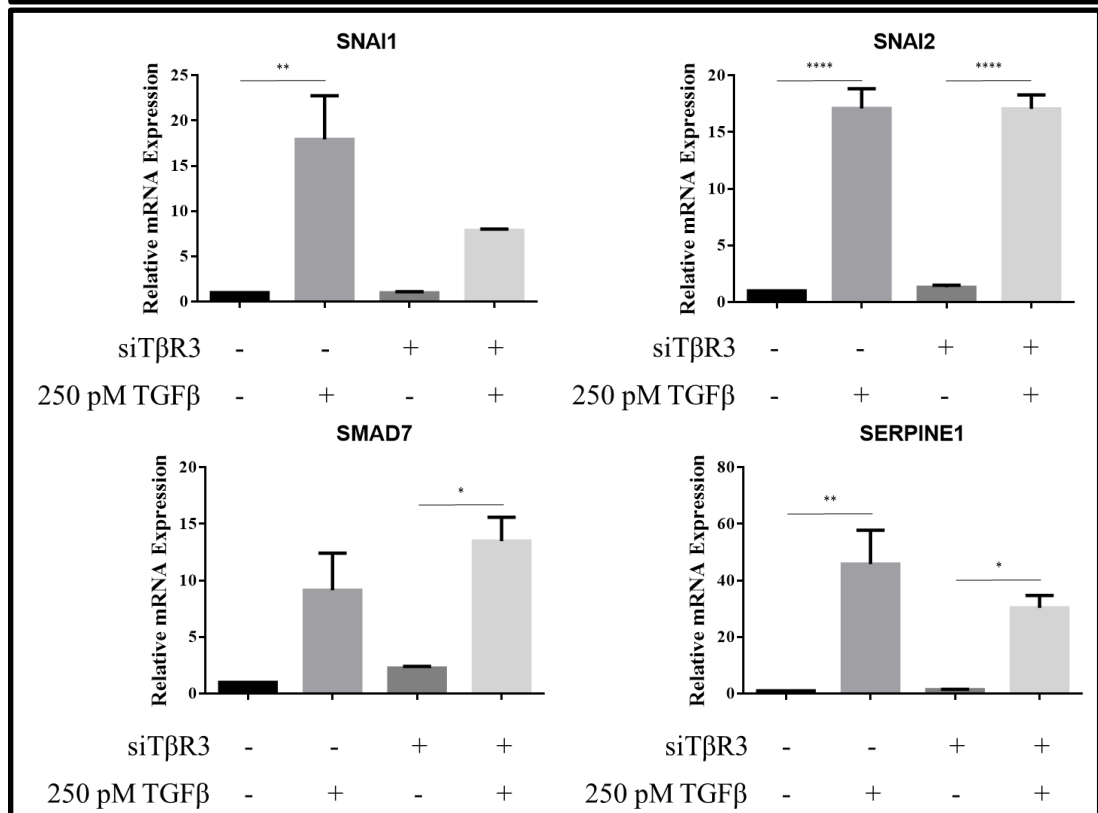


Figure 3.7**Figure 3.7 TGF β -dependent transcription in response to T β R3 knockdown**

H1299 (a) and A549 (b) cells were transfected with 12.5 nM siT β R3 or siControl, incubated for 48 hours at 37°C, and serum-starved overnight. Cells were then treated with 250 pM TGF β for 24 hours and total RNA was isolated. qPCR analysis was carried out as described in the materials and methods section and graphed. (One-way ANOVA; Mean \pm SEM; N=3; *p<0.05, **p<0.01, ***p<0.001, ****p<0.0001)

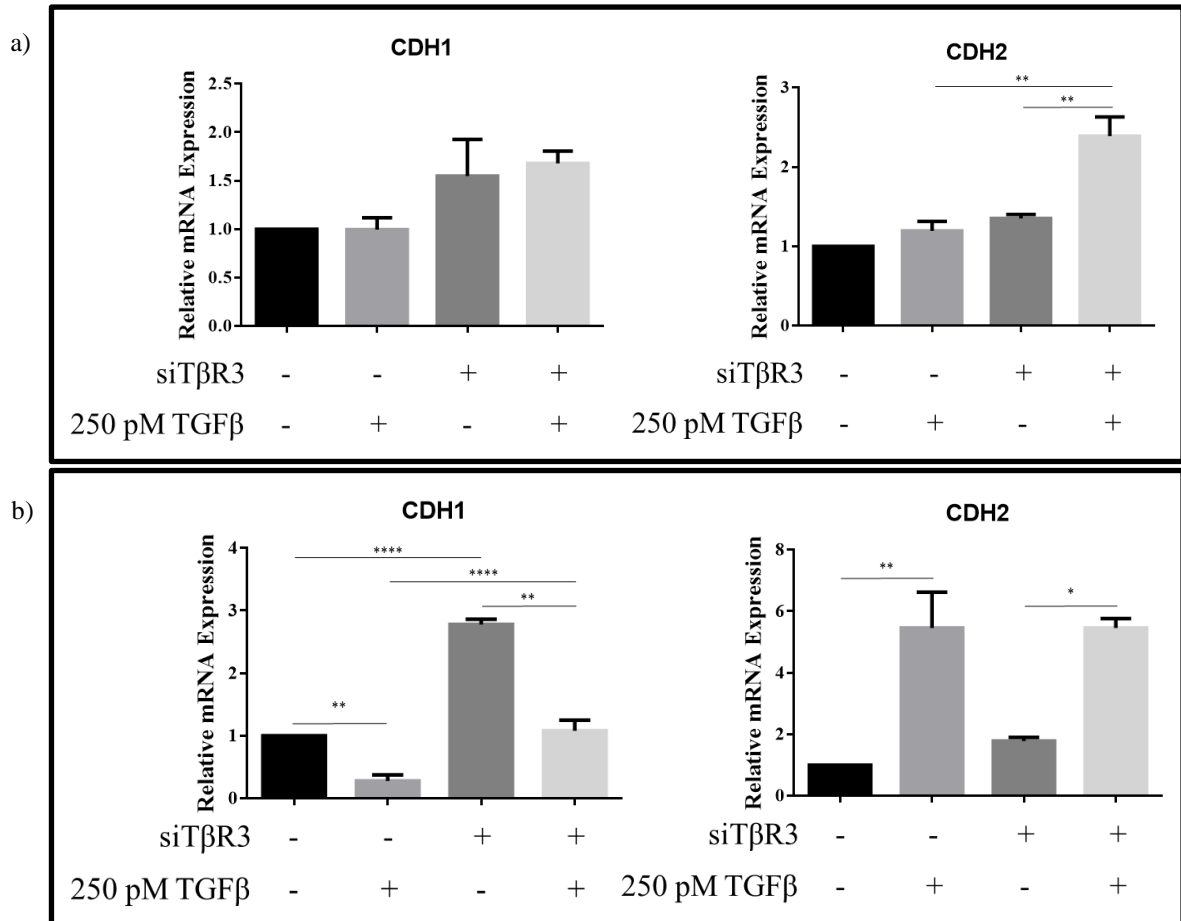


Figure 3.8 Expression of cadherin mRNA in the absence of TβR3

Relative mRNA expression of E- and N-cadherin. H1299 (a) and A549 (b) cells were transfected with 12.5 nM siTβR3 or siControl, incubated for 48 hours at 37°C, and serum-starved overnight. Cells were then treated with 250 pM TGFβ for 24 hours and total RNA was isolated. qPCR analysis was carried out as described in the materials and methods section and graphed. (One-way ANOVA; Mean ± SEM; N=3; *p<0.05, **p<0.01, ****p<0.0001)

Therefore, while N-cadherin transcription was not found to be TGF β dependent in control H1299 cells, N-cadherin mRNA levels were significantly increased following TGF β administration in T β R3 knockdown cells.

Since TGF β signaling has been shown to modulate EMT protein markers, we next explored the expression of E-cadherin and N-cadherin to determine whether T β R3 expression influences downstream phenotypic changes. Following supplementation with 250 pM TGF β for 0, 24, or 48 hours, A549 cells showed a canonical E- to N- cadherin shift. However, knockdown of T β R3 dampened the TGF β -dependent cadherin shift (**Figure 3.10**). Surprisingly, H1299 cells demonstrated an increase in both E-cadherin and N-cadherin over time (**Figure 3.9**). However, as seen with the A549 cells, T β R3 knockdown interfered with TGF β -dependent alteration in E- and N-cadherin levels. T β R3 silenced cells did not exhibit an increase in N-cadherin protein levels in response to TGF β , although control cells did. Together, these results suggest that the knockdown of T β R3 dampens the ability of TGF β to induce an E to N cadherin shift in both A549 and H1299 cells, which is consistent with the hypothesis that T β R3 promotes TGF β -signaling.

When comparing E-cadherin protein expression to mRNA expression, basal expression was observed to be consistently increased in T β R3 knockdown cells. Corresponding to protein expression, mRNA levels were also reduced following TGF β exposure in A549 cells and increased in H1299 cells. However, inconsistencies were present when examining these relationships with N-cadherin. Protein expression level was reduced in response to TGF β stimulation, while mRNA expression was significantly increased in both cell lines. The disconnect between mRNA and protein expression of N-cadherin in the presence of TGF β suggests a complex interplay between mRNA and protein expression, so I further

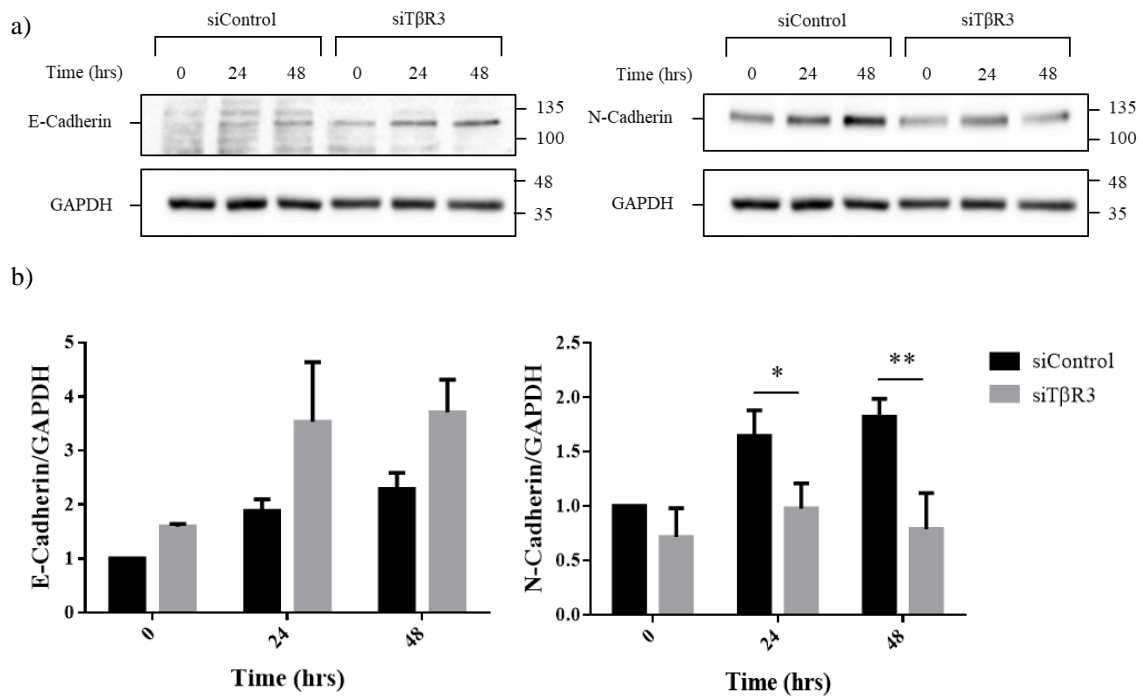


Figure 3.9 TβR3 knockdown on TGFβ-dependent cadherin shift in H1299 cells

a) H1299 cells were transfected with 12.5 nM siTβR3 or siControl, incubated for 48 hours at 37°C, and serum-starved overnight. Cells were then treated with 250 pM TGFβ for the indicated time points and lysed. Cell lysates were then subjected to western blotting for E-cadherin, N-cadherin or GAPDH (loading control).

b) Three separate experiments were carried out as described in panel a, imaged and quantitated using the BioRad QuantityOne software. (Two-way ANOVA; Mean ± SD; N=3; Tukey's post-hoc *p<0.05, **p<0.01)

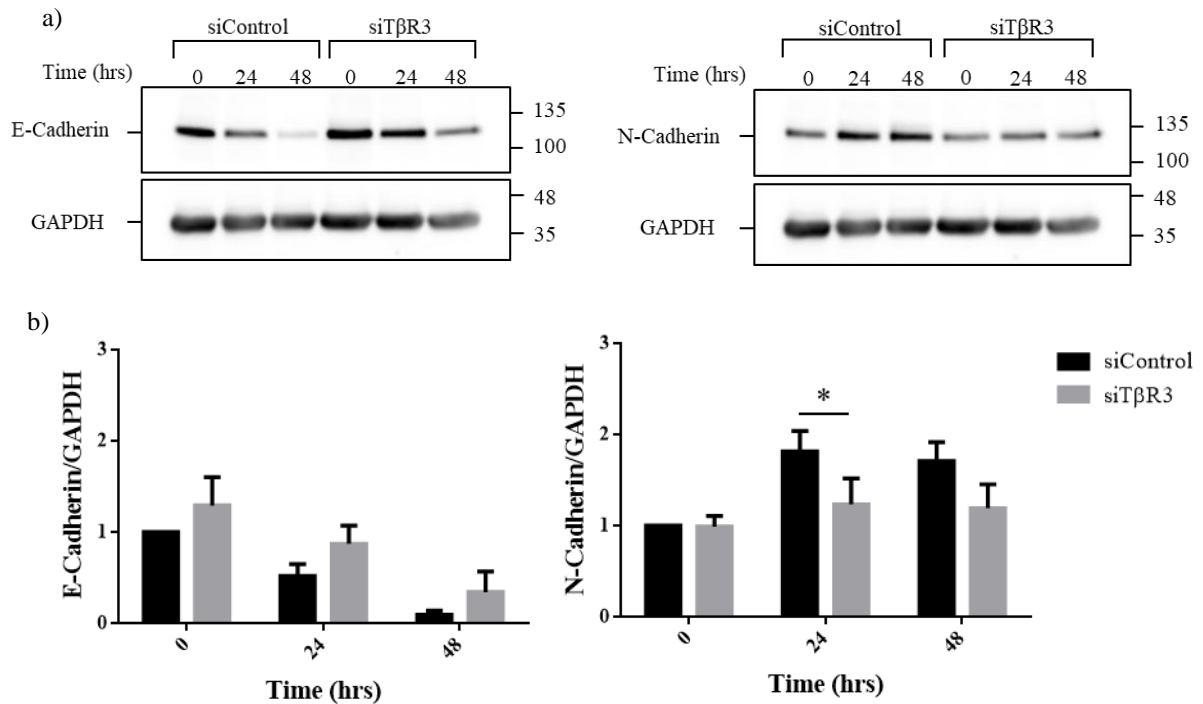


Figure 3.10 TβR3 knockdown on TGFβ-dependent cadherin shift in A549 cells

a) A549 cells were transfected with 12.5 nM siTβR3 or siControl, incubated for 48 hours at 37°C, and serum-starved overnight. Cells were then treated with 250 pM TGFβ for the indicated time points and lysed. Cell lysates were then subjected to western blotting for E-cadherin, N-cadherin or GAPDH (loading control).

b) Three separate experiments were carried out as described in panel a, imaged and quantitated using the BioRad QuantityOne software. (Two-way ANOVA; Mean ± SD; N=3; Tukey's post-hoc *p<0.05)

mined the microarray data for microRNAs that may alter EMT processes. Specifically, microRNAs targeting E-cadherin repressors SNAIL, ZEB1/2, or E-cadherin directly, would have the ability to modulate E-cadherin mRNA levels. However, the expression of an important subset of EMT-regulating microRNAs, including the mir200 and mir30 families, were unaffected by T β R3 knockdown (**Appendix Table 5**).

As described in the introduction, the processes of autophagy and epithelial-to-mesenchymal transition are related and positively correlated; i.e., as autophagy is induced, so is EMT. As such, I used the autophagy protein LC3B as a marker of EMT and observed that its expression is markedly reduced in both A549 and H1299 cells following T β R3 knockdown. A significant decrease was found in LC3B1 in A549 cells, regardless of TGF β administration (**Figure 3.12**). Similar results were found in H1299 cells, with T β R3 knockdown reducing expression of both LC3B1 and LC3B2 (**Figure 3.11**). However, significance was only seen following 48 hours of TGF β incubation.

Based on my observations that EMT markers were affected by T β R3 silencing, I next investigated if this would result in altered cell migration or invasion.

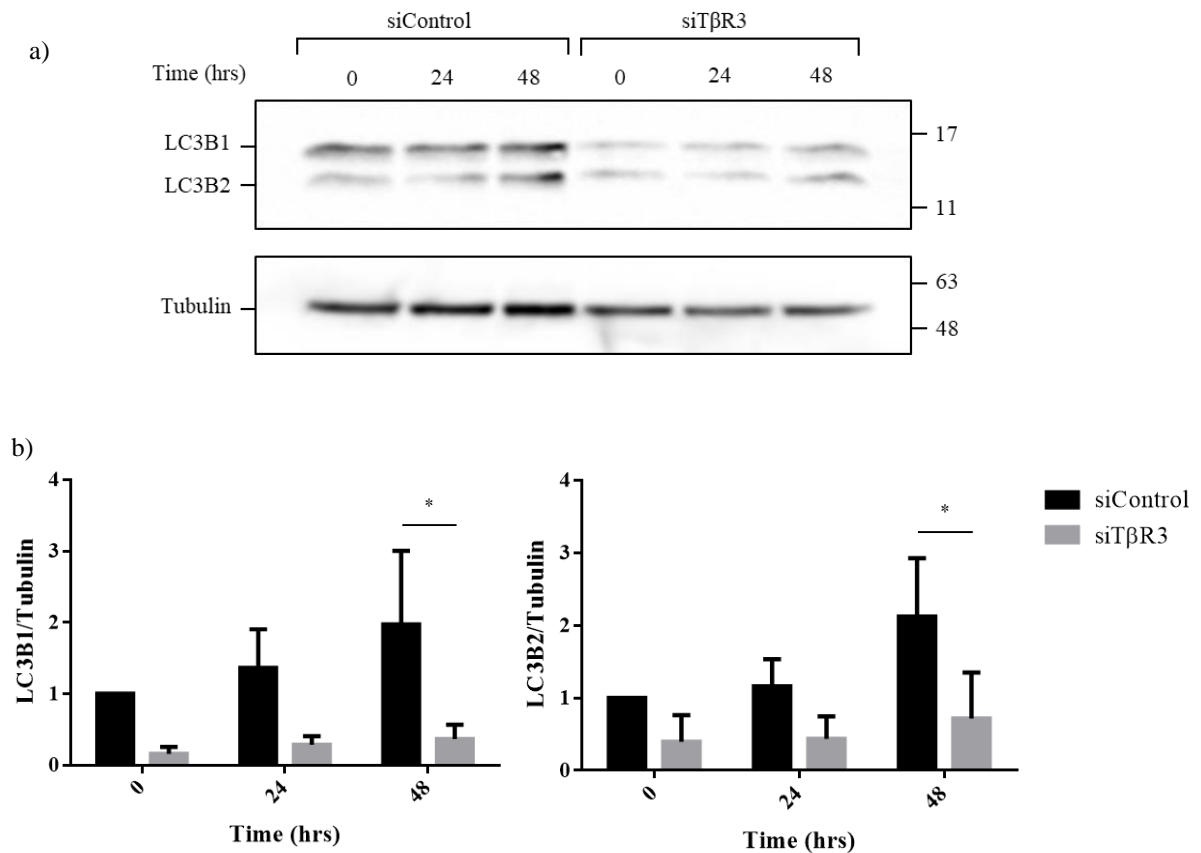


Figure 3.11 LC3B expression in H1299 cells following TβR3 knockdown

a) H1299 cells were transfected with 12.5 nM siTβR3 or siControl for 48 hours, serum-starved overnight, and treated with 250 pM TGFβ. Cell lysates were then subjected to western blotting for LC3B or tubulin (loading control).

b) Three separate experiments were carried out as described in panel a. LC3B1 and LC3B2 were imaged and quantitated using the BioRad QuantityOne software. (Two-way ANOVA; Mean ± SD; N=3; Tukey's post-hoc *p<0.05)

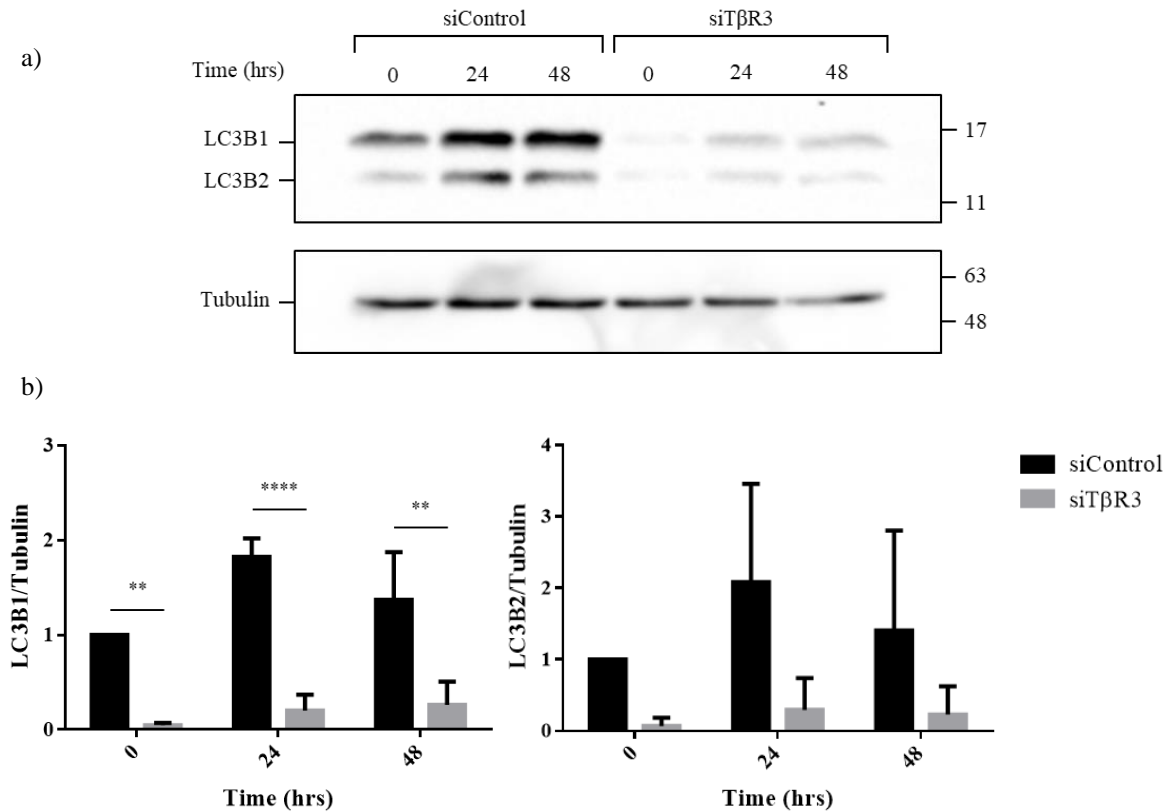


Figure 3.12 LC3B expression in A549 cells following TβR3 knockdown

a) A549 cells were transfected with 12.5 nM siTβR3 or siControl for 48 hours, serum-starved overnight, and treated with 250 pM TGFβ. Cell lysates were then subjected to western blotting for LC3B or tubulin (loading control).

b) Three separate experiments were carried out as described in panel a. LC3B1 and LC3B2 were imaged and quantitated using the BioRad QuantityOne software. (Two-way ANOVA; Mean ± SD; N=3; Tukey's post-hoc **p<0.01, ****p<0.0001)

3.3 Cell migration and invasion in the absence of T β R3

Since cellular EMT was reduced in both A549 and H1299 cells following T β R3 knockdown, it was expected that the invasive potential of these cells would correspondingly be reduced. Transwell assays were coated with Matrigel to measure H1299 cell invasion. Following seeding and a 24-hour incubation period, cellular invasion through Matrigel was significantly decreased in T β R3 knockdown cells when compared to control cells (**Figure 3.13**).

We next sought to determine whether the role of T β R3 in TGF β signaling and cadherin shift could also reduce phenotypic changes in cell migration. Cell migration was investigated using transwell assays. Contrary to my expectations, A549 and H1299 cells exhibited a significantly greater migratory ability following T β R3 knockdown (**Figure 3.14**). Additionally, a greater number of H1299 cells migrated when compared to A549 cells. Since H1299 cells had previously metastasized to the lymph node, they may be more mesenchymal than A549 cells and possess a greater migratory potential.

The diametrically opposite effect of T β R3 silencing on cell migration vs. invasion suggested that a complex interplay of gene expression could be regulating effects. I therefore assessed this via microarray analysis.

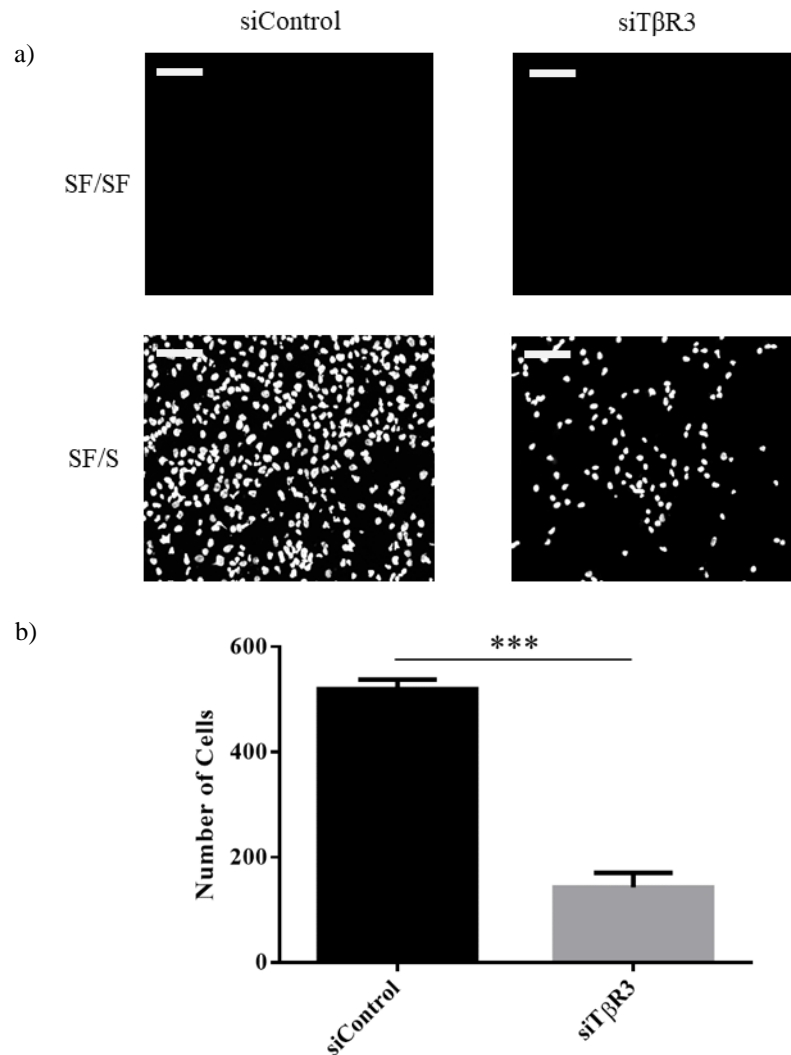


Figure 3.13 The number of H1299 cells that invaded through Matrigel following TβR3 knockdown

(a) H1299 cells were transfected with 12.5 nM siTβR3 or siControl, incubated for 48 hours, and serum-starved for 4 hours. Following trypsinization, 50,000 cells were seeded into Transwell chambers (24-well, 8 μm pores) coated with 50 μL Matrigel (0.9 μg/μL) for 30 mins at 37°C. Media containing 0.2% FBS (SF) was placed in the upper chamber, and either 0.2% or 10% FBS (S) in the lower chamber. Following 24 hours of incubation at 37°C, the cells were fixed with 4% PFA, permeabilized with 0.25% Triton X-100, and stained using DAPI. Scale bar = 100 μm.

(b) The number of cells that migrated through the filter was counted using ImageJ using 5 representative fields per cover slip and graphed. (Unpaired t-test; Mean ± SEM; N=3; ***p<0.001)

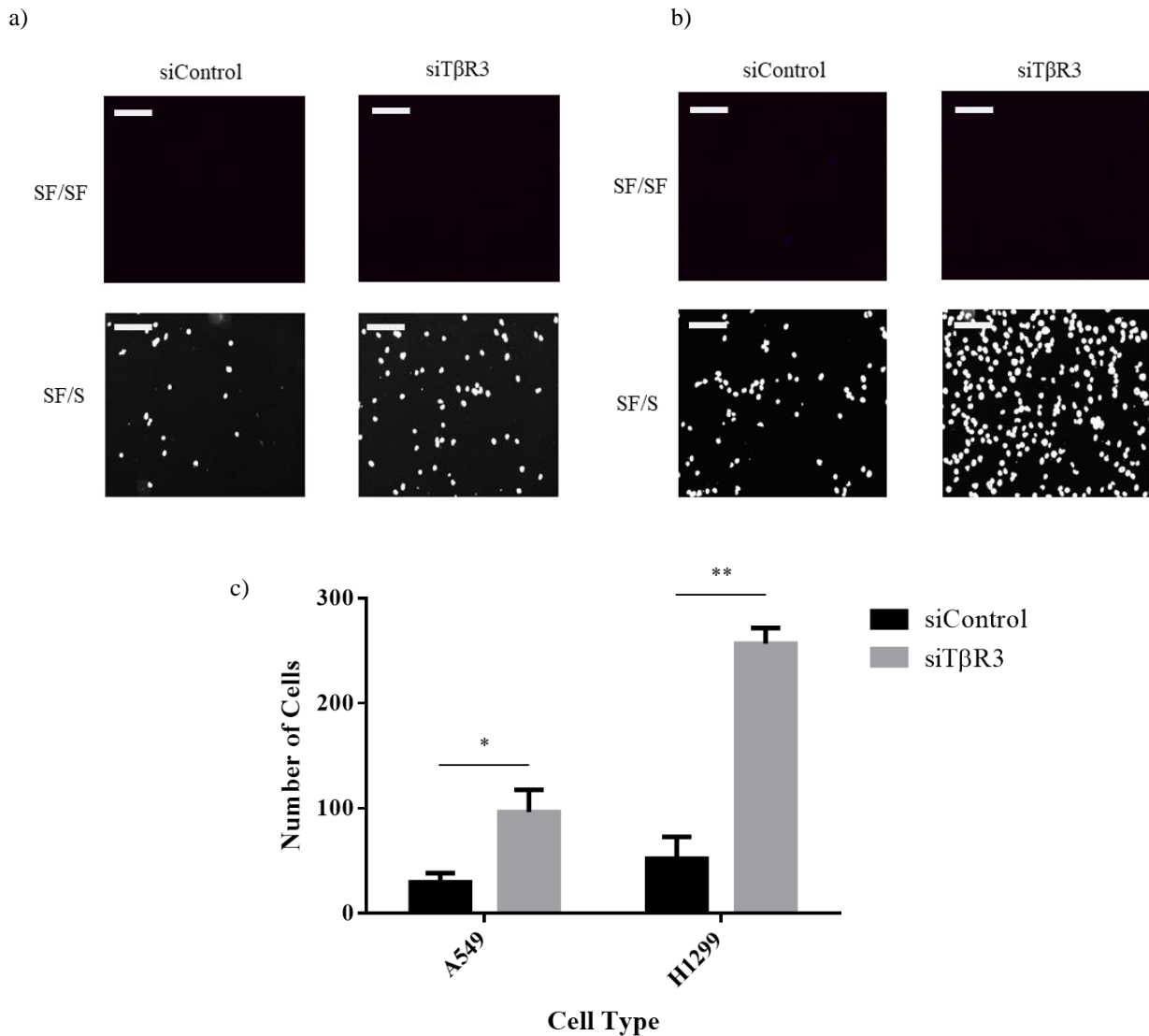


Figure 3.14 The number of A549 and H1299 cells that migrated following TβR3 knockdown

A549 (a) or H1299 (b) cells were transfected with 12.5 nM siTβR3 or siControl, incubated for 48 hours, and serum-starved for 4 hours. Following trypsinization, 50,000 cells were seeded into Transwell chambers (24-well, 8 μm pores). Media containing 0.2% FBS (SF) was placed in the upper chamber, and either 0.2% (SF) or 10% FBS (S) in the lower chamber. Following 24 hours of incubation at 37°C, the cells were fixed with 4% PFA, permeabilized with 0.25% Triton X-100, and stained using DAPI. Scale bar = 100 μm.

c) The number of migrated cells was counted using ImageJ using 5 representative fields per cover slip and graphed. (Unpaired t-test; Mean ± SEM; N=3; ***p<0.001)

3.4 Changes in mRNA expression

3.4.1 Microarray Analysis

The disconnect between cellular migration and invasion following T β R3 knockdown motivated the assessment of gene transcription on a wider scale. RNA isolated from H1299 cells following T β R3 knockdown was then analyzed by microarray gene chip analyses (**Figure 3.15**). The most upregulated gene encoded matrix metalloproteinase 1 (MMP1), with cells expressing +7.59-fold more MMP1 mRNA following T β R3 knockdown when compared to control (**Figure 3.15a**). Notable genes of interest, including prickle planar cell polarity protein 1 (PRICKLE1, +3.98), hepatocyte growth factor receptor (MET, +3.43), and the notch receptor ligand jagged 1 (JAG1, +2.85), were also significantly upregulated. In addition to MMP1, MMP14 was the only other matrix metalloproteinase to exhibit significant alteration, with a fold-change of +1.78. Notably, the transcription of genes involved in TGF β signaling (Smad2, Smad4, Smad7) and EMT (E-cadherin, N-cadherin, Snail, Slug) did not demonstrate significant changes. Numerous genes involved in cell cycling and DNA replication were significantly downregulated, including cyclins E2 (CCNE2, -3.82), A2 (CCNA2, -3.00), and B2 (CCNB2, -2.53), in addition to various cell division cycle proteins (CDC25C, CDC45, CDCA2) and cyclin-dependent kinases (CDK1, CDK14). ZEB2, a Smad-binding transcriptional repressor of E-cadherin displayed a fold-change of -1.81, but curiously, the expression of its paralog, ZEB1, was unchanged. qPCR was employed to validate the accuracy of the microarray, which was confirmed as no significant change was seen between mRNA expression levels between the two techniques (**Figure 3.15b**).

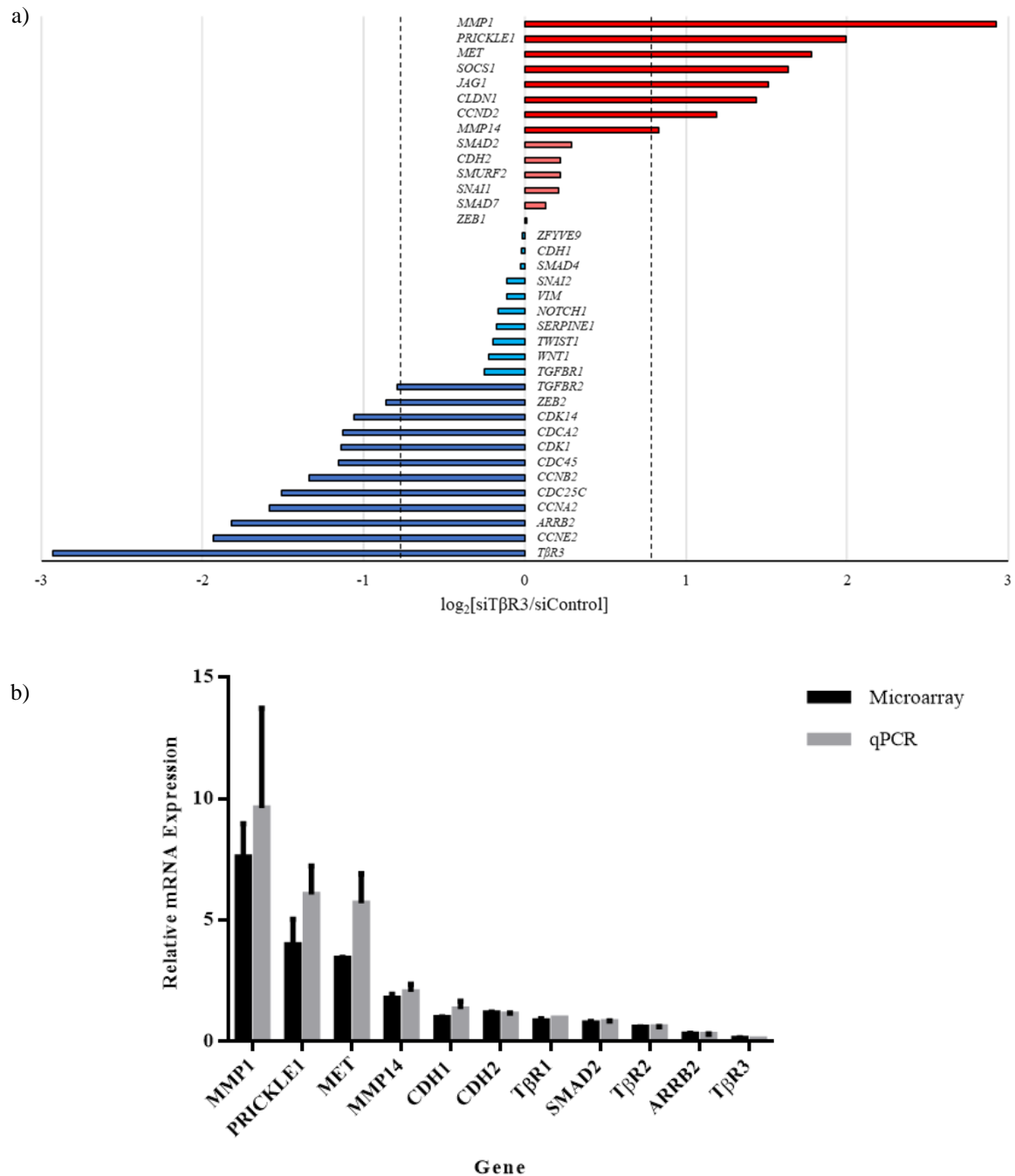


Figure 3.15 mRNA expression of selected genes from H1299 microarray analysis

Selected genes (most up- and downregulated genes, as well as the genes of TGFβ signaling members) from (a) Affymetrix Human GeneChip 2.0 Microarray mRNA analysis (N=2) and (b) validation by qPCR (Mean ± SEM; N=3) of H1299 cells transfected with 12.5 nM siTβR3 or siControl and incubated at 37°C for 48 hours. Black dashed line denotes ±1.75 fold-change. Total RNA was isolated and microarray technique was performed by London Regional Genomics Center.

Quantitative polymerase chain reactions were also performed on mRNA isolated from both A549 and H1299 cells following T β R3 knockdown and stimulation with TGF β . Measuring the mRNA expression of MMP1 and MMP14 would both validate microarray findings, as well as determine the effect of TGF β ligand on the upregulation of these genes. MMP1 mRNA expression was significantly upregulated in both cell lines, following T β R3 knockdown and incubation with exogenous TGF β (**Figure 3.16**). MMP14 also demonstrated a significant increase in both basal and stimulated mRNA expression. Furthermore, T β R3 knockdown and TGF β presence displayed an additive effect on the expression of MMP1 and MMP14 in A549 cells. However, this relationship was synergistic in nature in H1299 cells.

3.4.2 Gene Ontology Analysis

Using a subset of genes that exhibited a minimum microarray fold-change of +2.00 (**Figure 3.17a**) or -2.00 (**Figure 3.17b**), separate gene ontology analyses were performed using the PANTHER Classification System to reveal cellular processes. The group of up-regulated genes displayed greatest affinity for the pathways of cardiac right ventricle morphogenesis and regulation of chromatin binding, demonstrating fold enrichments of 48.86 and 38.68, respectively. Mirroring findings from the microarray analysis, pathways involving mitotic and DNA regulation emerged from the group of genes that were significantly down-regulated.

Interestingly, two relevant pathways were revealed when analyzing the cohort of up-regulated genes: Regulation of chemotaxis and regulation of locomotion. These pathways possessed fold enrichments of 10.37 and 3.98, respectively, and supported transwell migration results. Inquiry into specific genes involved in these pathways yielded MET

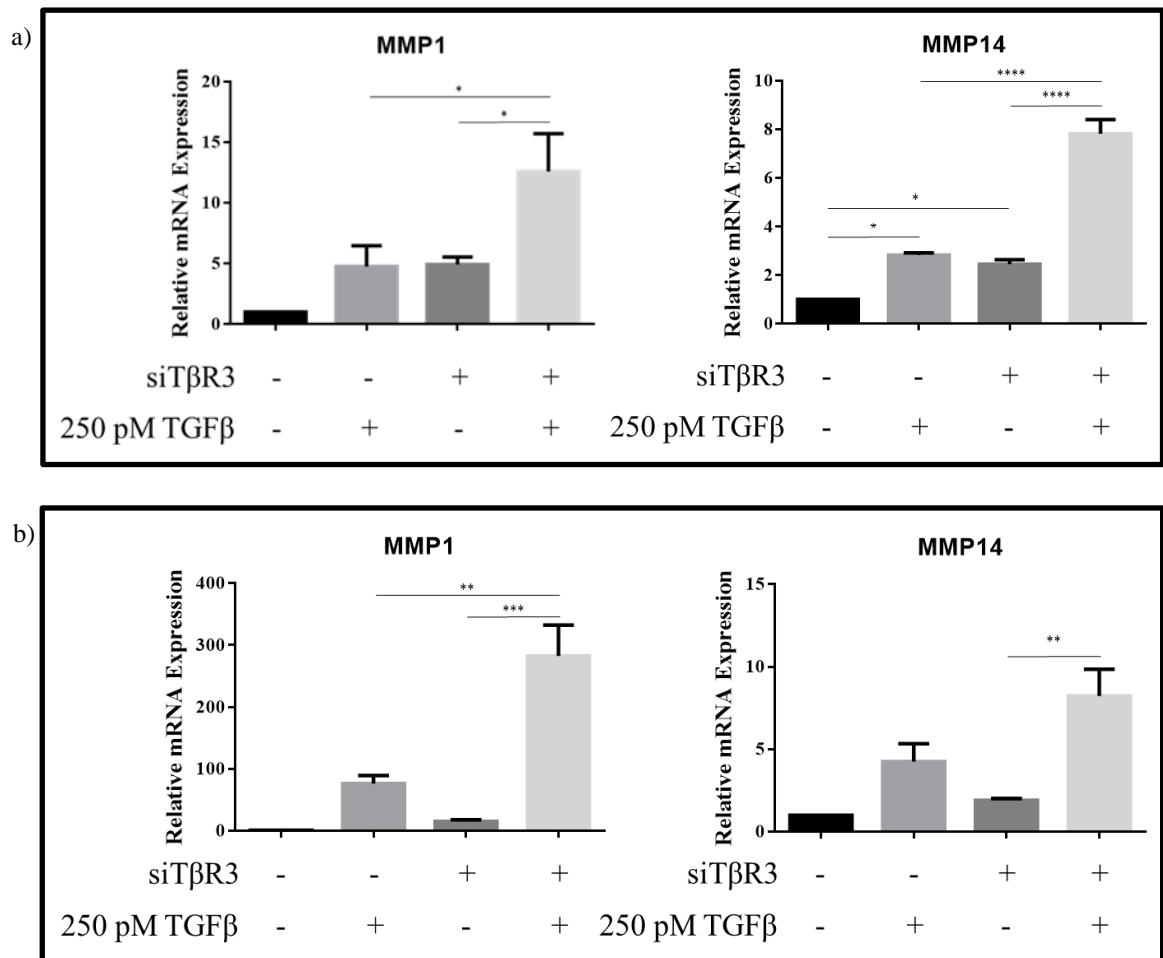
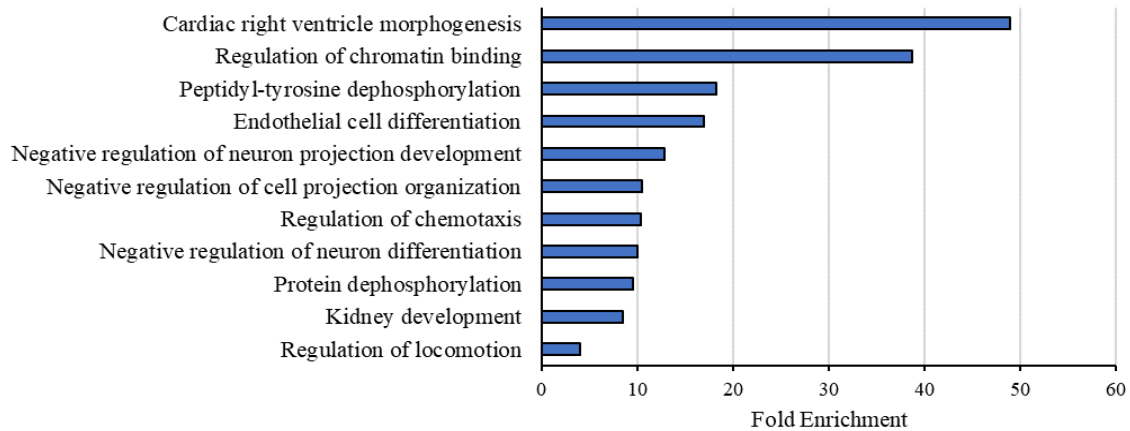


Figure 3.16 MMP1 and MMP14 mRNA expression following TβR3 knockdown

H1299 (a) and A549 (b) cells were transfected with 12.5 nM siTβR3 or siControl, incubated for 48 hours at 37°C, and serum-starved overnight. Cells were then treated with 250 pM TGFβ for 24 hours and total RNA was isolated. qPCR was carried out for MMP1 or MMP14. (Two-way ANOVA; +/- SEM; N=3; *p<0.05, **p<0.01, ***p<0.001, ****p<0.0001)

a)



b)

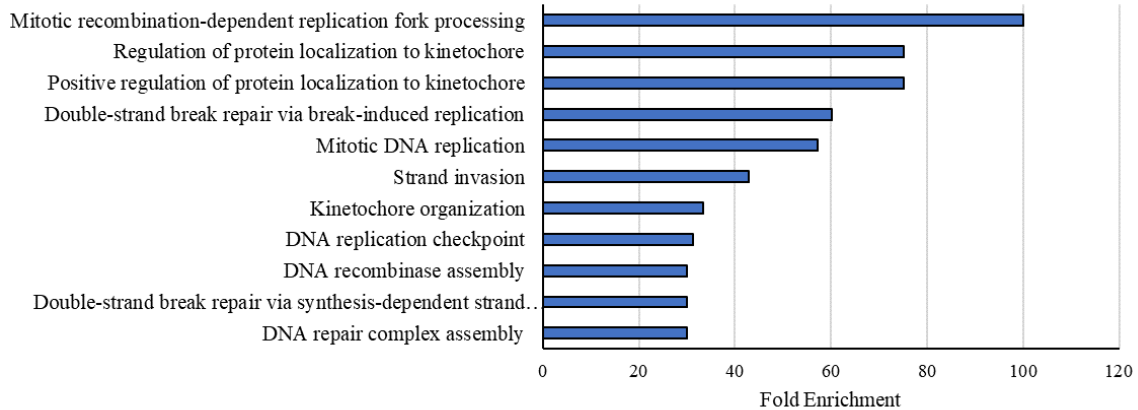


Figure 3.17 Gene ontology analysis of microarray mRNA expression

Pathways involving genes that exhibited a fold-change of +2.00 or greater (a), and -2.00 or less (b) as determined by microarray analysis of H1299 cells.

being involved in both regulation of chemotaxis and locomotion, while JAG1 is important in only the regulation of locomotion (**Figure 3.18; Table 3.1; Table 3.2**).

In this thesis, my results have demonstrated that the knockdown of T β R3 did not alter the phosphorylation of Smad2 in response to a gradient of TGF β concentrations, nor over time. Additionally, TGF β -dependent transcription was altered following T β R3 silencing, and cadherin expression was suppressed, along with LC3B expression, in both A549 and H1299 cells. Phenotypically, a greater number of cells migrated through Transwell assays in the absence of T β R3, while fewer cells invaded through a Matrigel plug. Finally, Microarray and qPCR analyses revealed the upregulation of MMP1 and MMP14, while gene ontology analysis reported the upregulation of genes involved in the regulation of chemotaxis and locomotion.

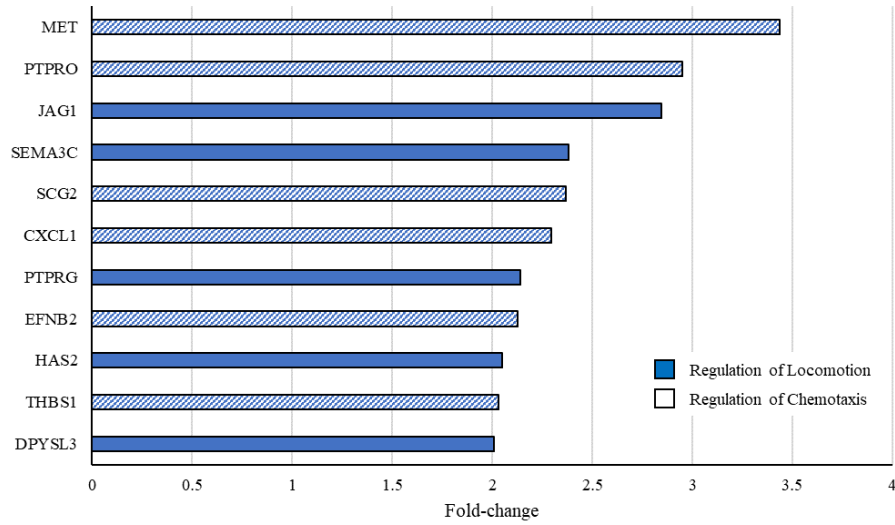


Figure 3.18 Specific upregulated genes that regulate locomotion and chemotaxis

Fold-change of genetic hits involved in chemotactic and locomotion pathways reported in gene ontology analysis.

Table 3.1 Regulation of Chemotaxis

<u>Gene</u>	<u>Protein</u>	<u>Average Microarray Fold-change</u>
THBS1	Thrombospondin-1	+2.03
SCG2	Secretogranin-2	+2.37
PTPRO	Receptor-type tyrosine-protein phosphatase O	+2.95
EFNB2	Ephrin-B2	+2.13
CXCL1	Growth-regulated alpha protein	+2.30
MET	Hepatocyte growth factor receptor	+3.43

Table 3.2 Regulation of Locomotion (including above)

<u>Gene</u>	<u>Protein</u>	<u>Microarray Fold-change</u>
DPYSL3	Dyhydropyrimidinase-related protein 3	+2.00
PTPRG	Receptor-type tyrosine-protein phosphatase gamma	+2.14
HAS2	Hyaluronan synthase 2	+2.05
JAG1	Jagged-1	+2.85
SEMA3C	Semaphorin-3C	+2.38

Discussion

4 Discussion

4.1 TGF β -dependent Smad2 signaling after knockdown of T β R3

Despite previous studies that demonstrated the role of T β R3 modulating TGF β signaling (**Figure 1.5**), neither H1299 nor A549 cells exhibited a change in relative Smad2 phosphorylation in response to a gradient of TGF β ligand (**Figures 3.3, 3.4**). Thus, T β R3 silencing may not alter the ability of T β R2 to associate with the TGF β ligand. Additionally, the knockdown of T β R3 was predicted to induce a faster return to basal Smad2 phosphorylation as measured by a washout time-course (**Figures 3.5, 3.6**). However, the relative phosphorylation of Smad2 following TGF β washout was not significantly different when comparing T β R3 knockdown to control in A549 or H1299 cells.

Interestingly, when investigating Smad2 phosphorylation in H1299 cells over time, a reduction in the expression of Smad2 was seen in both the presence and absence of TGF β ligand when compared to control (**Figure 3.5**). A reduction in Smad2 protein in H1299 suggests T β R3 expression may protect Smad2 linker regions from phosphorylation and downstream degradative pathways. Erk1/2 is active in phosphorylating serine residues in the linker region of Smad2 (Xu et al., 2012), which recruits E3 ubiquitin ligases to ubiquitinate Smad2 and promote proteasomal degradation. MMP14 has been implicated in activating Erk1/2 through the MAPK signaling cascade (Cepeda et al., 2017). An increased MMP14 expression following T β R3 silencing may therefore facilitate Erk1/2 activation, Smad2 linker phosphorylation, and subsequent degradation. Additionally, PI3K signaling has been shown to modulate Smad2 degradation. Yu et al. (2015) demonstrated that PI3K phosphorylation of specific tyrosine residues of the Smad2 linker region recruits ubiquitin

ligase Nedd4L. Thus, although the fraction of total Smad2 that is phosphorylated remains unchanged in response to T β R3 silencing, the reduction in absolute Smad2 phosphorylation may suppress downstream TGF β signaling and functional processes. Furthermore, T β R3 was more highly expressed in H1299 cells than in A549 cells, so protein knockdown may have had a more significant physiological impact in H1299 cells than in A549. Thus, silencing of T β R3 in H1299 cells may be more impactful on Smad2 expression than in A549 cells. As such, a knockdown of this receptor may have a greater impact on Smad-dependent TGF β signaling in H1299 cells by reducing absolute Smad2 phosphorylation through suppressed Smad2 expression, rather than by regulating kinase activity.

Contrary to my predictions, these results support the null hypothesis that the relative Smad2 phosphorylation level was not altered following T β R3 silencing. However, a reduction in Smad2 protein via linker phosphorylation and degradation in H1299 cells may hinder absolute Smad2 phosphorylation and suppress TGF β signaling. This finding supports my hypothesis, yet through the modulation of Smad2 expression rather than altering Smad2 phosphorylation.

4.2 TGF β -dependent EMT marker analysis

First, steady-state mRNA expression of TGF β responsive genes assessed transcriptional changes in A549 and H1299 cells following T β R3 silencing. Notably, T β R3 silencing in A549 cells prevented a significant increase in SNAI1 expression as was seen in control cells, and induced a significant increase in Smad7 expression, in response to TGF β in A549 cells (**Figure 3.7b**), suggesting that T β R3 silencing regulates transcription of different genes in different ways. However, in H1299 cells, a significant increase was seen in SNAI1 in T β R3 silenced cells treated with TGF β (**Figure 3.7a**). Thus, T β R3 silencing exhibits

differential regulation of transcriptional response to TGF β in a cell specific manner. Since mRNA expression is altered in both cell lines, together with unchanged TGF β -dependent Smad2 phosphorylation, it can be concluded that both cell lines retain intact TGF β signaling cascades despite T β R3 silencing.

Interestingly, differential TGF β response holds true for the CDH1 gene (E-cadherin). When examining mRNA expression of EMT markers, a significant increase in E-cadherin expression in A549 but not H1299 cells suggests T β R3 silencing shifts the cellular phenotype to a more epithelial state in certain cell contexts (**Figure 3.8**). A comparative increase in E-cadherin protein expression suggests a link between transcriptional and translational or degradative regulation of E-cadherin by T β R3 (**Figures 3.9, 3.10**). Therefore, silencing T β R3 enhances E-cadherin steady-state mRNA levels, which results in increased E-cadherin protein generated by functional translational machinery. In addition to greater basal expression, E-cadherin responds to TGF β in a traditional manner, with both mRNA and protein expression decreasing in response to TGF β , following canonical EMT progression simply from a more epithelial baseline.

Interestingly, A549 cells expressed more E-cadherin protein than H1299 cells (**Figure 3.9, 3.10**). While A549 cells were removed from an adenocarcinoma primary tumor, localized in the lung, H1299 cells were excised from lymph node (Giard et al., 1973; Giaccone et al., 1992). Thus, H1299 cells have previously undergone metastatic processes, and may not be as epithelial as A549 cells. As a result, A549 cells may display changes in phenotypical EMT markers more clearly than H1299 cells.

Similar changes in the expression of both E-cadherin protein and mRNA suggests T β R3 primarily influences E-cadherin expression on a transcriptional level, and that downstream protein levels are adjusted accordingly. The expression of E- and N-cadherin is tightly regulated through separate and distinct processes. Since E-cadherin expression is suppressed by transcription factors including Zeb1, Zeb2, Snail, and Slug, a reduction in repressor protein expression may increase the basal and TGF β -induced expression of E-cadherin. The transcription factor ZEB2 represses the transcription of E-cadherin in response to TGF β signaling by binding the promoter region of CDH1 (Peinado et al., 2007). As observed by microarray analysis, the mRNA expression of ZEB2 was reduced following T β R3 silencing (**Figure 3.15a**). Mining of microarray data for microRNAs that repress E-cadherin transcription directly, or indirectly through transcription factors, yielded no significant change in expression (**Appendix Table 5**). Future studies investigating protein expression of repressive transcription factors may elucidate a mechanism by which T β R3 influences E-Cadherin transcription.

Autophagy processes have been linked to EMT and E-cadherin expression (Alizadeh et al., 2018; Dash et al., 2018). In support of a suppressed epithelial-to-mesenchymal transition, and increased expression of E-cadherin, LC3B expression was significantly reduced following T β R3 silencing (**Figures 3.11, 3.12**). Furthermore, the general reduction in LC3B expression, rather than the inhibition of LC3B1 cleavage to LC3B2, suggests that T β R3 silencing has an important upstream regulatory role in autophagy, independent of Atg4 cleavage of LC3B1 specifically. LC3B mRNA expression has been linked with Erk1/2 activation, demonstrating a regulatory pathway that is following atypical TGF β signaling (Kim et al., 2014). Since Pang et al. (2016) demonstrated that autophagosome

formation was necessary to degrade E-cadherin, a broad downregulation of LC3B may suppress this degradation pathway, leading to the increase in E-cadherin protein expression exhibited after T β R3 silencing.

From this, the influence of T β R3 on E-cadherin expression may be two-fold. My results showing increased E-cadherin mRNA expression following T β R3 knockdown, in conjunction with a reduction in the formation of autophagosomes, which have been shown to degrade E-cadherin (Pang et al., 2016), may result in elevated E-cadherin levels. However, my observations assessing the relationship between N-cadherin mRNA and protein expression was weaker. In A549 cells, N-cadherin mRNA was significantly increased in T β R3 silenced conditions when treated with TGF β , equal to or greater than expression in control cells (**Figure 3.8**). However, a significant increase in N-cadherin mRNA expression was observed in T β R3 silenced H1299 cells treated with TGF β , which was not seen in control cells. Together, these results demonstrate an inconsistency between transcriptional regulation of T β R3 with respect to specific genes and between cell lines. In stark contrast, N-cadherin protein expression remained consistent between the cell lines, with T β R3 silencing resulted in reduced TGF β -dependent induction (**Figures 3.9, 3.10**). A clear disconnect is between N-cadherin mRNA and protein expression suggests T β R3 may be involved in modulating N-cadherin translation or degradation.

Although the transcriptional regulation of E-cadherin is well established, the characterization of N-cadherin control is unclear. A study by Alexander et al. (2006) found that the nuclear accumulation of transcription factor Twist1 resulted in its association with an E-box element in the promoter region of CDH2, the gene encoding N-cadherin, and enhanced its transcription. Thus, Twist1 is not only an important regulator of E-cadherin

repression, but also induces N-cadherin expression. However, Twist1 mRNA expression was not altered following T β R3 silencing and the role of other EMT-regulating transcription factors like Snail, Slug, Zeb1, and Zeb2, in N-cadherin regulation is unknown at this time.

Interestingly, Cardenas et al. (2014) demonstrated that TGF β signaling facilitates global changes in DNA methylation during EMT. TGF β -dependent expression and activity of DNA methyltransferases (DNMT) has been shown to alter mRNA expression of genes associated with EMT, including COL1A1. Additionally, the methylation of histone H3 has been implicated in repressing the transcription of CDH1 (Cao et al., 2008). Furthermore, the pattern of DNA methylation is reversed following withdrawal of TGF β ligand (Cardenas et al., 2014). Thus, Smad-independent TGF β signaling may influence N-cadherin mRNA expression through altered DNA methylation and would be an interesting future study.

Recently, regulation of N-cadherin protein has also been linked to PI3K/PKC ζ /mTOR signaling pathway, independent from transcriptional changes (Palma-Nicolas & Lopez-Colome, 2013). Furthermore, Twist1 expression is transcriptionally regulated by PI3K activity, which suggests an overarching pathway that regulates N-cadherin transcription and translation through separate downstream events (Hao et al., 2012). Furthermore, N-cadherin protein can be targeted for proteolysis via plasmin and matrix metalloproteinase activity (Paradies & Grunwald, 1993). A study by Takino et al. (2014) showed that MMP14 expression reduces N-cadherin adhesion, and Covington et al. (2006) have also established that MMP14 expression is involved in N-cadherin cleavage. Therefore, opposing roles of PI3K in promoting N-cadherin translation, and upregulated MMP expression in degrading

N-cadherin, may result in unaltered N-cadherin protein expression in response to TGF β despite significantly increased mRNA levels.

While studies investigating N-cadherin mRNA and protein expression yielded significant differences in both cell lines, E-cadherin only exhibited significant changes in A549 cells at the mRNA level. Thus, T β R3 silencing may have a greater influence on the expression of N-cadherin than E-cadherin. Additionally, E-cadherin protein expression may be so tightly regulated that altering mRNA levels by knocking down T β R3 may not result in wide-spread phenotypical changes.

Prickle1, which encodes Prickle Planar Cell Polarity Protein 1, has been implicated in β -catenin-independent Wnt signaling (Daulat et al., 2012). Prickle1 is a homolog of planar cell polarity (PCP) proteins, which include the traditional Wnt signaling components of Frizzled and Dishevelled. PCPs, including Prickle1, are essential for the maintenance of epithelial apical-basal polarity, a characteristic that serves as a phenotypical epithelial marker to assess EMT (Tao et al., 2009). Since the mRNA expression of Prickle1 was found by microarray to be highly upregulated in H1299 cells following T β R3 silencing, this observation supports the enhanced epithelial state of T β R3 knockdown cells demonstrated by increased E-cadherin expression (**Figure 3.15**). Additionally, Prickle1 homolog Prickle4 was found to be upregulated (+2.00) by microarray, as was tight junction protein Claudin1 (+2.70) (**Appendix Table 1**). While H1299 cells do not demonstrate a significant increase in E-cadherin expression, the upregulation of other epithelial markers may serve to maintain an epithelial phenotype.

Together, a potential reduction of E-cadherin proteasomal degradation through autophagic processes, the upregulation of E-cadherin mRNA, and the heightened expression of Prickle1, Prickle4, and Claudin1 all suggest the maintenance of an epithelial phenotype. The increase in epithelial marker expression corresponded with a reduction in the protein level of mesenchymal marker N-cadherin, further supporting my hypothesis. However, the mechanism behind these phenotypic changes remains unclear.

4.3 Interplay between cell migration and invasion

As predicted following a phenotypic shift towards a more epithelial state, fewer H1299 cells invaded through a Matrigel plug (**Figure 3.13**). However, the cellular migratory potential in H1299 cells did not match the inhibited invasion exhibited following T β R3 knockdown (**Figure 3.14**). Thus, T β R3 may influence these functional characteristics via different mechanisms of action.

Cellular invasive potential is dependent on two qualities: the ability of a cell to degrade the surrounding extracellular matrix, and its capacity to move after ECM degradation. For a tumor cell to successfully invade, both its degradative and motile capabilities must be heightened. In my studies, since fewer cells were able to invade Matrigel plugs yet exhibited an enhanced ability to migrate when unobstructed, the inability to invade could be a result of reduced degradative function. Interestingly, this is countered by an increase in MMP1 and MMP14 steady-state mRNA levels in both cell lines when T β R3 is silenced, both basally and in the presence of TGF β (**Figure 3.16**). However, despite greater mRNA expression, a lack of increased MMP protein expression would still not explain MMP functional activity, nor a reduction in cell invasion, as a maintenance of similar enzyme abundance should correspond with a similar number of cells that can invade.

However, a reduction in MMP activity would impede extracellular matrix degradation. Normally activated via proteolytic cleavage and inhibited by TIMPs, functionally active MMP levels may be regulated by T β R3. Thus, repression of invasion may be a result of reduced MMP activation by plasmin, furin, or other MMPs, or by an upregulation of TIMPs to aberrantly block MMP-dependent ECM degradation. However, no significant changes in mRNA expression were found by microarray with regards to proteins that regulate MMP activity (**Appendix Table 4**). Additionally, a downregulation of MMP protein expression despite increased mRNA levels could implicate T β R3 in a mechanistic pathway that controls MMP proteolysis. As a secreted enzyme (Lu et al, 2011), the ability of MMP1 to interact with its substrates and perform its functional ability relies upon an intact secretory pathway. Thus, impairment of the secretory pathway by which MMP1 is exocytosed could result in the suppression of extracellular matrix degradation, leaving a robust obstacle through which cells are unable to transverse.

Although MMP expression and activity are necessary for cells to invade, the ability of MMPs to carry out their functions are limited to the substrates with which they interact. Specifically, MMP1 and MMP14 are collagenases, primarily responsible for degrading collagens I, II, and III (Lu et al., 2011). Matrigel is mainly composed of laminin and collagen IV (Corning). As such, formation of a Matrigel plug may create a barrier that is unable to be degraded by upregulated MMP1 and MMP14. Interestingly, recent studies have demonstrated that MMP14 expression is inversely proportional to invasive potential, finding that cancer cells expressing lower levels of MMP14 invaded 3D cultures at a greater rate than cells expressing higher levels of MMP14 (Cepeda et al., 2016; Yamamoto et al., 2008). Thus, the overexpression of MMP14 following T β R3 silencing may actually

hinder the ability of H1299 cells to invade through a Matrigel plug. As such, matrix metalloproteinases may have additional roles in modulating cell signaling through the proteolysis of other non-extracellular membrane components.

T β R3 has also been shown to inhibit the NF- κ B signaling pathway (Criswell et al., 2008), which is known to facilitate MMP1 expression (Nguyen et al., 2015). Thus, the silencing of T β R3 could permit NF- κ B signaling to increase MMP1 transcription. Additionally, β -arrestin2 has also been implicated in NF- κ B regulation. β -arrestin2 is a scaffolding protein that can bind the cytoplasmic C-terminal tail of T β R3 and induce its internalization. Interestingly, following T β R3 silencing, the mRNA expression of β -arrestin2 was downregulated (**Figure 3.15**). In addition to its role as a scaffolding protein, β -arrestin2 is also involved in modulating intracellular signaling cascades. β -arrestin2 has been shown to inhibit Traf6 signaling and the activation of its downstream targets, including NF- κ B (Wang et al., 2006; Xiao et al., 2015). Since β -arrestin2 mRNA expression was reduced, inhibition of Traf6 may be absent resulting in the enhancement of NF- κ B signaling. Thus, T β R3 may promote β -arrestin2 expression, or protect it from degradation, as a way to suppress NF- κ B. In either case, the reduction in T β R3 and β -arrestin2 expression can enhance NF- κ B signaling and promote MMP1 upregulation.

However, MMP14 transcriptional regulation is not mediated by NF- κ B activation, but elevated MMP14 activity has been shown to promote Erk1/2 phosphorylation and downstream NF- κ B activation (Cepeda et al., 2017). From these observations, an increase in MMP14 expression may initiate cell signaling processes to upregulate its fellow collagenase MMP1. Importantly, MMP14 transcription relies upon a promoter region that is distinct from that of other MMPs, as it lacks a conventional TATA-box domain. A

binding site for SP-1 transcription factor is vital for MMP14 transcription and provides a unique mechanism of MMP14 regulation in which T β R3 may be involved (Lohi et al., 2000). Furthermore, a transcription factor involved in the repression of E-cadherin, Snail, has been shown to collaborate with SP-1 to induce the transcription of MMPs. Since T β R3 silencing significantly upregulated Snail expression (**Figure 3.7**), its interaction with SP-1 may act as a facilitator of increased MMP1 and MMP14 expression. Finally, microRNA expression of oligomers that are responsible for regulating MMP expression was found to remain unchanged following T β R3 silencing (**Appendix Table 3**).

In contrast to my results, Gordon et al. (2009) proposed a mechanism by which T β R3 expression suppressed cellular invasion through inhibiting Smad1 phosphorylation. Smad1 is a substrate of the activin type 2 receptor in the BMP signaling pathway which is modulated by T β R3. However, when BMP-2, -4, or -7 ligand expressions are increased, T β R3 expression is reduced and Smad1 may be phosphorylated. Smad1 then translocates to the nucleus and enhances the expression of MMP2, which degrades the extracellular matrix to promote invasion. Thus, T β R3 involvement in BMP signaling may play a role in receptor expression, MMP activity, and downstream regulation of EMT and invasion.

Contrary to a suppressed invasive capability of H1299 cells following T β R3 silencing, both H1299 and A549 knockdown cells exhibited greater migratory potential than control cells (**Figure 3.14**). Examination of microarray data and subsequent gene ontology analyses revealed two interesting genes that were upregulated and involved in the regulation of chemotaxis and locomotion: MET and JAG1 (**Figure 3.18**)

MET, also referred to as the hepatocyte growth factor receptor (HGFR), is a receptor tyrosine kinase that is an established promoter of cell migration (Piater et al., 2015). The binding of HGF to MET initiates a phosphorylation of tyrosine residues and initiates the Ras/MAPK signaling pathway, culminating in Erk1/2 phosphorylation and the promotion of migration (Gonzalez et al., 2017). Furthermore, the upregulation of both Met protein and mRNA expression have been implicated in cell migration and tumor budding (Bradley et al., 2016). JAG1 codes for the protein Jagged1, a ligand for Notch receptors which is upregulated in various late stage cancers (Dai et al., 2014). Upon ligand-receptor association, cleavage of the Notch intracellular domain (NICD) by γ -secretase induces nuclear accumulation and progression of prostate, breast, and head and neck cancers (Dai et al., 2014). As such, the elevated expression of Jagged1 and Notch receptors promotes Notch signaling and has been implicated in the promotion of cell migration (Tang et al., 2017). Together, the upregulation of MET and JAG1 following T β R3 silencing may influence the increase in cellular migratory potential.

Thus, the invasive and migratory potential of A549 and H1299 cells is clearly influenced by T β R3 silencing. However, the inconsistencies between migration and invasion suggests the interplay of additional, non-canonical TGF β signaling pathways.

4.4 Summary of observations

In this thesis, I observed that T β R3 knockdown did not alter relative Smad2 phosphorylation in response to TGF β in the H1299 or A549 NSCLC cell lines, although total Smad2 expression was insignificantly reduced in H1299 cells. When examining E-cadherin mRNA and protein levels, significant change was only found in the increased mRNA expression in A549 cells. However, in both cell lines, N-cadherin mRNA

expression was significantly increased in response to TGF β , but protein levels were unaffected. Correlating with suppressed EMT transition, autophagic marker LC3B expression was reduced in both A549 and H1299 cells following T β R3 knockdown. Functionally, the invasive potential of H1299 cells was reduced, while more A549 and H1299 cells migrated through transwell assays.

Together, these results suggest that epithelial to mesenchymal transition, cell migration, and cell invasion, may be altered by atypical TGF β signaling. These processes have been shown to be regulated via mechanisms involving the PI3K, MAPK, and NF- κ B pathways, which are each modulated by TGF β ligand in a Smad-independent manner. T β R3 expression may protect the integrity of the Smad signaling pathway and following receptor knockdown, cells may access non-canonical TGF β cascades. Activation of various pathways may serve a purpose in modulating downstream processes independently, and in suppressing canonical Smad signaling by phosphorylating Smad linker regions to facilitate ubiquitination and degradation. Clearly, T β R3 expression is involved in controlling multiple signaling pathways, and its specific functions in modulating EMT transition, cell migration, and cell invasion are complex.

4.5 Limitations and Future Directions

In this study, T β R3 was transiently reduced by siRNA, thus limiting the length of time cellular processes could be monitored before T β R3 expression was reacquired. Developing stable cell lines that expressed shRNA against T β R3 would allow for long-term experiments to be conducted. The use of CRISPR-Cas9 gene editing technologies could also permanently remove T β R3 from each cell line for future testing.

Reducing T β R3 in cells that highly express T β R3, such as H1299, is an effective way to reveal specific processes with which it may be involved. However, the efficiency of the knockdown may not be sufficient to cause physiological changes in the event that the reduced expression level of T β R3 remains sufficient to perform its normal roles. Furthermore, reducing protein levels in cell lines that have low levels of receptor may not uncover small changes in signaling potential. Therefore, future studies investigating the overexpression of T β R3 in cells that express low basal receptor levels would be beneficial to demonstrate specific functions in a direct way. Furthermore, overexpression of mutant T β R3 that alter their interaction with TGF β (other TGF β receptors) may shed light on the mechanism of this system.

The transition of A549 and H1299 cells from an epithelial state to a mesenchymal phenotype was investigated via the measurement of E-cadherin and N-cadherin expression at a protein and mRNA level. Although these proteins represent the gold-standard of EMT markers, the use of additional epithelial markers, including ZO-1 and cytokeratin; and the mesenchymal markers, vimentin and α -smooth muscle actin (α SMA), would further reinforce the cadherin shift demonstrated by E- and N-cadherin.

My research primarily examined the protein and mRNA expression of EMT markers in response to TGF β over time, but cellular morphology was not investigated. Next, it would be worthwhile to examine cytoskeletal organization of actin in response to TGF β . In epithelial cells, actin is normally structured in a cortical fashion (Thiery et al., 2002). However, during EMT, actin is rearranged to form stress fibers and promote a migratory phenotype (Thiery et al., 2002). Fluorescence microscopy using Phalloidin, a polymerized

actin stain, could be employed to investigate any morphological changes exhibited in cells following T β R3 knockdown.

Although LC3B expression was studied to determine a connection between T β R3, the autophagic processes, and EMT, further experiments examining T β R3 knockdown on other autophagic markers, such as Atg5, Atg7, Beclin1, or p62 should be conducted. Together with electron microscopic techniques to visualize the formation of autophagosomes, altered expression of these markers would hone in on specific autophagic stages that are influenced by T β R3.

Functional analysis of cell migration was limited to transwell assays, which measure the ability of a cell to sense a chemotactic agent and migrate across a physical barrier. Thus, only amoeboid, chemotactic motility was investigated and measured the number of cells that were able to migrate a pre-established distance. As a result, the total distance traveled, velocity, and direction by which the cells migrated was not determined. Therefore, the use of single-cell tracking technologies to measure these outputs may provide greater insight into the specific migratory processes that are altered by T β R3. Additionally, employing wound-healing assays would take cell-cell signaling and contact into account when measuring migrated distance as a physiologically relevant cancerous mass. Finally, the use of μ -Slide Chemotaxis (Ibidi) would test the chemotaxis of a migrating cell sheet through a channel, rather than single cells through a membrane, acting as a comprehensive measure of cell migration, taking all the above factors into consideration.

To investigate how MMP1 and MMP14 upregulation impact cellular invasion, a number of processes should be investigated. First, protein expression should be compared to the

steady-state mRNA expression of the MMPs to confirm an upregulation of MMP zymogen. Next, zymographic techniques should be performed to assess the activity of MMP1 and MMP14 in degrading appropriate substrates (Leber & Balkwill, 1997). Finally, when examining cellular invasion through a Transwell assay, establishing a barrier using collagen I-III may place cells in a more appropriate physiological context with regards to their MMP expression. Also, instead of using a plug, a hanging droplet apparatus may be used to measure cellular invasion out of a spheroid of cells and matrix as a pseudo-*in vivo* technique (Tung et al., 2011).

Quantitative polymerase chain reactions and microarray techniques compare the relative steady-state mRNA expression of various genes. However, these analyses do not reveal changes in gene transcription. Incorporating a sequence encoding a luciferase enzyme into the promoter region of genes of interest would clarify the mechanism by which T β R3 influences mRNA expression. Finally, investigating the involvement of T β R3 expression in non-canonical TGF β signaling processes would reveal novel functions of the accessory receptor previously solely associated with the TGF β cascade.

Despite these limitations, my results suggest that T β R3 has a distinct role in modulating EMT and cellular motility and will be of interest to the field of TGF β cancer biology.

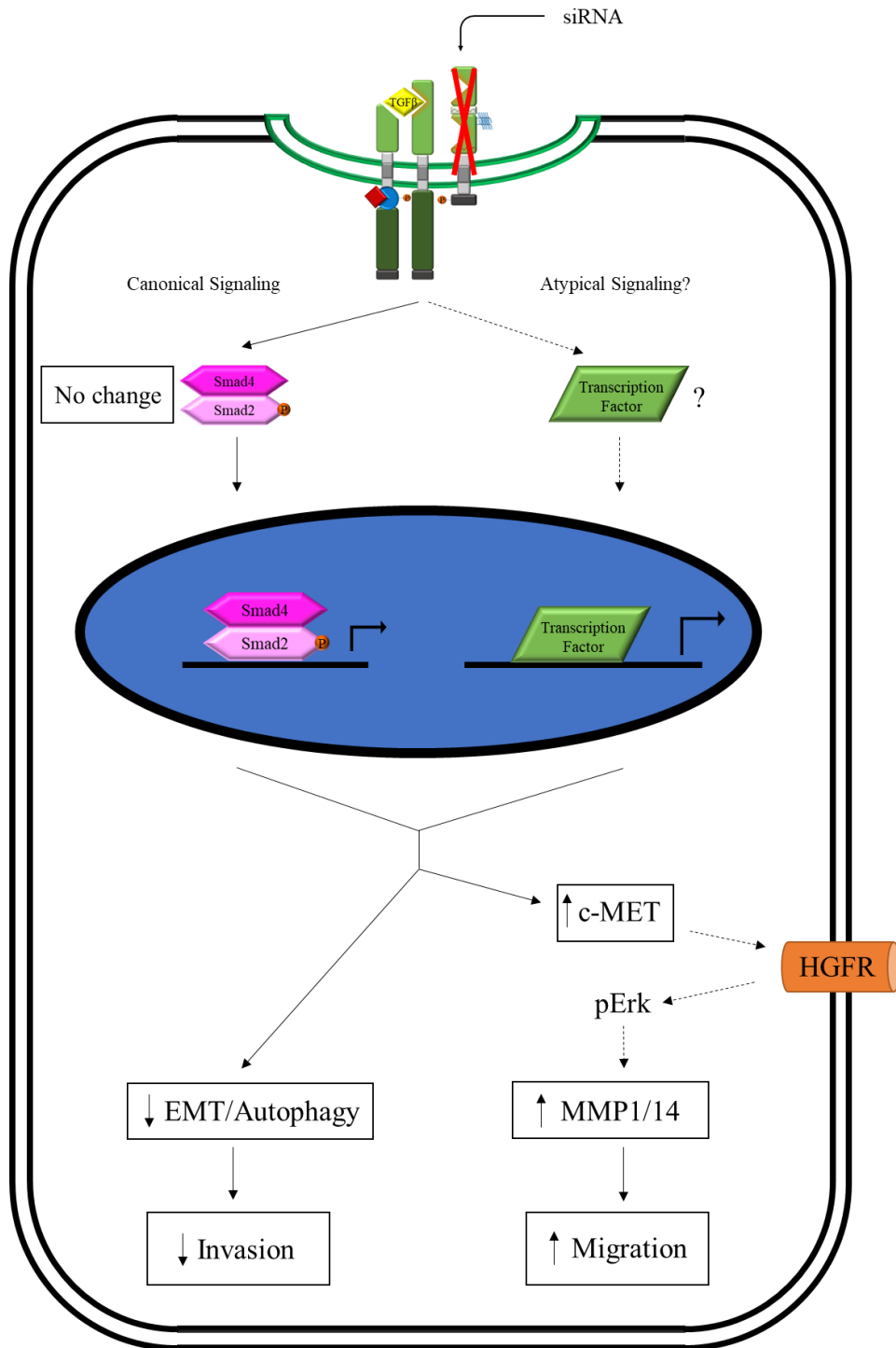


Figure 4.1 Proposed mechanism of TβR3 influence on cell migration and invasion

Black boxes signify results found in this thesis. Arrows demonstrate a sequence of processes, while dashed arrows suggest speculated mechanisms of action.

References

- Abba, M., Patil, N., & Allgayer, H. (2014). MicroRNAs in the regulation of MMPs and metastasis. *Cancers*, 6(2), 625–645.
- Akiyoshi, S., Inoue, H., Hanai, J., Kusanagi, K., Nemoto, N., Miyazono, K., & Kawabata, M. (1999). c-Ski acts as a transcriptional co-repressor in transforming growth factor-beta signaling through interaction with smads. *Journal of Biological Chemistry*, 274(49), 35269–35277.
- Alexander, N. R., Tran, N. L., Rekapally, H., Summers, C. E., Glackin, C., & Heimark, R. L. (2006). N-cadherin gene expression in prostate carcinoma is modulated by integrin-dependent nuclear translocation of Twist1. *Cancer Research*, 66(7), 3365–3369.
- Alizadeh, J., Glogowska, A., Thliveris, J., Kalantari, F., Shojaei, S., Hombach-Klonisch, S., ... Ghavami, S. (2018). Autophagy modulates transforming growth factor beta 1 induced epithelial to mesenchymal transition in non-small cell lung cancer cells. *Biochimica et Biophysica Acta (BBA) - Molecular Cell Research*, 1865(5), 749–768.
- Angadi, P. V., & Kale, A. D. (2015) Epithelial-mesenchymal transition – A fundamental mechanism in cancer progression: An overview. *Indian Journal of Health Sciences and Biomedical Research*, 8(2), 77–84.
- Apte, S. S., Fukai, N., Beier, D. R., & Olsen, B.R. (1997). The matrix metalloproteinase-14 (MMP-14) gene is structurally distinct from other MMP genes and is co-expressed with the TIMP-2 gene during mouse embryogenesis. *Journal of Biological Chemistry*, 272(41), 25511–25517.
- Attisano, L., Carcamo, J., Ventura, F., Weis, F. M., Massague, J., & Wrana, J. L. (1993). Identification of human activin and TGF beta type I receptors that form heteromeric kinase complexes with type II receptors. *Cell*, 75(4), 671–680.
- Baum, B., & Georgiou, M. (2011). Dynamics of adherens junctions in epithelial establishment, maintenance, and remodeling. *Journal of Cell Biology*, 192(6), 907–917.
- Bhowmick, N. A., Ghiassi, M., Bakin, A., Aakre, M., Lundquist, C. A., Engel, M. E. ... Moses, H. L. (2001). Transforming growth factor-beta1 mediates epithelial to mesenchymal transdifferentiation through a RhoA-dependent mechanism. *Molecular Biology of the Cell*, 12(1), 27–36.
- Blobe, G. C., Liu, X., Fang, S. J., How, T., & Lodish, H. F. (2001a). A novel mechanism for regulating transforming growth factor beta (TGF-beta) signaling. Functional modulation of type III TGF-beta receptor expression through interaction with the PDZ domain protein, GIPC. *Journal of Biological Chemistry*, 276(43), 39608–39617.

- Blobe, G. C., Schiemann, W. P., Pepin, M. C., Beauchemin, M., Moustakas, A., Lodish, H.F., & O'Connor-McCourt, M. D. (2001b). Functional roles for the cytoplasmic domain of the type III transforming growth factor beta receptor in regulating transforming growth factor beta signaling. *Journal of Biological Chemistry*, 276(26), 24627–24637.
- Bloom, G., Yang, I. V., Boulware, D., Kwong, K. Y., Coppola, D., Eschrich, S., ... Yeatman, T. J. (2004). Multi-platform, multi-site, microarray-based human tumor classification. *American Journal of Pathology*, 164(1), 9–16.
- Bradley, C. A., Dunne, P. D., Bingham, V., McQuaid, S., Khawaja, H., Craig, S., ... Van Schaeybroeck, S. (2016). Transcriptional upregulation of c-MET is associated with invasion and tumor budding in colorectal cancer. *Oncotarget*, 7(48), 78932–78945.
- Brew, K., & Nagase, H. (2010). The tissue inhibitors of metalloproteinases (TIMPs): an ancient family with structural and functional diversity. *Biochimica et Biophysica Acta (BBA) - Molecular Cell Research*, 1803(1), 55–71.
- Burrows, F. J., Derbyshire, E. J., Tazzari, P. L., Amlot, P., Gazdar, A. F., King, S. W., ... Thorpe, P. E. (1995). Up-regulation of endoglin on vascular endothelial cells in human solid tumors: implications for diagnosis and therapy. *Clinical Cancer Research*, 1(12), 1623–1634.
- Canadian Cancer Society's Advisory Committee on Cancer Statistics. (2017). *Canadian Cancer Statistics 2017*.
- Cao, Q., Yu, J., Dhanasekaran, S. M., Kim, J. H., Mani, R. S., Tomlins, S. A., ... Chinnaiyan, A. M. (2008). Repression of E-cadherin by the polycomb group protein EZH2 in cancer. *Oncogene*, 27(58), 7274–7284.
- Cardenas, H., Vieth, E., Lee, J., Segar, M., Liu, Y., Nephew, K. P., & Matei, D. (2014). TGF- β induces global changes in DNA methylation during the epithelial-to-mesenchymal transition in ovarian cancer cells. *Epigenetics*, 9(11), 1461–1472.
- Cepeda, M. A., Evered, C. L., Pelling, J. J. H., & Damjanovski, S. (2017). Inhibition of MT1-MMP proteolytic function and ERK1/2 signaling influences cell migration and invasion through changes in MMP-2 and MMP-9. *Journal of Cell Communication and Signaling*, 11, 167–179.
- Cepeda, M. A., Pelling, J. J. H., Evered, C. L., Williams, K. C., Freedman, Z., Stan, I., ... Damjanovski, S. (2016). Less is more: low expression of MT1-MMP is optimal to promote migration and tumorigenesis of breast cancer cells. *Molecular Cancer*, 15, 65.
- Cheifetz, S., Bellon, T., Cales, C., Vera, S., Bernabeu, C., Massague, J., & Letarte, M. (1992). Endoglin is a component of the transforming growth factor-beta receptor system in human endothelial cells. *Journal of Biological Chemistry*, 267(27), 19027–19030.

- Chen, W., Kirkbride, K. C., How, T., Nelson, C. D., Mo, J., Frederick, J. P., ... Blobel, G. C. (2003). Beta-arrestin 2 mediates endocytosis of type III TGF-beta receptor and down-regulation of its signaling. *Science*, *301*(5638), 1394–1397.
- Chun, T. H., Sabeh, F., Ota, I., Murphy, H., McDonagh, K. T., Holmbeck K., ... Weiss, S. J. (2004). MT1-MMP-dependent neovessel formation within the confines of the three-dimensional extracellular matrix. *Journal of Cell Biology*, *167*(4), 757–767.
- Covington, M. D., Burghardt, R. C., & Parrish, A. R. (2006). Ischemia-induced cleavage of cadherins in NRK cells requires MT1-MMP (MMP14). *American Journal of Physiology Renal Physiology*, *290*(1), 43–51.
- Covington, M. D., Burghardt, R. C., & Parrish, A. R. (2015). Ischemia-induced cleavage of cadherins in NRK cells requires MT1-MMP (MMP-14). *American Journal of Physiology-Renal Physiology*, *290*(1), 43–51.
- Criswell, T. L., Dumont, N., Barnett, J. V., & Arteaga, C. L. (2008). Knockdown of the Transforming Growth Factor-B Type III Receptor Impairs Motility and Invasion of Metastatic Cancer Cells. *Cancer Research*, *68*, 7304–7312.
- Dai, Y., Wilson, G., Huang, B., Peng, M., Teng, G., Zhang, D., ... Qiao, L. (2014). Silencing of Jagged1 inhibits cell growth and invasion in colorectal cancer. *Cell Death & Disease*, *5*(4), e1170.
- Dash, S., Sarashetti, P. M., Rajashekar, B., Chowdhury, R., & Mukherjee, S. (2018). TGF- β 2-induced EMT is dampened by inhibition of autophagy and TNF- α treatment. *Oncotarget*, *9*(5), 6433–6449.
- Daulat, A. M., Luu, O., Sing, A., Zhang, L., Wrana, J. L., McNeill, H., ... Angers, S. (2012). Mink1 regulates β -catenin-independent Wnt signaling via Prickle phosphorylation. *Molecular and Cellular Biology*, *32*(1), 173–185.
- de Caestecker, M. P., Piek, E., & Roberts, A. B. (2000). Role of transforming growth factor- β signaling in cancer. *Journal of the National Cancer Institute*, *92*(17), 1388–1402.
- Degenhardt, K., Mathew, R., Beaudoin, B., Bray, K., Anderson, D., Chen, G., ... White, E. (2006). Autophagy promotes tumor cell survival and restricts necrosis, inflammation, and tumorigenesis. *Cancer Cell*, *10*(1), 51–64.
- Deng, X., Bellis, S., Yan, Z., & Friedman, E. (1999). Differential responsiveness to autocrine and exogenous transforming growth factor (TGF) beta1 in cells with nonfunctional TGF-beta receptor type III. *Cell Growth & Differentiation*, *10*(1), 11–18.
- Di Guglielmo, G. M., Le Roy, C., Goodfellow, A. F., & Wrana, J. L. (2003). Distinct endocytic pathways regulate TGF-beta receptor signaling and turnover. *Nature Cell Biology*, *5*(5), 410–421.

- Docea, A. O., Mitrut, P., Grigore, D., Pirici, D., Calina, D. C., & Gofita, E. (2012). Immunohistochemical expression of TGF beta (TGF- β), TGF beta receptor 1 (TGFBR1), and Ki67 in intestinal variant of gastric adenocarcinomas. *Romanian Journal of Morphology and Embryology*, 53, 683–692.
- Dong, M., How, T., Kirkbride, K. C., Gordon, K. J., Lee, J. D., Hempel, N., ... Blobe, G. C. (2007). The type III TGF-beta receptor suppresses breast cancer progression. *Journal of Clinical Investigation*, 117(1), 206–217.
- Downward, J. (2004). PI 3-kinase, Akt, and cell survival. *Seminars in Cell and Developmental Biology*, 15(2), 177–182.
- Elliot, R. L., & Blobe, G. C. (2005). Role of transforming growth factor Beta in human cancer. *Journal of Clinical Oncology*, 23(9), 2078–2093.
- Esquela-Kerscher, A., & Slack, F. J. (2006). Oncomirs - microRNAs with a role in cancer. *Nature Reviews Cancer*, 6(4), 259–269.
- Finger, E. C., Lee, N. Y., You, H. J., & Blobe, G. C. (2008a). Endocytosis of the type III transforming growth factor- β (TGF- β) receptor through the clathrin-independent/lipid raft pathway regulates TGF- β signaling and receptor down-regulation. *Journal of Biological Chemistry*, 283(50), 34808–34818.
- Finger, E. C., Turley, R. S., Dong, M., How, T., Fields, T. A., & Blobe, G. C. (2008b). TbetaRIII suppresses non-small cell lung cancer invasiveness and tumorigenicity. *Carcinogenesis*, 28, 528–535.
- Flanders, K. C., Yang, Y. A., Herrmann, M., Chen, J., Mendoza, N., Mirza, A. M., & Wakefield, L. M. (2016). Quantitation of TGF-beta proteins in mouse tissues shows reciprocal changes in TGF-beta1 and TGF-beta3 in normal vs neoplastic mammary epithelium. *Oncotarget*, 7(25), 38164–38179.
- Fleming, N. I., Jorissen, R. N., Mouradov, D., Christie, M., Sakthianandeswaren, A., Palmieri, M. ... Sieber, O. M. (2013). SMAD2, SMAD3 and SMAD4 mutations in colorectal cancer. *Cancer Research*, 73(2), 725–735.
- Frantz, C., Stewart, K. M., & Weaver, V. M. (2010). The extracellular matrix at a glance. *Journal of Cell Science*, 123, 4195–4181.
- Fujita, Y., Krause, G., Scheffner, M., Zechner, D., Leddy, H. E., Behrens, J., ... Birchmeier, W. (2002). Hakai, a c-Cbl-like protein, ubiquitinates and induces endocytosis of the E-cadherin complex. *Nature Cell Biology*, 4(3), 222–231.
- Gatza, C. E., Oh, S. Y., & Blobe, G. C. (2010). Roles for the type III TGF-beta receptor in human cancer. *Cell Signaling*, 22(8), 1163–1174.

- Giaccone, G., Battey, J., Gazdar, A. F., Oie, H., Draoui, M., & Moody, T. W. (1992). Neuromedin B is present in lung cancer cell lines. *Cancer Research*, *52*(9), 2732–2736.
- Giard, D. J., Aaronson, S. A., Todaro, G. J., Arnstein, P., Kersey, J. H., Dosik, H., & Parks, W. P. (1973). In vitro cultivation of human tumors: establishment of cell lines derived from a series of solid tumors. *Journal of the National Cancer Institute*, *51*(5), 1417–1423.
- Gonzalez, M. N., de Mello, W., Butler-Browne, G. S., Silva-Barbosa, S. D., Mouly, V., Savino, W., & Riederer, I. (2017). HGF potentiates extracellular matrix-driven migration of human myoblasts: involvement of matrix metalloproteinases and MAPK/ERK pathway. *Skeletal Muscle*, *7*, 20.
- Gordon, K. J., Kirkbride, K. C., How, T., & Blobe, G. C. (2009). Bone morphogenic proteins induce pancreatic cancer cell invasiveness through a Smad1-dependent mechanism that involves matrix metalloproteinase-2. *Carcinogenesis*, *30*(2), 238–248.
- Grande, M., Franzen, A., Karlsson, J. O., Ericson, L. E., Heldin, N. E., & Nilsson, M. (2002). Transforming growth factor-beta and epidermal growth factor synergistically stimulate epithelial to mesenchymal transition (EMT) through a MEK-dependent mechanism in primary culture pig thyrocytes. *Journal of Cell Science*, *115*(22), 4227–4236.
- Gunaratne, A., & Di Guglielmo, G. M. (2013). Par6 is phosphorylated by aPKC to facilitate EMT. *Cell Adhesion & Migration*, *7*(4), 357–361.
- Hao, L., Ha, J. R., Kuzel, P., Garcia, E., & Persad, S. (2012). Cadherin switch from E- to N-cadherin in melanoma progression is regulated by the PI3K/PTEN pathway through Twist and Snail. *British Journal of Dermatology*, *166*(6), 1184–1197.
- Harris, T. J., & Tepass, U. (2010). Adherens junctions: from molecules to morphogenesis. *Nature Reviews Molecular Cell Biology*, *11*(7), 502–514.
- Hempel, N., How, T., Dong, M., Murphy, S. K., Fields, T. A., & Blobe, G. C. (2007). Loss of betaglycan expression in ovarian cancer: role in motility and invasion. *Cancer Research*, *67*(11), 5231–5238.
- Huang, T., Schor, S. L., & Hinck, A. P. (2014). Biological differences between TGF- β 1 and TGF β -3 correlate with differences in the rigidity and arrangement of their component monomers. *Biochemistry*, *53*(36), 5737–5749.
- Huang, C. H., Yang, W. H., Chang, S. Y., Tai, S. K., Tzeng, C. H., Kao, J. Y., ... Yang, M. H. (2009). Regulation of membrane-type 4 matrix metalloproteinase by SLUG contributes to hypoxia-mediated metastasis. *Neoplasia*, *11*(12), 1371–1382.

- Hynes, R. O., & Naba, A. (2012). Overview of the matrisome--an inventory of extracellular matrix constituents and functions. *Cold Spring Harbor Perspectives in Biology*, 4(1).
- Jackson, H. W., Defamie, V., Waterhouse, P., & Khokha, R. (2017). TIMPs: versatile extracellular regulators in cancer. *Nature Reviews Cancer*, 17(1), 38–53.
- Jiang, Y., Jiao, Y., Liu, Y., Zhang, Z., Wang, Z., Li, Y., ... Wang, D. (2018). Sinomenine hydrochloride inhibits the metastasis of human glioblastoma cells by suppressing the expression of matrix metalloproteinase-2/-9 and reversing the endogenous and exogenous epithelial-mesenchymal transition. *International Journal of Molecular Science*, 19, 844.
- Kaartinen, V., Haataja, L., Nagy, A., Heisterkamp, N., & Groffen, J. (2002). TGFbeta3-induced activation of RhoA/Rho-kinase pathway is necessary but not sufficient for epithelia-mesenchymal transdifferentiation: implications for palatogenesis. *International Journal of Molecular Medicine*, 9(6), 563–570.
- Kalluri, R., & Neilson, E. G. (2003). Epithelial-mesenchymal transition and its implications for fibrosis. *Journal of Clinical Investigation*, 112, 1776–1784.
- Kalluri, R., & Weinberg, R. A. (2009). The basics of epithelial-mesenchymal transition. *Journal of Clinical Investigation*, 119(6), 1420–1428.
- Kavsak, P., Rasmussen, R. K., Causing, C. G., Bonni, S., Zhu, H., Thomsen, G. H., & Wrana, J. L. (2000). Smad7 binds to Smurf2 to form an E3 ubiquitin ligase that targets the TGF beta receptor for degradation. *Molecular Cell*, 6(6), 1365–1375.
- Kim, J. H., Hong, S. K., Wu, P. K., Richards, A. L., Jackson, W. T., & Park, J. I. (2014). Raf/MEK/ERK can regulate cellular levels of LC3B and SQSTM1/p62 at expression levels. *Experimental Cell Research*, 327(2), 340–352.
- Kim, Y., Kugler, M. C., Wei, Y., Kim, K. K., Li, X., Brumwell, A. N., & Chapman H. A. (2009). Integrin alpha3beta1-dependent beta-catenin phosphorylation links epithelial Smad signaling to cell contacts. *Journal of Cell Biology*, 184(2), 309–322.
- Konrad, L., Scheiber, J. A., Völck-Badouin, E., Keilani, M. M., Laible, L., ... Hofmann, R. (2007). Alternative splicing of TGF-betas and their high-affinity receptors TβRI, TβRII and TβRIII (betaglycan) reveal new variants in human prostatic cells. *BMC Genomics*, 8(318).
- Kretschmar, M., Doody, J., Timokhina, I., & Massague, J. (1999) A mechanism of repression of TGFbeta/ Smad signaling by oncogenic Ras. *Genes & Development*, 13(7), 804–816.
- Leber, T. M., & Balkwill, F. R. (1997). Zymography: a single-step staining method for quantitation of proteolytic activity on substrate gels. *Analytical Biochemistry*, 249, 24–28.

- Li, Y., Yang, J., Dai, C., Wu, C., & Liu, Y. (2003). Role for integrin-linked kinase in mediating tubular epithelial to mesenchymal transition and renal interstitial fibrogenesis. *Journal of Clinical Investigation*, *112*(4), 503–516.
- Liu, F., Hata, A., Baker, J. C., Doody, J., Carcamo, J., Harland, R. M., & Massague, J. (1996). A human Mad protein acting as a BMP-regulated transcriptional activator. *Nature*, *381*(6583), 620–623.
- Liu, Y., Sun, X., Feng, J., Deng, L. L., Liu, Y., Li, B., ... Zhou, L. (2016). MT2-MMP induces proteolysis and leads to EMT in carcinomas. *Oncotarget*, *7*(30), 48193–48205.
- Liu, X. L., Xiao, K., Xue, B., Yang, D., Lei, Z., Shan, Y., & Zhang, H. T. (2013). Dual role of TGFBR3 in bladder cancer. *Oncology Reports*, *30*(3), 1301–1308.
- Lohi, J., Lehti, K., Valtanen, H., Parks, W. C., & Keski-Oja, J. (2000). Structural analysis and promoter characterization of human membrane-type matrix metalloproteinase-1 (MT1-MMP) gene. *Gene*, *242*(1-2), 75–86.
- Lopez-Casillas, F., Cheifetz, S., Doody, J., Andres, J. L., Lane, W. S., & Massague, J. (1991). Structure and expression of the membrane proteoglycan betaglycan, a component of the TGF-beta receptor system. *Cell*, *67*(4), 785–795.
- Lopez-Casillas, F., Payne, H. M., Andres, J. L., & Massague, J. (1994). Betaglycan can act as a dual modulator of TGF-beta access to signaling receptors: mapping of ligand binding and GAG attachment sites. *Journal of Cell Biology*, *124*(4), 557–568.
- Lopez-Casillas, F., Wrana, J. L., & Massague, J. (1993). Betaglycan presents ligand to the TGF beta signaling receptor. *Cell*, *73*(7), 1435–1444.
- Lu, P., Takai, K., Weaver, V. M., & Werb, Z. (2011). Extracellular matrix degradation and remodeling in development and disease. *Cold Spring Harbor Perspectives in Biology*, *3*.
- Massague, J. (1998). TGF-beta signal transduction. *Annual Review of Biochemistry*, *67*, 753–791.
- Masszi, A., Di Ciano, C., Sirokmany, G., Arthur, W. T., Rotstein, O. D., Wang, J. ... Kapus, A. (2003). Central role for Rho in TGF-beta1-induced alpha-smooth muscle actin expression during epithelial-mesenchymal transition. *American Journal of Physiology-Renal Physiology*, *284*(5), 911–924.
- Matsushita, M., Suzuki, N. N., Obara, K., Fujioka, Y., Ohsumi, Y., & Inagaki, F. (2007). Structure of Atg5.Atg6, a complex essential for autophagy. *Journal of Biological Chemistry*, *282*(9), 6763–6772.
- Mayo, L. D., & Donner, D. B. (2002). The PTEN, Mdm2, p53 tumor suppressor-oncoprotein network. *Trends in Biochemical Sciences*, *27*(9), 462–467.

- McLean, S., & Di Guglielmo, G. M. (2010). TGF β (transforming growth factor β) receptor type III directs clathrin-mediated endocytosis of TGF β receptor types I and II. *Biochemical Journal*, 429(1), 137–145.
- Mendoza, V., Vilchis-Landeros, M. M., Mendoza-Hernandez, G., Huang, T., Villarreal, M. M., Hinck, A. P., ... Montiel, J. L. (2009). Betaglycan has two independent domains required for high affinity TGF- β binding: proteolytic cleavage separates the domains and inactivates the neutralizing activity of the soluble receptor. *Biochemistry*, 48(49), 11755–11765.
- Mlcochova, H., Machackova, T., Rabien, A., Radova, L., Fabian, P., Iliev, R., ... Slaby, O. (2016). Epithelial-mesenchymal transition- associated microRNA/mRNA signature is linked to metastasis and prognosis in clear-cell renal cell carcinoma. *Scientific Reports*, 6, 31852.
- Nguyen, C. H., Senfter, D., Basilio, J., Hozlner, S., Stadler, S., Krieger, S., ... Krupitza, G. (2015). NF- κ B contributes to MMP1 expression in breast cancer spheroids causing paracrine PAR1 activation and disintegrations in the lymph endothelial barrier in vitro. *Oncotarget*, 6(36), 39262–39275.
- Nitta, T., Sato, Y., Shan Ren, X., Harada, K., Sasaki, M., Hirano, S., & Nakanuma, Y. (2014). Autophagy may promote carcinoma cell invasion and correlate with poor prognosis in cholangiocarcinoma. *International Journal of Clinical and Experimental Pathology*, 7(8), 4913–4921.
- Okada, A., Bellocq, J. P., Rouyer, N., Chenard, M. P., Rio, M. C., Chambo, P., & Basset, P. (1995). Membrane-type matrix metalloproteinase (MT-MMP) gene is expressed in stromal cells of human colon, breast, and head and neck carcinomas. *Proceedings of the National Academy of Science*, 92(7), 2730–2724.
- Ota, I., Li, X. Y., Hu, Y., & Weiss, S. J. (2009). Induction of a MT1-MMP and MT2-MMP-dependent basement membrane transmigration program in cancer cells by Snail1. *Proceedings of the National Academy of Science*, 106(48), 20318–20323.
- Paget, S. (1889). The distribution of secondary growths in cancer of the breast. *Lancet*, 133(3421), 571–573.
- Pahwa, S., Stawikowski, M. J., & Fields, G. B. (2014). Monitoring and inhibiting MT1-MMP during cancer initiation and progression. *Cancers*, 6(1), 416–435.
- Palma-Nicolas, J. P., & Lopez-Colome, A. M. (2013). Thrombin induces slug-mediated E-cadherin transcriptional repression and the parallel up-regulation of N-cadherin by a transcription-independent mechanism in RPE cells. *Journal of Cellular Physiology*, 228(3), 581–589.
- Pang, M., Wang, H., Rao, P., Zhao, Y., Xie, J., Cao, Q., ... Zheng, G. (2016). Autophagy links β -catenin and Smad signaling to promote epithelial-mesenchymal transition via

- upregulation of integrin linked kinase. *International Journal of Biochemistry and Cell Biology*, 76, 123–134.
- Paradies, N. E., & Grunwald, G. B. (1993). Purification and characterization of NCAD90, a soluble endogenous form of N-cadherin, which is generated by proteolysis during retinal development and retains adhesive and neurite-promoting function. *Journal of Neuroscience Research*, 36(1), 33–45.
- Parzych, K. R., & Klionski, D. J. (2014). An overview of autophagy: Morphology, mechanism, and regulation. *Antioxidants & Redox Signaling*, 20(3), 460–473.
- Pei, D., & Weiss, S. J. (1995). Furin-dependent intracellular activation of the human stromelysin zymogen. *Nature*, 375(6528), 244–247.
- Peinado, H., Olmeda, D., & Cano, A. (2007). Snail, Zeb and bHLH factors in tumour progression: an alliance against the epithelial phenotype. *Nature Reviews Cancer*, 7(6), 415–428.
- Piater, B., Doerner, A., Guenther, R., Kolmar, H., & Hock, B. (2015). Aptamers binding to c-Met inhibiting tumor cell migration. *PLoS One*, 10(12), e0142412.
- Pommier, Y., Sordet, O., Antony, S., Hayward, R. L., & Kohn, K. W. (2004). Apoptosis defects and chemotherapy resistance: molecular interaction maps and networks. *Oncogene*, 23(16), 2934–2949.
- Principe, D. R., Doll, J. A., Bauer, J., Jung, B., Munshi, H. G., Bartholin, L., ... Grippo, P. J. (2014). TGF- β : Duality of function between tumor prevention and carcinogenesis. *Journal of the National Cancer Institute*, 106(2), 1–16.
- Rahimi, R. A., & Leof, E. B. (2007). TGF-beta signaling: a tale of two responses. *Journal of Cellular Biochemistry*, 102(3), 593–608.
- Riihimäki, M., Hemminki, A., Fallah, M., Thomsen, H., Sundquist, K., Sundquist, J., & Hemminki, K. (2014). Metastatic sites and survival in lung cancer. *Lung Cancer*, 86(1), 78–84.
- Robertson, I. B., & Rifkin, D. B. (2013). Unchaining the beast; insights from structural and evolutionary studies on TGF β secretion, sequestration, and activation. *Cytokine Growth Factor Reviews*, 4, 355–372.
- Roskoski, R. (2012). ERK1/2 MAP kinases: structure, function, and regulation. *Pharmacological Research*, 66(2), 105–143.
- Sakamoto, T., & Seiki, M. (2009). Cytoplasmic tail of MT1-MMP regulates macrophage motility independently from its protease activity. *Genes to Cells*, 14(5), 617–626.

- Sato, H., Takino, T., Okada, Y., Cao, J., Shinagawa, A., Yamamoto, E., & Seiki, M. (1994). A matrix metalloproteinase expressed on the surface of invasive tumour cells. *Nature*, *370*(6484), 61–65.
- Satoo, K., Noda, N. N., Kumeta, H., Fujioka, Y., Mizushima, N., Ohsumi, Y., & Inagaki, F. (2009). The structure of Atg4B-LC3 complex reveals the mechanism of LC3 processing and delipidation during autophagy. *EMBO Journal*, *28*(9), 1341–1350.
- Schliekelman, P., & Liu, S. (2014). Quantifying the effect of competition for detection between coeluting peptides on detection probabilities in mass-spectrometry-based proteomics. *Journal Proteome Research*, *13*(2), 348–361.
- Schramek, H., Feifel, E., Marschitz, I., Golochtchapova, N., Gstraunthaler, G., & Montesano, R. (2003). Loss of active MEK1-ERK1/2 restores epithelial phenotype and morphogenesis in transdifferentiated MDCK cells. *American Journal of Physiology-Cell Physiology*, *285*(3), 652–661.
- Schultz-Cherry, S., & Murphy-Ullrich, J. E. (1993). Thrombospondin causes activation of latent transforming growth factor-beta secreted by endothelial cells by a novel mechanism. *Journal of Cell Biology*, *122*(4), 923–932.
- Shi, Y., Wang, Y. F., Jayaraman, L., Yang, H., Massague, J., & Pavletich, N. P. (1998). Crystal structure of a Smad MH1 domain bound to DNA: insights on DNA binding in TGF-beta signaling. *Cell*, *94*(5), 585–594.
- Siegel, P. M., & Massague, J. (2003). Cytostatic and apoptotic actions of TGF- β in homeostasis and cancer. *Nature Reviews Cancer*, *3*, 807–821.
- Sohail, A., Sun, Q., Zhao, H., Bernardo, M. M., Cho, J. A., & Fridman, R. (2008). MT4- (MMP17) and MTP-MMP (MMP25), A unique set of membrane-anchored matrix metalloproteinases: properties and expression in cancer. *Cancer Metastasis Reviews*, *27*(2), 289–302.
- Sounni, N. E., Rozanov, D. V., Remacle, A. G., Golubkov, V. S., Noel, A., & Strongin, A. Y. (2010). Timp-2 binding with cellular MT1-MMP stimulates invasion-promoting MEK/ERK signaling in cancer cells. *International Journal of Cancer*, *126*(5), 1067–1078.
- Statistics Canada. (2015). Canadian tobacco, alcohol, and drugs survey (CTADS) 2013. *Health Canada*.
- Stroschein, S. L., Wang, W., Zhou, S., Zhou, Q., & Luo, K. (1999). Negative feedback regulation of TGF-beta signaling by the SnoN oncoprotein. *Science*, *286*(5440), 771–774.
- Strutz, F., Zeisberg, M., Ziyadeh, F. N., Yang, C. Q., Kalluri, R., Muller, G. A., & Neilson, E. G. (2002). Role of basic fibroblast growth factor-2 in epithelial-mesenchymal transformation. *Kidney International*, *61*(5), 1714–1728.

- Sun, L., & Chen, C. (1997). Expression of transforming growth factor β type III receptor suppresses tumorigenicity of human breast cancer MDA-MB-231 cells. *Journal of Biological Chemistry*, 272(40), 25367–25372.
- Takino, T., Yoshimoto, T., Nakada, M., Li, Z., Domoto, T., Kawashiri, S., & Sato, H. (2014). Membrane-type 1 matrix metalloproteinase regulates fibronectin assembly and N-cadherin adhesion. *Biochemical and Biophysical Research Communications*, 450(2), 1016–1020.
- Tang, G., Weng, Z., Song, J., & Chen, Y. (2017). Reversal effect of Jagged1 signaling inhibition on CCI4-induced hepatic fibrosis in rats. *Oncotarget*, 8(37), 60778–60788.
- Tang, K., & Xu, H. (2015). Prognostic value of meta-signature miRNAs in renal cell carcinoma: an integrated miRNA expression profiling analysis. *Scientific Reports*, 5, 10272.
- Tao, H., Suzuki, M., Kiyonari, H., Abe, T., Sasaoka, T., Ueno, N. (2009). Mouse prickle1, the homolog of a PCP gene, is essential for epiblast apical-basal polarity. *Proceedings of the National Academy of Science*, 106(34), 14426–14431.
- Tazat, K., Hector-Greene, M., Blobe, G.C., & Henis, Y. I. (2015). T β RIII independently binds type I and type II TGF- β receptors to inhibit TGF- β signaling. *Molecular Biology of the Cell*, 26(19), 3535–3545.
- Terai, K., Call, M. K., Liu, H., Saika, S., Liu, C. Y., Hayashi, Y., ... Kao, W. W. (2011). Crosstalk between TGF-beta and MAPK signaling during corneal wound healing. *Investigative Ophthalmology & Visual Science*, 52(11), 8208–8215.
- Thiery, J. P. (2002). Epithelial-mesenchymal transitions in tumor progression. *Nature Reviews Cancer*, 2, 442–454.
- Thompson, E. W., & Haviv, I. (2011). The social aspects of EMT-MET plasticity. *Nature Medicine*, 17(9), 1048–1049.
- Tsukazaki, T., Chiang, T. A., Davison, A. F., Attisano, L., & Wrana J. L. (1998). SARA, a FYVE domain protein that recruits Smad2 to the TGFbeta receptor. *Cell*, 95(6), 779–791.
- Tung, Y. C., Hsiao, A. Y., Allen, S. G., Torisawa, Y., Ho, M., & Takayama, S. (2011). High-throughput 3D spheroid culture and drug testing using a 384 hanging drop array. *Analyst*, 136(3), 473–478.
- Turley, R. S., Finger, E. C., Hempel, N., How, T., Fields, T. A., & Blobe, G. C. (2007). The type III transforming growth factor-beta receptor as a novel tumor suppressor gene in prostate cancer. *Cancer Research*, 67(3), 1090–1098.
- U.S. National Institutes of Health. (2016). *SEER Cancer Statistics Review, 1975-2013*.

- Velasco-Loyden, G., Arribas, J., & Lopez-Casillas, F. (2004). The shedding of betaglycan is regulated by pervanadate and mediated by membrane type matrix metalloprotease-1. *Journal of Biological Chemistry*, 279(9), 7721–7733.
- Vi, L., Boo, S., Sayedyahosseini, S., Singh, R., McLean, S., Di Guglielmo, G. M., & Dagnino, L. (2015). Modulation of type II TGF- β receptor degradation by integrin-linked kinase. *Journal of Investigative Dermatology*, 135(3), 885–894.
- Vi, L., de Lasa, C., Di Guglielmo, G. M., & Dagnino, L. (2011). Integrin-linked kinase is required for TGF- β 1 induction of dermal myofibroblast differentiation. *Journal of Investigative Dermatology*, 131, 586–593.
- Wang, X. F., Lin, H. Y., Ng-Eaton, E., Downward, J., Lodish, H. F., & Weinberg, R. A. (1991). Expression cloning and characterization of the TGF-beta type III receptor. *Cell*, 67(4), 797–805.
- Wang, Y., Tang, Y., Teng, L., Wu, Y., Zhao, X., & Pei, G. (2006). Association of beta-arrestin and TRAF6 negatively regulates Toll-like receptor-interleukin 1 receptor signaling. *Nature Immunology*, 7(2), 139–147.
- Watson, W. L., & Berg, J.W. (1962). Oat cell lung cancer. *Cancer*, 15, 759–768.
- Whitby, D. J., & Ferguson, M. W. (1991). Immunohistochemical localization of growth factors in fetal wound healing. *Developmental Biology*, 147(1), 207–215.
- Wrana, J. L. (2000). Regulation of Smad activity. *Cell*, 100(2), 189–192.
- Wrana, J. L., Attisano, L., Wieser, R., Ventura, F., & Massague, J. (1994). Mechanism of activation of the TGF-beta receptor. *Nature*, 370(6488), 341–347.
- Wu, J., Chen, X., Liu, X., Huang, S., He, C., Chen, B., & Liu, Y. (2018). Autophagy regulates TGF- β 2-induced epithelial-mesenchymal transition in human retinal pigment epithelium cells. *Molecular Medicine Reports*, 17, 3607–3614.
- Wu, J. W., Fairman, R., Penry, J., & Shi, Y. (2001a). Formation of a stable heterodimer between Smad2 and Smad4. *Journal of Biological Chemistry*, 276, 20688–20694.
- Wu, J. W., Hu, M., Chai, J., Seoane, J., Huse, M., Li, C. ... Shi, Y. (2001b). Crystal Structure of a phosphorylated Smad2. Recognition of phosphoserine by the MH2 domain and insights on Smad Function in TGF-beta signaling. *Molecular Cell*, 8(6), 1277–89.
- Wu, J. W., Krawitz, A. R., Chai, J., Li, W., Zhang, F., Luo, K., & Shi, Y. (2002). Structural mechanism of Smad4 recognition by the nuclear oncoprotein Ski: insights on Ski-mediated repression of TGF-beta signaling. *Cell*, 111(3), 357–367.

- Xiao, N., Li, H., Mei, W., & Cheng, J. (2015). SUMOylation attenuates human β -arrestin 2 inhibition of IL-1R/TRAF6 signaling. *Journal of Biological Chemistry*, *290*(4), 1927–1935.
- Xu, J., Lamouille, S., & Derynck, R. (2009). TGF- β -induced epithelial to mesenchymal transition. *Cell Research*, *19*(2), 156–172.
- Xu, D., Li, D., Lu, Z., Dong, X., & Wang, X. (2016). Type III TGF- β receptor inhibits cell proliferation and migration in salivary glands adenoid cystic carcinoma by suppressing NF- κ B signaling. *Oncology Reports*, *35*(1), 267–274.
- Xu, P., Liu, J., & Derynck, R. (2012). Post-translational regulation of TGF- β receptor and Smad signaling. *FEBS Letters*, *586*(14), 1871–1884.
- Xu, L., & Massague, J. (2004). Nucleocytoplasmic shuttling of signal transducers. *Nature Reviews Molecular Cell Biology*, *5*(3), 209–219.
- Yamamoto, H., Noura, S., Okami, J., Uemura, M., Takemasa, I., Ikeda, M., ... Mori, M. (2008). Overexpression of MT1-MMP is insufficient to increase experimental liver metastasis of human colon cancer cells. *International Journal of Molecular Medicine*, *22*(6), 757–761.
- Yang, J., & Liu, Y. (2001). Dissection of key events in tubular epithelial to myofibroblast transition and its implications in renal interstitial fibrosis. *American Journal of Pathology*, *159*(4), 1465–1475.
- Ye, X., & Weinberg, R. A. (2016). Epithelial-mesenchymal plasticity: A central regulator of cancer progression. *Trends in Cell Biology*, *25*(11), 675–686.
- You, H. J., How, T., & Blobel, G. C. (2009). The type III transforming growth factor-beta receptor negatively regulates nuclear factor kappa B signaling through its interaction with beta-arrestin2. *Carcinogenesis*, *30*(8), 1281–1287.
- Yu, J. S. L., Ramasamy, T. S., Murphy, N., Holt, M. K., Czapiewski, R., Wei, S. K. & Cui, W. (2015). PI3K/mTORC2 regulates TGF- β /Activin signaling by modulating Smad2/3 activity via linker phosphorylation. *Nature Communications*, *6*, 7212.
- Yu, Q., & Stamenkovic, I. (2000). Cell surface-localized matrix metalloproteinase-9 proteolytically activates TGF-beta and promotes tumor invasion and angiogenesis. *Genes & Development*, *14*, 163–176.
- Zakrzewski, P. K., Nowacka-Zawisza, M., Semczuk, A., Rechberger, T., Galczynski, K., & Krajewska, W. M. (2016). Significance of TGFBR3 allelic loss in the deregulation of TGF β signaling in primary human endometrial carcinomas. *Oncology Reports*, *35*(2), 932–938.

- Zavadil, J., Cermak, L., Soto-Nieves, N., & Bottinger, E. P. (2004). Integration of TGF-beta/Smad and Jagged1/Notch signaling in epithelial-to-mesenchymal transition. *The EMBO Journal*, 23(5), 1155–1165.
- Zeisberg, M., Hanai, J., Sugimoto, H., Mannoto, T., Charytan, D., Strutz, F., & Kalluri, R. (2003). BMP-7 counteracts TGF-beta1-induced epithelial-to-mesenchymal transition and reverses chronic renal injury. *Nature Medicine*, 9(7), 964–968.
- Zhang, Z., Liu, Z. B., Ren, W. M., Ye, X. G., & Zhang, Y. Y. (2012). The miR-200 family regulates the epithelial-mesenchymal transition induced by EGF/EGFR in anaplastic thyroid cancer cells. *International Journal of Molecular Medicine*, 30(4), 856–862.
- Zhang, S., Sun, W. Y., Wu., J. J., Gu, Y. J., & Wei, W. (2016). Decreased expression of the type III TGF- β receptor enhances metastasis and invasion in hepatocarcinoma progression. *Oncology Reports*, 35(4), 2373–2381.
- Zhang, W., Zhang, T., Jin, R., Zhao, H., Hu, J., Feng, B., ... Wang, M. (2014). MicroRNA-301a promotes migration and invasion by targeting TGFBR2 in human colorectal cancer. *Journal of Experimental & Clinical Cancer Research*, 33(113), 1–13.
- Zheng, F., He, K., Li, X., Zhao, D., Sun, F., Zhang, Y., ... Lu, Y. (2013). Transient overexpression of TGFBR3 induces apoptosis in human nasopharyngeal carcinoma CNE-2Z cells. *Bioscience Reports*, 33(2).
- Zhou, B. P., & Hung, M. C. (2002). Novel targets of Akt, p21(Cip1/WAF1), and MDM2. *Seminars in Oncology*, 29(3), 62–70.

Appendix

Appendix Table 1 Genes upregulated in Microarray analysis $\geq +1.75$ fold-change (165 genes)

Gene Symbol	Assignment	Average Fold-Change
MMP1	NM_001145938 // RefSeq // Homo sapiens matrix metalloproteinase 1 (MMP1), transcript var	7.587845
PRICKLE1	NM_001144881 // RefSeq // Homo sapiens prickle homolog 1 (PRICKLE1), transcript variant	3.98391
MET	NM_000245 // RefSeq // Homo sapiens MET proto-oncogene, receptor tyrosine kinase (MET).	3.43446
HMBOX1	XM_005273635 // RefSeq // PREDICTED: Homo sapiens homeobox containing 1 (HMBOX1), trans	3.16948
SOCS1	NM_003745 // RefSeq // Homo sapiens suppressor of cytokine signaling 1 (SOCS1), mRNA. /	3.099
PTPMT1	NM_001143984 // RefSeq // Homo sapiens protein tyrosine phosphatase, mitochondrial 1 (P	2.975635
PTPRO	NM_002848 // RefSeq // Homo sapiens protein tyrosine phosphatase, receptor type, O (PTP	2.95122
JAG1	NM_000214 // RefSeq // Homo sapiens jagged 1 (JAG1), mRNA. // chr20 // 100 // 92 // 23	2.84577
SERPINB7	NM_001040147 // RefSeq // Homo sapiens serpin peptidase inhibitor, clade B (ovalbumin),	2.830065
PIP4K2A	NM_005028 // RefSeq // Homo sapiens phosphatidylinositol-5-phosphate 4-kinase, type II,	2.7278
NRBF2	NM_001282405 // RefSeq // Homo sapiens nuclear receptor binding factor 2 (NRBF2), trans	2.7113
CLDN1	NM_021101 // RefSeq // Homo sapiens claudin 1 (CLDN1), mRNA. // chr3 // 94 // 89 // 16	2.70308
PYGO2	NM_138300 // RefSeq // Homo sapiens pygopus family PHD finger 2 (PYGO2), mRNA. // chr1	2.698445
CRH	NM_000756 // RefSeq // Homo sapiens corticotropin releasing hormone (CRH), mRNA. // chr	2.682165
KLC1	ENST00000348520 // ENSEMBL // kinesin light chain 1 [gene_biotype:protein_coding transc	2.51896
CALU	NM_001130674 // RefSeq // Homo sapiens calumenin (CALU), transcript variant 2, mRNA. //	2.51797
HIST1H2BG	NM_003518 // RefSeq // Homo sapiens histone cluster 1, H2bg (HIST1H2BG), mRNA. // chr6	2.49148
PTPN1	NM_001278618 // RefSeq // Homo sapiens protein tyrosine phosphatase, non-receptor type	2.472065
TSC22D2	ENST00000361875 // ENSEMBL // TSC22 domain family, member 2 [gene_biotype:protein_codin	2.471215
SLC2A3	NM_006931 // RefSeq // Homo sapiens solute carrier family 2 (facilitated glucose transp	2.429165
CHAF1B	XM_011529753 // RefSeq // PREDICTED: Homo sapiens chromatin assembly factor 1, subunit	2.41733
HIST1H2BC	ENST00000314332 // ENSEMBL // histone cluster 1, H2bc [gene_biotype:protein_coding tran	2.417155
SPP1	NM_000582 // RefSeq // Homo sapiens secreted phosphoprotein 1 (SPP1), transcript varian	2.403515
GPAT3	NM_001256421 // RefSeq // Homo sapiens glycerol-3-phosphate acyltransferase 3 (GPAT3),	2.396755
OR2A42	NM_001001802 // RefSeq // Homo sapiens olfactory receptor, family 2, subfamily A, membe	2.388755
SEMA3C	NM_006379 // RefSeq // Homo sapiens sema domain, immunoglobulin domain (Ig), short basi	2.382555
SOX4	NM_003107 // RefSeq // Homo sapiens SRY (sex determining region Y)-box 4 (SOX4), mRNA.	2.37484
SCG2	NM_003469 // RefSeq // Homo sapiens secretogranin II (SCG2), mRNA. // chr2 // 100 // 68	2.366255

EHP1L1	NM_001099409 // RefSeq // Homo sapiens EH domain binding protein 1-like 1 (EHP1L1), mR	2.362085
CALB2	NM_001740 // RefSeq // Homo sapiens calbindin 2 (CALB2), transcript variant CALB2, mRNA	2.359335
CNR1	NM_001160226 // RefSeq // Homo sapiens cannabinoid receptor 1 (brain) (CNR1), transcrip	2.35512
PDIA4	NM_004911 // RefSeq // Homo sapiens protein disulfide isomerase family A, member 4 (PDI)	2.34272
ARL4C	NM_001282431 // RefSeq // Homo sapiens ADP-ribosylation factor-like 4C (ARL4C), transcr	2.32081
CXCL1	NM_001511 // RefSeq // Homo sapiens chemokine (C-X-C motif) ligand 1 (melanoma growth s	2.296395
CCND2	NM_001759 // RefSeq // Homo sapiens cyclin D2 (CCND2), mRNA. // chr12 // 100 // 62 // 1	2.282615
PGGT1B	XM_005272020 // RefSeq // PREDICTED: Homo sapiens protein geranylgeranyltransferase typ	2.27886
LOC286437	NR_039980 // RefSeq // Homo sapiens uncharacterized LOC286437 (LOC286437), long non-cod	2.25092
DNER	NM_139072 // RefSeq // Homo sapiens delta/notch-like EGF repeat containing (DNER), mRNA	2.2351
WSB1	NM_015626 // RefSeq // Homo sapiens WD repeat and SOCS box containing 1 (WSB1), transcr	2.23316
FLRT3	NM_013281 // RefSeq // Homo sapiens fibronectin leucine rich transmembrane protein 3 (F	2.201595
CYB5D1	NM_144607 // RefSeq // Homo sapiens cytochrome b5 domain containing 1 (CYB5D1), mRNA. /	2.196315
FAM49B	NM_001256763 // RefSeq // Homo sapiens family with sequence similarity 49, member B (FA	2.189425
LOC105373538	XR_923158 // RefSeq // PREDICTED: Homo sapiens uncharacterized LOC105373538 (LOC1053735	2.165175
TDG	NM_003211 // RefSeq // Homo sapiens thymine DNA glycosylase (TDG), mRNA. // chr12 // 10	2.15107
PTPN14	NM_005401 // RefSeq // Homo sapiens protein tyrosine phosphatase, non-receptor type 14	2.14654
PTPRG	NM_002841 // RefSeq // Homo sapiens protein tyrosine phosphatase, receptor type, G (PTP	2.138735
EFNB2	NM_004093 // RefSeq // Homo sapiens ephrin-B2 (EFNB2), mRNA. // chr13 // 100 // 100 //	2.12732
HOXB5	NM_002147 // RefSeq // Homo sapiens homeobox B5 (HOXB5), mRNA. // chr17 // 100 // 74 //	2.122855
MYO10	NM_012334 // RefSeq // Homo sapiens myosin X (MYO10), mRNA. // chr5 // 100 // 83 // 33	2.110515
RNU6-57P	ENST00000411348 // ENSEMBL // RNA, U6 small nuclear 57, pseudogene [gene_biotype:snRNA	2.10814
MIR548A1	NR_030312 // RefSeq // Homo sapiens microRNA 548a-1 (MIR548A1), microRNA. // chr6 // 10	2.10333
EYA3	NM_001282560 // RefSeq // Homo sapiens EYA transcriptional coactivator and phosphatase	2.098615
IGFL4	ENST00000595006 // ENSEMBL // IGF-like family member 4 [gene_biotype:protein_coding tra	2.098035
MT1X	NM_005952 // RefSeq // Homo sapiens metallothionein 1X (MT1X), mRNA. // chr16 // 100 //	2.09164
B3GALT1	NM_020981 // RefSeq // Homo sapiens UDP-Gal:betaGlcNAc beta 1,3-galactosyltransferase,	2.09153
MCL1	NM_001197320 // RefSeq // Homo sapiens myeloid cell leukemia 1 (MCL1), transcript varia	2.09069
ANKRD52	NM_173595 // RefSeq // Homo sapiens ankyrin repeat domain 52 (ANKRD52), mRNA. // chr12	2.083575
HMBOX1	NM_001135726 // RefSeq // Homo sapiens homeobox containing 1 (HMBOX1), transcript varia	2.079915
TMEM2	NM_001135820 // RefSeq // Homo sapiens transmembrane protein 2 (TMEM2), transcript vari	2.0798
B4GALT1	NM_001497 // RefSeq // Homo sapiens UDP-Gal:betaGlcNAc beta 1,4-galactosyltransferase,	2.054165
HAS2	NM_005328 // RefSeq // Homo sapiens hyaluronan synthase 2 (HAS2), mRNA. // chr8 // 100	2.048335
NABP1	ENST00000410026 // ENSEMBL // nucleic acid binding protein 1 [gene_biotype:protein_codi	2.03921

THBS1	NM_003246 // RefSeq // Homo sapiens thrombospondin 1 (THBS1), mRNA. // chr15 // 100 //	2.029965
FAM217B	NM_001190826 // RefSeq // Homo sapiens family with sequence similarity 217, member B (F)	2.02722
SPRY1	NM_001258038 // RefSeq // Homo sapiens sprouty RTK signaling antagonist 1 (SPRY1), tran	2.021935
UNC13A	NM_001080421 // RefSeq // Homo sapiens unc-13 homolog A (C. elegans) (UNC13A), mRNA. //	2.018905
PLD5	NM_001195811 // RefSeq // Homo sapiens phospholipase D family, member 5 (PLD5), transcr	2.01615
LOC105376694	XR_931876 // RefSeq // PREDICTED: Homo sapiens uncharacterized LOC105376694 (LOC1053766	2.012215
ANKRD1	NM_014391 // RefSeq // Homo sapiens ankyrin repeat domain 1 (cardiac muscle) (ANKRD1),	2.01199
PRICKLE4	ENST00000335515 // ENSEMBL // prickle homolog 4 [gene_biotype:protein_coding transcript	2.009555
DPYSL3	NM_001197294 // RefSeq // Homo sapiens dihydropyrimidinase-like 3 (DPYSL3), transcript	2.00606
ZFP14	NM_001297619 // RefSeq // Homo sapiens ZFP14 zinc finger protein (ZFP14), transcript va	2.00576
ZNF783	XM_005249929 // RefSeq // PREDICTED: Homo sapiens zinc finger family member 783 (ZNF783	2.003635
PPP2R1B	NM_001177562 // RefSeq // Homo sapiens protein phosphatase 2, regulatory subunit A, bet	1.989705
CDS1	NM_001263 // RefSeq // Homo sapiens CDP-diacylglycerol synthase (phosphatidate cytidyly	1.98269
TGFB2	NM_001135599 // RefSeq // Homo sapiens transforming growth factor, beta 2 (TGFB2), tran	1.977195
GATSL2	NM_001145064 // RefSeq // Homo sapiens GATS protein-like 2 (GATSL2), mRNA. // chr7 // 1	1.97662
SLC36A1	NM_001308150 // RefSeq // Homo sapiens solute carrier family 36 (proton/amino acid symp	1.97038
RRS1	NM_015169 // RefSeq // Homo sapiens ribosome biogenesis regulator homolog (RRS1), mRNA.	1.96967
STX12	NM_177424 // RefSeq // Homo sapiens syntaxin 12 (STX12), mRNA. // chr1 // 100 // 68 //	1.965035
RBPJ	NM_005349 // RefSeq // Homo sapiens recombination signal binding protein for immunoglob	1.96131
FAM46A	NM_017633 // RefSeq // Homo sapiens family with sequence similarity 46, member A (FAM46	1.954995
TIAM1	NM_003253 // RefSeq // Homo sapiens T-cell lymphoma invasion and metastasis 1 (TIAM1),	1.940475
MIR365A	NR_029854 // RefSeq // Homo sapiens microRNA 365a (MIR365A), microRNA. // chr16 // 100	1.938085
MAPKAP1	NM_001006617 // RefSeq // Homo sapiens mitogen-activated protein kinase associated prot	1.93674
MIR4655	NR_039799 // RefSeq // Homo sapiens microRNA 4655 (MIR4655), microRNA. // chr7 // 100 /	1.934215
CNR1	NM_001160226 // RefSeq // Homo sapiens cannabinoid receptor 1 (brain) (CNR1), transcrip	1.924605
ZNF157	NM_003446 // RefSeq // Homo sapiens zinc finger protein 157 (ZNF157), mRNA. // chrX //	1.924055
SBNO1	NM_001167856 // RefSeq // Homo sapiens strawberry notch homolog 1 (Drosophila) (SBNO1),	1.9178
LOC105373538	XR_923158 // RefSeq // PREDICTED: Homo sapiens uncharacterized LOC105373538 (LOC1053735	1.91522
AK4	NM_001005353 // RefSeq // Homo sapiens adenylate kinase 4 (AK4), transcript variant 1,	1.913045
FAM32A	NM_014077 // RefSeq // Homo sapiens family with sequence similarity 32, member A (FAM32	1.912335
BARX2	NM_003658 // RefSeq // Homo sapiens BARX homeobox 2 (BARX2), mRNA. // chr11 // 100 // 5	1.912105
KDM7A	NM_030647 // RefSeq // Homo sapiens lysine (K)-specific demethylase 7A (KDM7A), mRNA. /	1.898755
DDX58	NM_014314 // RefSeq // Homo sapiens DEAD (Asp-Glu-Ala-Asp) box polypeptide 58 (DDX58),	1.89858
SSFA2	NM_001130445 // RefSeq // Homo sapiens sperm specific antigen 2 (SSFA2), transcript var	1.89748

GUSBP1	NR_027026 // RefSeq // Homo sapiens glucuronidase, beta pseudogene 1 (GUSBP1), transcri	1.897305
MIR4441	NR_039643 // RefSeq // Homo sapiens microRNA 4441 (MIR4441), microRNA. // chr2 // 100 /	1.89599
CYB561D1	NM_001134400 // RefSeq // Homo sapiens cytochrome b561 family, member D1 (CYB561D1), tr	1.884945
GAS2L1	NM_001278730 // RefSeq // Homo sapiens growth arrest-specific 2 like 1 (GAS2L1), transc	1.880455
MRPL45	NM_001278279 // RefSeq // Homo sapiens mitochondrial ribosomal protein L45 (MRPL45), tr	1.87827
SPRY4	NM_001127496 // RefSeq // Homo sapiens sprouty RTK signaling antagonist 4 (SPRY4), tran	1.87776
TCEB3	NM_003198 // RefSeq // Homo sapiens transcription elongation factor B (SIII), polypepti	1.873875
TMEM145	NM_173633 // RefSeq // Homo sapiens transmembrane protein 145 (TMEM145), mRNA. // chr19	1.86874
TNFRSF21	NM_014452 // RefSeq // Homo sapiens tumor necrosis factor receptor superfamily, member	1.86786
CUEDC1	NM_001271875 // RefSeq // Homo sapiens CUE domain containing 1 (CUEDC1), transcript var	1.866395
PTPRZ1	NM_001206838 // RefSeq // Homo sapiens protein tyrosine phosphatase, receptor-type, Z p	1.86588
BANF1	NM_001143985 // RefSeq // Homo sapiens barrier to autointegration factor 1 (BANF1), tra	1.862805
GOPC	NM_001017408 // RefSeq // Homo sapiens golgi-associated PDZ and coiled-coil motif conta	1.862395
MIR31HG	NR_027054 // RefSeq // Homo sapiens MIR31 host gene (MIR31HG), long non-coding RNA. //	1.86227
KRTAP2-3	NM_001165252 // RefSeq // Homo sapiens keratin associated protein 2-3 (KRTAP2-3), mRNA.	1.861415
FHOD1	NM_013241 // RefSeq // Homo sapiens formin homology 2 domain containing 1 (FHOD1), mRNA	1.85921
CPPED1	NM_001099455 // RefSeq // Homo sapiens calcineurin-like phosphoesterase domain containi	1.85535
PLSCR4	NM_001128304 // RefSeq // Homo sapiens phospholipid scramblase 4 (PLSCR4), transcript v	1.85202
TRUB2	NM_015679 // RefSeq // Homo sapiens TruB pseudouridine (psi) synthase family member 2 (1.848545
CLIP4	NM_001287527 // RefSeq // Homo sapiens CAP-GLY domain containing linker protein family,	1.84656
ZNHIT6	NM_001170670 // RefSeq // Homo sapiens zinc finger, HIT-type containing 6 (ZNHIT6), tra	1.84486
LIPH	NM_139248 // RefSeq // Homo sapiens lipase, member H (LIPH), mRNA. // chr3 // 100 // 90	1.843155
LOC105374749	XR_925976 // RefSeq // PREDICTED: Homo sapiens uncharacterized LOC105374749 (LOC1053747	1.83801
SNORD114-1	NR_003193 // RefSeq // Homo sapiens small nucleolar RNA, C/D box 114-1 (SNORD114-1), sm	1.83693
RHOB	NM_004040 // RefSeq // Homo sapiens ras homolog family member B (RHOB), mRNA. // chr2 /	1.83475
RNF43	NM_001305544 // RefSeq // Homo sapiens ring finger protein 43 (RNF43), transcript varia	1.83369
MAGEA6	ENST00000412733 // ENSEMBL // melanoma antigen family A6 [gene_biotype:protein_coding t	1.826145
INPP5F	NM_001243194 // RefSeq // Homo sapiens inositol polyphosphate-5-phosphatase F (INPP5F),	1.82158
VGLL4	NM_001128219 // RefSeq // Homo sapiens vestigial-like family member 4 (VGLL4), transcri	1.81722
MIR1587	NR_039763 // RefSeq // Homo sapiens microRNA 1587 (MIR1587), microRNA. // chrX // 100 /	1.817035
C15orf48	NM_032413 // RefSeq // Homo sapiens chromosome 15 open reading frame 48 (C15orf48), tra	1.816345
GABPA	NM_001197297 // RefSeq // Homo sapiens GA binding protein transcription factor, alpha s	1.81563
ERCC5	NM_000123 // RefSeq // Homo sapiens excision repair cross-complementation group 5 (ERCC	1.814955
HIST2H2BF	NM_001161334 // RefSeq // Homo sapiens histone cluster 2, H2bf (HIST2H2BF), transcript	1.8133

THSD7A	NM_015204 // RefSeq // Homo sapiens thrombospondin, type I, domain containing 7A (THSD7)	1.811745
MYH8	NM_002472 // RefSeq // Homo sapiens myosin, heavy chain 8, skeletal muscle, perinatal (1.80751
RCHY1	NM_001009922 // RefSeq // Homo sapiens ring finger and CHY zinc finger domain containin	1.801645
TNFRSF10D	NM_003840 // RefSeq // Homo sapiens tumor necrosis factor receptor superfamily, member	1.800885
PPP3CB	NM_001142353 // RefSeq // Homo sapiens protein phosphatase 3, catalytic subunit, beta i	1.7959
MAGEA12	NM_001166386 // RefSeq // Homo sapiens melanoma antigen family A12 (MAGEA12), transcrip	1.79377
SGK1	NM_001143676 // RefSeq // Homo sapiens serum/glucocorticoid regulated kinase 1 (SGK1),	1.792335
ARHGDI	NM_001185077 // RefSeq // Homo sapiens Rho GDP dissociation inhibitor (GDI) alpha (ARHG	1.791955
CEP170P1	NR_003135 // RefSeq // Homo sapiens centrosomal protein 170kDa pseudogene 1 (CEP170P1),	1.78878
MAP2	NM_001039538 // RefSeq // Homo sapiens microtubule-associated protein 2 (MAP2), transcr	1.78864
HIST1H2BD	NM_021063 // RefSeq // Homo sapiens histone cluster 1, H2bd (HIST1H2BD), transcript var	1.788425
RASSF8	NM_001164746 // RefSeq // Homo sapiens Ras association (RalGDS/AF-6) domain family (N-t	1.78679
B3GALT1	XM_005246931 // RefSeq // PREDICTED: Homo sapiens UDP-Gal:betaGlcNAc beta 1,3-galactosy	1.7843
FBXL19-AS1	NR_024348 // RefSeq // Homo sapiens FBXL19 antisense RNA 1 (head to head) (FBXL19-AS1),	1.78243
PPFIBP1	NM_001198915 // RefSeq // Homo sapiens PTPRF interacting protein, binding protein 1 (li	1.7789
ZNF626	NM_001076675 // RefSeq // Homo sapiens zinc finger protein 626 (ZNF626), transcript var	1.776355
MMP14	NM_004995 // RefSeq // Homo sapiens matrix metalloproteinase 14 (membrane-inserted) (MMP	1.776015
CWC15	NM_016403 // RefSeq // Homo sapiens CWC15 spliceosome-associated protein (CWC15), mRNA.	1.7755
WDR83	NM_001099737 // RefSeq // Homo sapiens WD repeat domain 83 (WDR83), transcript variant	1.77217
LOC105376235	XR_930270 // RefSeq // PREDICTED: Homo sapiens uncharacterized LOC105376235 (LOC1053762	1.77159
FOXP2	NM_001172766 // RefSeq // Homo sapiens forkhead box P2 (FOXP2), transcript variant 5, m	1.769185
VAMP4	NM_001185127 // RefSeq // Homo sapiens vesicle-associated membrane protein 4 (VAMP4), t	1.769
P3H2	NM_001134418 // RefSeq // Homo sapiens prolyl 3-hydroxylase 2 (P3H2), transcript varian	1.768995
MBTPS1	NM_003791 // RefSeq // Homo sapiens membrane-bound transcription factor peptidase, site	1.76674
GPR155	NM_001033045 // RefSeq // Homo sapiens G protein-coupled receptor 155 (GPR155), transcr	1.76206
KATNAL1	NM_001014380 // RefSeq // Homo sapiens katanin p60 subunit A-like 1 (KATNAL1), transcri	1.760585
MIR548AM	NR_039762 // RefSeq // Homo sapiens microRNA 548am (MIR548AM), microRNA. // chrX // 100	1.758735
EIF3B	NM_001037283 // RefSeq // Homo sapiens eukaryotic translation initiation factor 3, subu	1.756245
OPHN1	NM_002547 // RefSeq // Homo sapiens oligophrenin 1 (OPHN1), mRNA. // chrX // 100 // 89	1.756205
PREPL	NM_001042385 // RefSeq // Homo sapiens prolyl endopeptidase-like (PREPL), transcript va	1.755085
SCX	NM_001080514 // RefSeq // Homo sapiens scleraxis bHLH transcription factor (SCX), mRNA.	1.7548
GPCPD1	NM_019593 // RefSeq // Homo sapiens glycerophosphocholine phosphodiesterase 1 (GPCPD1),	1.754265
H3F3AP4	NR_002315 // RefSeq // Homo sapiens H3 histone, family 3A, pseudogene 4 (H3F3AP4), non-	1.75039
RASA3	NM_007368 // RefSeq // Homo sapiens RAS p21 protein activator 3 (RASA3), mRNA. // chr13	1.75039

Appendix Table 2 Genes downregulated in Microarray ≤ -1.75 fold-change (441 genes)

Gene Symbol	Assignment	Average Fold-Change
TGFBR3	NM_001195683 // RefSeq // Homo sapiens transforming growth factor, beta receptor III (T)	-7.6191
ULBP1	NM_025218 // RefSeq // Homo sapiens UL16 binding protein 1 (ULBP1), mRNA. // chr6 // 10	-4.62948
SLC35F1	NM_001029858 // RefSeq // Homo sapiens solute carrier family 35, member F1 (SLC35F1), m	-4.51595
APOLD1	ENST00000534843 // ENSEMBL // apolipoprotein L domain containing 1 [gene_biotype:protei	-3.9413
CCNE2	NM_057749 // RefSeq // Homo sapiens cyclin E2 (CCNE2), mRNA. // chr8 // 100 // 67 // 18	-3.82031
HIST1H1B	NM_005322 // RefSeq // Homo sapiens histone cluster 1, H1b (HIST1H1B), mRNA. // chr6 //	-3.77962
GUCY1B3	NM_000857 // RefSeq // Homo sapiens guanylate cyclase 1, soluble, beta 3 (GUCY1B3), tra	-3.73332
BLM	NM_000057 // RefSeq // Homo sapiens Bloom syndrome, RecQ helicase-like (BLM), transcrip	-3.56194
ARRB2	NM_001257328 // RefSeq // Homo sapiens arrestin, beta 2 (ARRB2), transcript variant 3,	-3.53547
BRCA2	NM_000059 // RefSeq // Homo sapiens breast cancer 2, early onset (BRCA2), mRNA. // chr1	-3.4322
TICRR	NM_001308025 // RefSeq // Homo sapiens TOPBP1-interacting checkpoint and replication re	-3.23973
SGOL1	NM_001012409 // RefSeq // Homo sapiens shugoshin-like 1 (S. pombe) (SGOL1), transcript	-3.23506
HIST1H3G	NM_003534 // RefSeq // Homo sapiens histone cluster 1, H3g (HIST1H3G), mRNA. // chr6 //	-3.22531
FAM72D	NM_207418 // RefSeq // Homo sapiens family with sequence similarity 72, member D (FAM72	-3.18314
HIST1H2BH	NM_003524 // RefSeq // Homo sapiens histone cluster 1, H2bh (HIST1H2BH), mRNA. // chr6	-3.17553
TYMS	NM_001071 // RefSeq // Homo sapiens thymidylate synthetase (TYMS), mRNA. // chr18 // 10	-3.14754
MASTL	NM_001172303 // RefSeq // Homo sapiens microtubule associated serine/threonine kinase-1	-3.10531
STC1	NM_003155 // RefSeq // Homo sapiens stanniocalcin 1 (STC1), mRNA. // chr8 // 100 // 86	-3.09791
HIST1H3F	NM_021018 // RefSeq // Homo sapiens histone cluster 1, H3f (HIST1H3F), mRNA. // chr6 //	-3.0844
SERPINB9	NM_004155 // RefSeq // Homo sapiens serpin peptidase inhibitor, clade B (ovalbumin), me	-3.04552
CCNA2	NM_001237 // RefSeq // Homo sapiens cyclin A2 (CCNA2), mRNA. // chr4 // 100 // 100 // 2	-3.00154
SKA1	NM_001039535 // RefSeq // Homo sapiens spindle and kinetochore associated complex subun	-2.98977
FBXO43	NM_001029860 // RefSeq // Homo sapiens F-box protein 43 (FBXO43), transcript variant 2,	-2.94798
HIST2H3A	NM_001005464 // RefSeq // Homo sapiens histone cluster 2, H3a (HIST2H3A), mRNA. // chr1	-2.93141
HIST2H3A	NM_001005464 // RefSeq // Homo sapiens histone cluster 2, H3a (HIST2H3A), mRNA. // chr1	-2.93141
MKI67	NM_001145966 // RefSeq // Homo sapiens marker of proliferation Ki-67 (MKI67), transcrip	-2.87658
PCNA	NM_002592 // RefSeq // Homo sapiens proliferating cell nuclear antigen (PCNA), transcri	-2.87572
FAM111B	NM_001142703 // RefSeq // Homo sapiens family with sequence similarity 111, member B (F	-2.87548
PLPP1	NM_003711 // RefSeq // Homo sapiens phospholipid phosphatase 1 (PLPP1), transcript vari	-2.86974
CDC25C	NM_001287582 // RefSeq // Homo sapiens cell division cycle 25C (CDC25C), transcript var	-2.85109
PBK	NM_001278945 // RefSeq // Homo sapiens PDZ binding kinase (PBK), transcript variant 2,	-2.85087

HIST1H3E	NM_003532 // RefSeq // Homo sapiens histone cluster 1, H3e (HIST1H3E), mRNA. // chr6 //	-2.81285
RNF10	NM_014868 // RefSeq // Homo sapiens ring finger protein 10 (RNF10), mRNA. // chr12 // 1	-2.80049
XRCC2	NM_005431 // RefSeq // Homo sapiens X-ray repair complementing defective repair in Chin	-2.79875
SGMS2	NM_001136257 // RefSeq // Homo sapiens sphingomyelin synthase 2 (SGMS2), transcript var	-2.7831
MYBL2	NM_001278610 // RefSeq // Homo sapiens v-myb avian myeloblastosis viral oncogene homolo	-2.78231
SLC7A11	NM_014331 // RefSeq // Homo sapiens solute carrier family 7 (anionic amino acid transpo	-2.77462
ATAD5	NM_024857 // RefSeq // Homo sapiens ATPase family, AAA domain containing 5 (ATAD5), mRN	-2.75198
POLQ	NM_199420 // RefSeq // Homo sapiens polymerase (DNA directed), theta (POLQ), mRNA. // c	-2.73644
PPDPF	NM_024299 // RefSeq // Homo sapiens pancreatic progenitor cell differentiation and prol	-2.7147
TSPAN6	NM_001278740 // RefSeq // Homo sapiens tetraspanin 6 (TSPAN6), transcript variant 2, mR	-2.71416
KIF15	NM_020242 // RefSeq // Homo sapiens kinesin family member 15 (KIF15), mRNA. // chr3 //	-2.7103
ENPP1	NM_006208 // RefSeq // Homo sapiens ectonucleotide pyrophosphatase/phosphodiesterase 1	-2.70423
KIF24	NM_194313 // RefSeq // Homo sapiens kinesin family member 24 (KIF24), mRNA. // chr9 //	-2.70389
MARCKS	NM_002356 // RefSeq // Homo sapiens myristoylated alanine-rich protein kinase C substra	-2.66908
EME1	NM_001166131 // RefSeq // Homo sapiens essential meiotic structure-specific endonucleas	-2.66487
ASNS	NM_001178075 // RefSeq // Homo sapiens asparagine synthetase (glutamine-hydrolyzing) (A	-2.652
NSA2	NM_001271665 // RefSeq // Homo sapiens NSA2 ribosome biogenesis homolog (NSA2), transcr	-2.64196
MNS1	NM_018365 // RefSeq // Homo sapiens meiosis-specific nuclear structural 1 (MNS1), mRNA.	-2.63135
CKAP2L	NM_001304361 // RefSeq // Homo sapiens cytoskeleton associated protein 2-like (CKAP2L),	-2.59652
HIST1H2AM	NM_003514 // RefSeq // Homo sapiens histone cluster 1, H2am (HIST1H2AM), mRNA. // chr6	-2.58476
CDT1	NM_030928 // RefSeq // Homo sapiens chromatin licensing and DNA replication factor 1 (C	-2.58378
NEIL3	NM_018248 // RefSeq // Homo sapiens nei-like DNA glycosylase 3 (NEIL3), mRNA. // chr4 /	-2.58248
HIST1H3J	ENST00000479986 // ENSEMBL // histone cluster 1, H3j [gene_biotype:protein_coding trans	-2.58117
FANCI	NM_001113378 // RefSeq // Homo sapiens Fanconi anemia, complementation group I (FANCI),	-2.57447
CENPQ	NM_018132 // RefSeq // Homo sapiens centromere protein Q (CENPQ), mRNA. // chr6 // 100	-2.57397
DLGAP5	NM_001146015 // RefSeq // Homo sapiens discs, large (Drosophila) homolog-associated pro	-2.57062
BRCA1	NM_007294 // RefSeq // Homo sapiens breast cancer 1, early onset (BRCA1), transcript va	-2.54913
CENPF	NM_016343 // RefSeq // Homo sapiens centromere protein F, 350/400kDa (CENPF), mRNA. //	-2.54742
MKNK2	NM_017572 // RefSeq // Homo sapiens MAP kinase interacting serine/threonine kinase 2 (M	-2.53381
CCNB2	NM_004701 // RefSeq // Homo sapiens cyclin B2 (CCNB2), mRNA. // chr15 // 100 // 79 // 2	-2.52602
SRRM2	NM_016333 // RefSeq // Homo sapiens serine/arginine repetitive matrix 2 (SRRM2), mRNA.	-2.51062
YBX2	NM_015982 // RefSeq // Homo sapiens Y box binding protein 2 (YBX2), mRNA. // chr17 // 1	-2.50458
TSPAN13	NM_014399 // RefSeq // Homo sapiens tetraspanin 13 (TSPAN13), mRNA. // chr7 // 100 // 7	-2.49473
C5	NM_001735 // RefSeq // Homo sapiens complement component 5 (C5), mRNA. // chr9 // 100 /	-2.49208

TPM4	NM_001145160 // RefSeq // Homo sapiens tropomyosin 4 (TPM4), transcript variant Tpm4.1.	-2.49028
HORMAD1	NM_001199829 // RefSeq // Homo sapiens HORMA domain containing 1 (HORMAD1), transcript	-2.48965
FADS1	NM_013402 // RefSeq // Homo sapiens fatty acid desaturase 1 (FADS1), mRNA. // chr11 //	-2.48957
PHGDH	NM_006623 // RefSeq // Homo sapiens phosphoglycerate dehydrogenase (PHGDH), mRNA. // ch	-2.48909
FANCA	NM_000135 // RefSeq // Homo sapiens Fanconi anemia, complementation group A (FANCA), tr	-2.48745
EXO1	NM_003686 // RefSeq // Homo sapiens exonuclease 1 (EXO1), transcript variant 3, mRNA. /	-2.48328
TRIM6	NM_001003818 // RefSeq // Homo sapiens tripartite motif containing 6 (TRIM6), transcrip	-2.48296
RAD51	NM_001164269 // RefSeq // Homo sapiens RAD51 recombinase (RAD51), transcript variant 4.	-2.48137
FAM64A	NM_001195228 // RefSeq // Homo sapiens family with sequence similarity 64, member A (FA	-2.48059
CENPK	NM_001267038 // RefSeq // Homo sapiens centromere protein K (CENPK), transcript variant	-2.47994
HTR1D	NM_000864 // RefSeq // Homo sapiens 5-hydroxytryptamine (serotonin) receptor 1D, G prot	-2.4733
GINS2	NM_016095 // RefSeq // Homo sapiens GINS complex subunit 2 (Psf2 homolog) (GINS2), mRNA	-2.46952
HIST1H2BI	NM_003525 // RefSeq // Homo sapiens histone cluster 1, H2bi (HIST1H2BI), mRNA. // chr6	-2.46158
E2F7	NM_203394 // RefSeq // Homo sapiens E2F transcription factor 7 (E2F7), mRNA. // chr12 /	-2.46125
KIF20A	NM_005733 // RefSeq // Homo sapiens kinesin family member 20A (KIF20A), mRNA. // chr5 /	-2.4581
COMMD8	NM_017845 // RefSeq // Homo sapiens COMM domain containing 8 (COMMD8), mRNA. // chr4 //	-2.45305
KIF18B	NM_001264573 // RefSeq // Homo sapiens kinesin family member 18B (KIF18B), transcript v	-2.44763
SLC7A5	NM_003486 // RefSeq // Homo sapiens solute carrier family 7 (amino acid transporter lig	-2.44165
HIST1H2AB	NM_003513 // RefSeq // Homo sapiens histone cluster 1, H2ab (HIST1H2AB), mRNA. // chr6	-2.4379
GPR19	NM_006143 // RefSeq // Homo sapiens G protein-coupled receptor 19 (GPR19), mRNA. // chr	-2.43532
MCM10	NM_018518 // RefSeq // Homo sapiens minichromosome maintenance 10 replication initiatio	-2.42739
KIF11	NM_004523 // RefSeq // Homo sapiens kinesin family member 11 (KIF11), mRNA. // chr10 //	-2.41916
KNTC1	NM_014708 // RefSeq // Homo sapiens kinetochore associated 1 (KNTC1), mRNA. // chr12 //	-2.41799
ARID3B	NM_001307939 // RefSeq // Homo sapiens AT rich interactive domain 3B (BRIGHT-like) (ARI	-2.4156
MIF4GD	NM_001242498 // RefSeq // Homo sapiens MIF4G domain containing (MIF4GD), transcript var	-2.4132
TNFRSF9	NM_001561 // RefSeq // Homo sapiens tumor necrosis factor receptor superfamily, member	-2.41134
HIST1H3B	NM_003537 // RefSeq // Homo sapiens histone cluster 1, H3b (HIST1H3B), mRNA. // chr6 //	-2.4016
DTL	NM_001286229 // RefSeq // Homo sapiens denticleless E3 ubiquitin protein ligase homolog	-2.39383
CDCA8	NM_001256875 // RefSeq // Homo sapiens cell division cycle associated 8 (CDCA8), transc	-2.39189
DEPDC1	NM_001114120 // RefSeq // Homo sapiens DEP domain containing 1 (DEPDC1), transcript var	-2.39187
ZIK1	NM_001010879 // RefSeq // Homo sapiens zinc finger protein interacting with K protein 1	-2.37509
NTAN1	NM_001270766 // RefSeq // Homo sapiens N-terminal asparagine amidase (NTAN1), transcrip	-2.37377
SPAG5	NM_006461 // RefSeq // Homo sapiens sperm associated antigen 5 (SPAG5), mRNA. // chr17	-2.36951
CDKN3	NM_001130851 // RefSeq // Homo sapiens cyclin-dependent kinase inhibitor 3 (CDKN3), tra	-2.36825

GSG2	NM_031965 // RefSeq // Homo sapiens germ cell associated 2 (haspin) (GSG2), mRNA. // ch	-2.36041
TOB2P1	NR_002936 // RefSeq // Homo sapiens transducer of ERBB2, 2 pseudogene 1 (TOB2P1), non-c	-2.35917
STAG3	NM_001282716 // RefSeq // Homo sapiens stromal antigen 3 (STAG3), transcript variant 2,	-2.3581
ASPM	NM_001206846 // RefSeq // Homo sapiens abnormal spindle microtubule assembly (ASPM), tr	-2.34388
ORC1	NM_001190818 // RefSeq // Homo sapiens origin recognition complex, subunit 1 (ORC1), tr	-2.34261
NDC80	NM_006101 // RefSeq // Homo sapiens NDC80 kinetochore complex component (NDC80), mRNA.	-2.33825
MIR634	NR_030364 // RefSeq // Homo sapiens microRNA 634 (MIR634), microRNA. // chr17 // 100 //	-2.33724
SPC25	NM_020675 // RefSeq // Homo sapiens SPC25, NDC80 kinetochore complex component (SPC25).	-2.3364
LRRCC1	NM_033402 // RefSeq // Homo sapiens leucine rich repeat and coiled-coil centrosomal pro	-2.33023
CBX1	NM_001127228 // RefSeq // Homo sapiens chromobox homolog 1 (CBX1), transcript variant 2	-2.32889
ARL17A	uc010wwt.2 // UCSC Genes // Homo sapiens ADP-ribosylation factor-like 17A (ARL17A), tra	-2.32815
PTTG1	NM_001282382 // RefSeq // Homo sapiens pituitary tumor-transforming 1 (PTTG1), transcri	-2.32531
TOP2A	NM_001067 // RefSeq // Homo sapiens topoisomerase (DNA) II alpha 170kDa (TOP2A), mRNA.	-2.31916
RPL23AP53	NR_003572 // RefSeq // Homo sapiens ribosomal protein L23a pseudogene 53 (RPL23AP53), n	-2.31843
NCAPH	NM_001281710 // RefSeq // Homo sapiens non-SMC condensin I complex, subunit H (NCAPH).	-2.31523
PLK4	NM_001190799 // RefSeq // Homo sapiens polo-like kinase 4 (PLK4), transcript variant 2,	-2.31308
SYNE2	NM_015180 // RefSeq // Homo sapiens spectrin repeat containing, nuclear envelope 2 (SYN	-2.30654
GINS4	NM_032336 // RefSeq // Homo sapiens GINS complex subunit 4 (Sld5 homolog) (GINS4), mRNA	-2.30582
AUNIP	NM_001287490 // RefSeq // Homo sapiens aurora kinase A and ninein interacting protein (-2.30536
SKA3	NM_001166017 // RefSeq // Homo sapiens spindle and kinetochore associated complex subun	-2.29483
HIST1H1E	NM_005321 // RefSeq // Homo sapiens histone cluster 1, H1e (HIST1H1E), mRNA. // chr6 //	-2.29437
ARSB	NM_000046 // RefSeq // Homo sapiens arylsulfatase B (ARSB), transcript variant 1, mRNA.	-2.28673
SLC1A5	NM_001145144 // RefSeq // Homo sapiens solute carrier family 1 (neutral amino acid tran	-2.28431
RAD54L	NM_001142548 // RefSeq // Homo sapiens RAD54-like (S. cerevisiae) (RAD54L), transcript	-2.28079
TTK	NM_001166691 // RefSeq // Homo sapiens TTK protein kinase (TTK), transcript variant 2,	-2.28067
MTBP	NM_022045 // RefSeq // Homo sapiens MDM2 binding protein (MTBP), mRNA. // chr8 // 100 /	-2.28056
MXRA8	NM_001282582 // RefSeq // Homo sapiens matrix-remodelling associated 8 (MXRA8), transcr	-2.27993
ALDH1L2	NM_001034173 // RefSeq // Homo sapiens aldehyde dehydrogenase 1 family, member L2 (ALDH	-2.27302
TIMM21	NM_014177 // RefSeq // Homo sapiens translocase of inner mitochondrial membrane 21 homo	-2.26865
HMGB2	NM_001130688 // RefSeq // Homo sapiens high mobility group box 2 (HMGB2), transcript va	-2.26709
C1orf112	NM_018186 // RefSeq // Homo sapiens chromosome 1 open reading frame 112 (C1orf112), mRN	-2.25193
NET1	NM_001047160 // RefSeq // Homo sapiens neuroepithelial cell transforming 1 (NET1), tran	-2.24356
LOC105374104	XR_924474 // RefSeq // PREDICTED: Homo sapiens uncharacterized LOC105374104 (LOC1053741	-2.24206
QIQN5815	AY358807 // GenBank // Homo sapiens clone DNA129580 QIQN5815 (UNQ5815) mRNA, complete c	-2.24121

HIST1H2AJ	NM_021066 // RefSeq // Homo sapiens histone cluster 1, H2aj (HIST1H2AJ), mRNA. // chr6	-2.24093
ESCO2	NM_001017420 // RefSeq // Homo sapiens establishment of sister chromatid cohesion N-ace	-2.23819
CDC45	NM_001178010 // RefSeq // Homo sapiens cell division cycle 45 (CDC45), transcript varia	-2.22858
SLC25A40	NM_018843 // RefSeq // Homo sapiens solute carrier family 25, member 40 (SLC25A40), mRN	-2.22491
MELK	NM_001256685 // RefSeq // Homo sapiens maternal embryonic leucine zipper kinase (MELK),	-2.2229
NUF2	NM_031423 // RefSeq // Homo sapiens NUF2, NDC80 kinetochore complex component (NUF2), t	-2.21993
FBN1	NM_000138 // RefSeq // Homo sapiens fibrillin 1 (FBN1), mRNA. // chr15 // 100 // 92 //	-2.21078
RNASEH2A	NM_006397 // RefSeq // Homo sapiens ribonuclease H2, subunit A (RNASEH2A), mRNA. // chr	-2.21014
HMMR	NM_001142556 // RefSeq // Homo sapiens hyaluronan-mediated motility receptor (RHAMM) (H	-2.2026
FLJ36000	NR_027084 // RefSeq // Homo sapiens uncharacterized FLJ36000 (FLJ36000), long non-codin	-2.20157
LOC729732	NR_047662 // RefSeq // Homo sapiens uncharacterized LOC729732 (LOC729732), long non-cod	-2.20116
CDK1	NM_001170406 // RefSeq // Homo sapiens cyclin-dependent kinase 1 (CDK1), transcript var	-2.20087
FANCD2	NM_001018115 // RefSeq // Homo sapiens Fanconi anemia, complementation group D2 (FANCD2	-2.19693
RRM2	NM_001034 // RefSeq // Homo sapiens ribonucleotide reductase M2 (RRM2), transcript vari	-2.19325
DMC1	NM_001278208 // RefSeq // Homo sapiens DNA meiotic recombinase 1 (DMC1), transcript var	-2.19226
PRIM1	NM_000946 // RefSeq // Homo sapiens primase, DNA, polypeptide 1 (49kDa) (PRIM1), mRNA.	-2.19159
HIST1H1C	NM_005319 // RefSeq // Homo sapiens histone cluster 1, H1c (HIST1H1C), mRNA. // chr6 //	-2.19158
HIST1H2BM	NM_003521 // RefSeq // Homo sapiens histone cluster 1, H2bm (HIST1H2BM), mRNA. // chr6	-2.19058
LOC389831	NM_001242480 // RefSeq // Homo sapiens uncharacterized LOC389831 (LOC389831), mRNA. //	-2.18987
TK1	NM_003258 // RefSeq // Homo sapiens thymidine kinase 1, soluble (TK1), mRNA. // chr17 //	-2.18966
TXNDC16	NM_001160047 // RefSeq // Homo sapiens thioredoxin domain containing 16 (TXNDC16), tran	-2.18921
CDCA2	NM_152562 // RefSeq // Homo sapiens cell division cycle associated 2 (CDCA2), mRNA. //	-2.18685
CEP128	NM_152446 // RefSeq // Homo sapiens centrosomal protein 128kDa (CEP128), mRNA. // chr14	-2.18442
ZNF318	NM_014345 // RefSeq // Homo sapiens zinc finger protein 318 (ZNF318), mRNA. // chr6 //	-2.18214
PRC1	NM_001267580 // RefSeq // Homo sapiens protein regulator of cytokinesis 1 (PRC1), trans	-2.17532
CLSPN	NM_001190481 // RefSeq // Homo sapiens claspin (CLSPN), transcript variant 2, mRNA. //	-2.17491
CENPE	NM_001286734 // RefSeq // Homo sapiens centromere protein E, 312kDa (CENPE), transcript	-2.17471
LOC105376944	XR_936590 // RefSeq // PREDICTED: Homo sapiens uncharacterized LOC105376944 (LOC1053769	-2.17244
CHAC1	NM_001142776 // RefSeq // Homo sapiens ChaC glutathione-specific gamma-glutamylcyclotra	-2.17196
KIFC1	NM_002263 // RefSeq // Homo sapiens kinesin family member C1 (KIFC1), mRNA. // chr6 //	-2.16841
BIRC5	NM_001012270 // RefSeq // Homo sapiens baculoviral IAP repeat containing 5 (BIRC5), tra	-2.16823
NUSAP1	NM_001243142 // RefSeq // Homo sapiens nucleolar and spindle associated protein 1 (NUSA	-2.15713
ARHGAP11B	OTTHUMT00000430733 // Havana transcript // Rho GTPase activating protein 11B[<i>gene_bioty</i>	-2.15201
MCM8	NM_001281520 // RefSeq // Homo sapiens minichromosome maintenance 8 homologous recomb	-2.15079

EIF4EBP1	NM_004095 // RefSeq // Homo sapiens eukaryotic translation initiation factor 4E binding	-2.14859
ZNF257	NM_033468 // RefSeq // Homo sapiens zinc finger protein 257 (ZNF257), mRNA. // chr19 //	-2.14772
BORA	NM_001286746 // RefSeq // Homo sapiens bora, aurora kinase A activator (BORA), transcri	-2.14507
ZNF362	NM_152493 // RefSeq // Homo sapiens zinc finger protein 362 (ZNF362), mRNA. // chr1 //	-2.13866
HIST1H4B	NM_003544 // RefSeq // Homo sapiens histone cluster 1, H4b (HIST1H4B), mRNA. // chr6 //	-2.13846
PLK1	NM_005030 // RefSeq // Homo sapiens polo-like kinase 1 (PLK1), mRNA. // chr16 // 100 //	-2.13694
PDS5B	NM_015032 // RefSeq // Homo sapiens PDS5 cohesin associated factor B (PDS5B), mRNA. //	-2.12941
ASF1B	NM_018154 // RefSeq // Homo sapiens anti-silencing function 1B histone chaperone (ASF1B	-2.12772
PSMG2	NM_020232 // RefSeq // Homo sapiens proteasome (prosome, macropain) assembly chaperone	-2.12637
MAP1B	NM_005909 // RefSeq // Homo sapiens microtubule-associated protein 1B (MAP1B), mRNA. //	-2.11948
MMD	NM_012329 // RefSeq // Homo sapiens monocyte to macrophage differentiation-associated (-2.11831
LMNB2	NM_032737 // RefSeq // Homo sapiens lamin B2 (LMNB2), mRNA. // chr19 // 100 // 94 // 29	-2.11778
C7orf60	NM_152556 // RefSeq // Homo sapiens chromosome 7 open reading frame 60 (C7orf60), mRNA.	-2.11543
NCAPG	NM_022346 // RefSeq // Homo sapiens non-SMC condensin I complex, subunit G (NCAPG), tra	-2.11229
FAM222B	NM_001077498 // RefSeq // Homo sapiens family with sequence similarity 222, member B (F	-2.11169
XK	NM_021083 // RefSeq // Homo sapiens X-linked Kx blood group (XK), mRNA. // chrX // 100	-2.0995
CLMP	NM_024769 // RefSeq // Homo sapiens CXADR-like membrane protein (CLMP), mRNA. // chr11	-2.08887
CDK14	NM_001287135 // RefSeq // Homo sapiens cyclin-dependent kinase 14 (CDK14), transcript v	-2.08755
DSCC1	NM_024094 // RefSeq // Homo sapiens DNA replication and sister chromatid cohesion 1 (DS	-2.08379
ZNF732	NM_001137608 // RefSeq // Homo sapiens zinc finger protein 732 (ZNF732), mRNA. // chr4	-2.07746
TEX15	NM_031271 // RefSeq // Homo sapiens testis expressed 15 (TEX15), mRNA. // chr8 // 100 //	-2.07638
FOPNL	NM_001304497 // RefSeq // Homo sapiens FGFR1OP N-terminal like (FOPNL), transcript vari	-2.07263
LOC105370623	XR_915902 // RefSeq // PREDICTED: Homo sapiens uncharacterized LOC105370623 (LOC1053706	-2.06905
MDC1	NM_014641 // RefSeq // Homo sapiens mediator of DNA-damage checkpoint 1 (MDC1), mRNA. /	-2.06881
NFATC3	NM_004555 // RefSeq // Homo sapiens nuclear factor of activated T-cells, cytoplasmic, c	-2.06809
ECT2	NM_001258315 // RefSeq // Homo sapiens epithelial cell transforming 2 (ECT2), transcrip	-2.06422
STIL	NM_001048166 // RefSeq // Homo sapiens SCL/TAL1 interrupting locus (STIL), transcript v	-2.06414
MYL9	NM_006097 // RefSeq // Homo sapiens myosin, light chain 9, regulatory (MYL9), transcrip	-2.06385
CDC6	NM_001254 // RefSeq // Homo sapiens cell division cycle 6 (CDC6), mRNA. // chr17 // 100	-2.05956
ZBED8	NM_001303251 // RefSeq // Homo sapiens zinc finger, BED-type containing 8 (ZBED8), tran	-2.05872
KIF14	NM_001305792 // RefSeq // Homo sapiens kinesin family member 14 (KIF14), transcript var	-2.05825
ETV4	NM_001079675 // RefSeq // Homo sapiens ets variant 4 (ETV4), transcript variant 2, mRNA	-2.05774
LINC01096	NR_015450 // RefSeq // Homo sapiens long intergenic non-protein coding RNA 1096 (LINC01	-2.05319
RTKN2	NM_001282941 // RefSeq // Homo sapiens rhotekin 2 (RTKN2), transcript variant 2, mRNA.	-2.0494

DIAPH3	NM_001042517 // RefSeq // Homo sapiens diaphanous-related formin 3 (DIAPH3), transcript	-2.04876
HIST1H2AI	NM_003509 // RefSeq // Homo sapiens histone cluster 1, H2ai (HIST1H2AI), mRNA. // chr6	-2.04656
LOC105373133	XM_011508982 // RefSeq // PREDICTED: Homo sapiens uncharacterized LOC105373133 (LOC1053)	-2.04589
MEAT6	NR_131926 // RefSeq // Homo sapiens melanoma-associated transcript 6 (MEAT6), long non-	-2.04357
CKAP2	NM_001098525 // RefSeq // Homo sapiens cytoskeleton associated protein 2 (CKAP2), trans	-2.03953
LOC257396	NR_034107 // RefSeq // Homo sapiens uncharacterized LOC257396 (LOC257396), transcript v	-2.03846
MCM5	NM_006739 // RefSeq // Homo sapiens minichromosome maintenance complex component 5 (MCM)	-2.03843
CENPU	NM_024629 // RefSeq // Homo sapiens centromere protein U (CENPU), transcript variant 1,	-2.03755
C9orf84	NM_001080551 // RefSeq // Homo sapiens chromosome 9 open reading frame 84 (C9orf84), tr	-2.03306
EFEMP1	NM_001039348 // RefSeq // Homo sapiens EGF containing fibulin-like extracellular matrix	-2.02715
DEPDC1B	NM_001145208 // RefSeq // Homo sapiens DEP domain containing 1B (DEPDC1B), transcript v	-2.02609
OIP5	NM_007280 // RefSeq // Homo sapiens Opa interacting protein 5 (OIP5), mRNA. // chr15 //	-2.02582
PKMYT1	NM_001258450 // RefSeq // Homo sapiens protein kinase, membrane associated tyrosine/thr	-2.02559
ZWINT	NM_001005413 // RefSeq // Homo sapiens ZW10 interacting kinetochore protein (ZWINT), tr	-2.0218
RPL39L	NM_052969 // RefSeq // Homo sapiens ribosomal protein L39-like (RPL39L), mRNA. // chr3	-2.01873
TBC1D22A-AS1	NR_122047 // RefSeq // Homo sapiens TBC1D22A antisense RNA 1 (TBC1D22A-AS1), long non-c	-2.0186
CEP55	NM_001127182 // RefSeq // Homo sapiens centrosomal protein 55kDa (CEP55), transcript va	-2.01809
EZR	NM_001111077 // RefSeq // Homo sapiens ezrin (EZR), transcript variant 2, mRNA. // chr6	-2.01395
RBL1	NM_002895 // RefSeq // Homo sapiens retinoblastoma-like 1 (RBL1), transcript variant 1,	-2.01384
TRO	NM_001039705 // RefSeq // Homo sapiens trophinin (TRO), transcript variant 6, mRNA. //	-2.01381
RFC3	NM_002915 // RefSeq // Homo sapiens replication factor C (activator 1) 3, 38kDa (RFC3),	-2.01231
SUZ12	NM_015355 // RefSeq // Homo sapiens SUZ12 polycomb repressive complex 2 subunit (SUZ12)	-2.00955
EBAG9	NM_001278938 // RefSeq // Homo sapiens estrogen receptor binding site associated, antig	-2.00784
DDIAS	NM_145018 // RefSeq // Homo sapiens DNA damage-induced apoptosis suppressor (DDIAS), mR	-2.0062
KIF5C	NM_004522 // RefSeq // Homo sapiens kinesin family member 5C (KIF5C), transcript varian	-2.00381
CENPA	NM_001042426 // RefSeq // Homo sapiens centromere protein A (CENPA), transcript variant	-2.00203
ZWILCH	NM_001287821 // RefSeq // Homo sapiens zwilch kinetochore protein (ZWILCH), transcript	-1.99939
FOXM1	NM_001243088 // RefSeq // Homo sapiens forkhead box M1 (FOXM1), transcript variant 4, m	-1.99913
IQGAP3	NM_178229 // RefSeq // Homo sapiens IQ motif containing GTPase activating protein 3 (IQ)	-1.9938
LOC101926892	NR_110653 // RefSeq // Homo sapiens uncharacterized LOC101926892 (LOC101926892), long n	-1.99268
MCM3	NM_001270472 // RefSeq // Homo sapiens minichromosome maintenance complex component 3 (-1.9913
CENPN	NM_001100624 // RefSeq // Homo sapiens centromere protein N (CENPN), transcript variant	-1.989
BUB1	NM_001278616 // RefSeq // Homo sapiens BUB1 mitotic checkpoint serine/threonine kinase	-1.98889

LOC105370496	XR_915613 // RefSeq // PREDICTED: Homo sapiens uncharacterized LOC105370496 (LOC1053704)	-1.98868
FANCB	NM_001018113 // RefSeq // Homo sapiens Fanconi anemia, complementation group B (FANCB),	-1.98421
EML1	NM_001008707 // RefSeq // Homo sapiens echinoderm microtubule associated protein like 1	-1.98099
STOX1	NM_001130159 // RefSeq // Homo sapiens storkhead box 1 (STOX1), transcript variant 3, m	-1.98062
LRR1	NM_152329 // RefSeq // Homo sapiens leucine rich repeat protein 1 (LRR1), transcript va	-1.97781
KIF20B	NM_001284259 // RefSeq // Homo sapiens kinesin family member 20B (KIF20B), transcript v	-1.97745
CCNE1	NM_001238 // RefSeq // Homo sapiens cyclin E1 (CCNE1), mRNA. // chr19 // 100 // 100 //	-1.97705
AKT3	NM_001206729 // RefSeq // Homo sapiens v-akt murine thymoma viral oncogene homolog 3 (A	-1.97689
DNA2	NM_001080449 // RefSeq // Homo sapiens DNA replication helicase/nuclease 2 (DNA2), tran	-1.97594
SIMC1	NM_001308195 // RefSeq // Homo sapiens SUMO-interacting motifs containing 1 (SIMC1), tr	-1.97594
CDC20	NM_001255 // RefSeq // Homo sapiens cell division cycle 20 (CDC20), mRNA. // chr1 // 10	-1.97374
DUSP3	NM_004090 // RefSeq // Homo sapiens dual specificity phosphatase 3 (DUSP3), mRNA. // ch	-1.97355
CEP57	NM_001243776 // RefSeq // Homo sapiens centrosomal protein 57kDa (CEP57), transcript va	-1.97149
UBL7-AS1	NR_038448 // RefSeq // Homo sapiens UBL7 antisense RNA 1 (head to head) (UBL7-AS1), tra	-1.96607
RMND5A	NM_022780 // RefSeq // Homo sapiens required for meiotic nuclear division 5 homolog A (-1.96548
ITGB3BP	NM_001206739 // RefSeq // Homo sapiens integrin beta 3 binding protein (beta3- endonexin	-1.96401
DSN1	NM_001145315 // RefSeq // Homo sapiens DSN1 homolog, MIS12 kinetochore complex componen	-1.96374
AURKB	NM_001256834 // RefSeq // Homo sapiens aurora kinase B (AURKB), transcript variant 2, m	-1.96293
KNSTRN	NM_001142761 // RefSeq // Homo sapiens kinetochore-localized astrin/SPAG5 binding prote	-1.96223
MIR130B	NR_029845 // RefSeq // Homo sapiens microRNA 130b (MIR130B), microRNA. // chr22 // 100	-1.96164
AGBL2	NM_024783 // RefSeq // Homo sapiens ATP/GTP binding protein-like 2 (AGBL2), mRNA. // ch	-1.95597
ZNF680	NM_001130022 // RefSeq // Homo sapiens zinc finger protein 680 (ZNF680), transcript var	-1.95506
HIST1H4K	NM_003541 // RefSeq // Homo sapiens histone cluster 1, H4k (HIST1H4K), mRNA. // chr6 //	-1.95383
LAMP3	NM_014398 // RefSeq // Homo sapiens lysosomal-associated membrane protein 3 (LAMP3), mR	-1.95296
MEIOB	NM_001163560 // RefSeq // Homo sapiens meiosis specific with OB domains (MEIOB), transc	-1.95292
TTF2	NM_003594 // RefSeq // Homo sapiens transcription termination factor, RNA polymerase II	-1.95057
HADH	NM_001184705 // RefSeq // Homo sapiens hydroxyacyl-CoA dehydrogenase (HADH), transcript	-1.9487
FAM225A	NR_024366 // RefSeq // Homo sapiens family with sequence similarity 225, member A (non-	-1.94812
PRR14	NM_024031 // RefSeq // Homo sapiens proline rich 14 (PRR14), mRNA. // chr16 // 96 // 10	-1.94609
RAD51AP1	NM_001130862 // RefSeq // Homo sapiens RAD51 associated protein 1 (RAD51AP1), transcrip	-1.94598
LOC729088	XR_951689 // RefSeq // PREDICTED: Homo sapiens uncharacterized LOC729088 (LOC729088), m	-1.94595
MCM7	NM_001278595 // RefSeq // Homo sapiens minichromosome maintenance complex component 7 (-1.94178
KIF2C	NM_001297655 // RefSeq // Homo sapiens kinesin family member 2C (KIF2C), transcript var	-1.94093
LIG3	ENST00000378526 // ENSEMBL // ligase III, DNA, ATP-dependent [gene_biotype:protein_codi	-1.94081

SOBP	NM_018013 // RefSeq // Homo sapiens sine oculis binding protein homolog (SOBP), mRNA. /	-1.9385
LCLAT1	NM_001002257 // RefSeq // Homo sapiens lysocardiolipin acyltransferase 1 (LCLAT1), tran	-1.93616
CEP162	NM_001286206 // RefSeq // Homo sapiens centrosomal protein 162kDa (CEP162), transcript	-1.93355
SMC4	NM_001002800 // RefSeq // Homo sapiens structural maintenance of chromosomes 4 (SMC4),	-1.9333
HJURP	NM_001282962 // RefSeq // Homo sapiens Holliday junction recognition protein (HJURP), t	-1.93232
NDRG1	NM_001135242 // RefSeq // Homo sapiens N-myc downstream regulated 1 (NDRG1), transcript	-1.9301
TROAP	NM_001100620 // RefSeq // Homo sapiens trophinin associated protein (TROAP), transcript	-1.92979
GINS1	NM_021067 // RefSeq // Homo sapiens GINS complex subunit 1 (Psf1 homolog) (GINS1), mRNA	-1.92743
POLA2	NM_002689 // RefSeq // Homo sapiens polymerase (DNA directed), alpha 2, accessory subun	-1.92498
SGOL2	NM_001160033 // RefSeq // Homo sapiens shugoshin-like 2 (S. pombe) (SGOL2), transcript	-1.92472
USP1	NM_001017415 // RefSeq // Homo sapiens ubiquitin specific peptidase 1 (USP1), transcrip	-1.92398
EMP2	NM_001424 // RefSeq // Homo sapiens epithelial membrane protein 2 (EMP2), mRNA. // chr1	-1.92346
PTENP1	NR_023917 // RefSeq // Homo sapiens phosphatase and tensin homolog pseudogene 1 (functi	-1.92251
CENPI	NM_006733 // RefSeq // Homo sapiens centromere protein I (CENPI), mRNA. // chrX // 100	-1.92228
ATP11A	NM_015205 // RefSeq // Homo sapiens ATPase, class VI, type 11A (ATP11A), transcript var	-1.92057
FAM65A	NM_001193522 // RefSeq // Homo sapiens family with sequence similarity 65, member A (FA	-1.91896
MCM2	NM_004526 // RefSeq // Homo sapiens minichromosome maintenance complex component 2 (MCM	-1.91833
MUC1	NM_001018016 // RefSeq // Homo sapiens mucin 1, cell surface associated (MUC1), transcr	-1.91794
SHCBP1	NM_024745 // RefSeq // Homo sapiens SHC SH2-domain binding protein 1 (SHCBP1), mRNA. //	-1.91675
UBE2C	NM_001281741 // RefSeq // Homo sapiens ubiquitin-conjugating enzyme E2C (UBE2C), transc	-1.91653
PROSER1	NM_025138 // RefSeq // Homo sapiens proline and serine rich 1 (PROSER1), mRNA. // chr13	-1.91487
TGOLN2	NM_001206840 // RefSeq // Homo sapiens trans-golgi network protein 2 (TGOLN2), transcri	-1.91374
HIST1H4C	NM_003542 // RefSeq // Homo sapiens histone cluster 1, H4c (HIST1H4C), mRNA. // chr6 //	-1.91322
GAS2L3	NM_001303130 // RefSeq // Homo sapiens growth arrest-specific 2 like 3 (GAS2L3), transc	-1.90984
MTFR2	NM_001099286 // RefSeq // Homo sapiens mitochondrial fission regulator 2 (MTFR2), trans	-1.90928
PDCD4	NM_001199492 // RefSeq // Homo sapiens programmed cell death 4 (neoplastic transformati	-1.90912
BRIP1	NM_032043 // RefSeq // Homo sapiens BRCA1 interacting protein C-terminal helicase 1 (BR	-1.90746
TMPO-AS1	NR_027157 // RefSeq // Homo sapiens TMPO antisense RNA 1 (TMPO-AS1), long non-coding RN	-1.90716
ANLN	NM_001284301 // RefSeq // Homo sapiens anillin actin binding protein (ANLN), transcript	-1.90631
ORC6	NM_014321 // RefSeq // Homo sapiens origin recognition complex, subunit 6 (ORC6), trans	-1.90481
DOCK11	NM_144658 // RefSeq // Homo sapiens dedicator of cytokinesis 11 (DOCK11), mRNA. // chrX	-1.90208
LOC101927978	XR_429768 // RefSeq // PREDICTED: Homo sapiens uncharacterized LOC101927978 (LOC1019279	-1.90171
LOC101929475	XR_242755 // RefSeq // PREDICTED: Homo sapiens uncharacterized LOC101929475 (LOC1019294	-1.89932
TAS2R30	ENST00000539585 // ENSEMBL // taste receptor, type 2, member 30 [gene_biotype:protein_c	-1.8989

CSTF3-AS1	NR_034027 // RefSeq // Homo sapiens CSTF3 antisense RNA 1 (head to head) (CSTF3-AS1), 1	-1.89843
MIR644A	NR_030374 // RefSeq // Homo sapiens microRNA 644a (MIR644A), microRNA. // chr20 // 100	-1.89717
LOC729987	NR_046088 // RefSeq // Homo sapiens uncharacterized LOC729987 (LOC729987), long non-cod	-1.89649
NPR2	NM_003995 // RefSeq // Homo sapiens natriuretic peptide receptor 2 (NPR2), mRNA. // chr	-1.89617
BASP1	NM_001271606 // RefSeq // Homo sapiens brain abundant, membrane attached signal protein	-1.89362
POLE	NM_006231 // RefSeq // Homo sapiens polymerase (DNA directed), epsilon, catalytic subun	-1.89189
FAM161A	NM_001201543 // RefSeq // Homo sapiens family with sequence similarity 161, member A (F	-1.89113
POLE2	NM_001197330 // RefSeq // Homo sapiens polymerase (DNA directed), epsilon 2, accessory	-1.89109
MDM1	NM_001205028 // RefSeq // Homo sapiens Mdm1 nuclear protein (MDM1), transcript variant	-1.89068
LOC728755	XR_110268 // RefSeq // PREDICTED: Homo sapiens uncharacterized LOC728755 (LOC728755), t	-1.89014
SCML2	NM_006089 // RefSeq // Homo sapiens sex comb on midleg-like 2 (Drosophila) (SCML2), tra	-1.88981
MCM4	NM_005914 // RefSeq // Homo sapiens minichromosome maintenance complex component 4 (MCM	-1.88922
LOC101929140	NR_120423 // RefSeq // Homo sapiens uncharacterized LOC101929140 (LOC101929140), long n	-1.88758
ARHGAP11A	NM_001286479 // RefSeq // Homo sapiens Rho GTPase activating protein 11A (ARHGAP11A), t	-1.88685
RPGRIP1L	NM_001127897 // RefSeq // Homo sapiens RPGRIP1-like (RPGRIP1L), transcript variant 2, m	-1.88681
RAD54B	NM_001205262 // RefSeq // Homo sapiens RAD54 homolog B (S. cerevisiae) (RAD54B), transc	-1.88542
WDHD1	NM_001008396 // RefSeq // Homo sapiens WD repeat and HMG-box DNA binding protein 1 (WDH	-1.88414
MGME1	NM_001310338 // RefSeq // Homo sapiens mitochondrial genome maintenance exonuclease 1 (-1.88245
KIF5A	NM_004984 // RefSeq // Homo sapiens kinesin family member 5A (KIF5A), mRNA. // chr12 //	-1.8816
SFXN2	NM_178858 // RefSeq // Homo sapiens sideroflexin 2 (SFXN2), mRNA. // chr10 // 100 // 83	-1.87955
AMOT	NM_001113490 // RefSeq // Homo sapiens angiomin (AMOT), transcript variant 1, mRNA. /	-1.87808
GGH	NM_003878 // RefSeq // Homo sapiens gamma-glutamyl hydrolase (conjugase, foyllypolygamma	-1.87685
PARPBP	NM_017915 // RefSeq // Homo sapiens PARP1 binding protein (PARPBP), mRNA. // chr12 // 1	-1.87651
CABYR	NM_001308231 // RefSeq // Homo sapiens calcium binding tyrosine-(Y)-phosphorylation reg	-1.87627
SLC1A4	NM_001193493 // RefSeq // Homo sapiens solute carrier family 1 (glutamate/neutral amino	-1.87597
TAS2R31	NM_176885 // RefSeq // Homo sapiens taste receptor, type 2, member 31 (TAS2R31), mRNA.	-1.87416
NUP54	NM_001278603 // RefSeq // Homo sapiens nucleoporin 54kDa (NUP54), transcript variant 2,	-1.87409
KIAA1524	NM_020890 // RefSeq // Homo sapiens KIAA1524 (KIAA1524), mRNA. // chr3 // 100 // 88 //	-1.87288
HOXD4	NM_014621 // RefSeq // Homo sapiens homeobox D4 (HOXD4), mRNA. // chr2 // 100 // 58 //	-1.86893
FANCG	NM_004629 // RefSeq // Homo sapiens Fanconi anemia, complementation group G (FANCG), mR	-1.86851
PLCB4	NM_000933 // RefSeq // Homo sapiens phospholipase C, beta 4 (PLCB4), transcript variant	-1.86727
TRIP13	NM_001166260 // RefSeq // Homo sapiens thyroid hormone receptor interactor 13 (TRIP13),	-1.86307
ARID2	NM_152641 // RefSeq // Homo sapiens AT rich interactive domain 2 (ARID, RFX-like) (ARID	-1.86176
GLI1	NM_001160045 // RefSeq // Homo sapiens GLI family zinc finger 1 (GLI1), transcript vari	-1.86078

CASC5	NM_144508 // RefSeq // Homo sapiens cancer susceptibility candidate 5 (CASC5), transcri	-1.86076
SLC6A8	NM_001142805 // RefSeq // Homo sapiens solute carrier family 6 (neurotransmitter transp	-1.85991
GADD45B	NM_015675 // RefSeq // Homo sapiens growth arrest and DNA-damage-inducible, beta (GADD4	-1.85935
DHFR	NM_000791 // RefSeq // Homo sapiens dihydrofolate reductase (DHFR), transcript variant	-1.85934
CENPW	NM_001012507 // RefSeq // Homo sapiens centromere protein W (CENPW), transcript variant	-1.859
MIR54802	NR_039605 // RefSeq // Homo sapiens microRNA 5480-2 (MIR54802), microRNA. // chr20 // 1	-1.85846
GTSE1	NM_016426 // RefSeq // Homo sapiens G-2 and S-phase expressed 1 (GTSE1), mRNA. // chr22	-1.85696
UBE2T	NM_001310326 // RefSeq // Homo sapiens ubiquitin-conjugating enzyme E2T (UBE2T), transc	-1.85677
FAM46D	NM_001170574 // RefSeq // Homo sapiens family with sequence similarity 46, member D (FA	-1.85511
CCDC18	NM_001306076 // RefSeq // Homo sapiens coiled-coil domain containing 18 (CCDC18), trans	-1.85401
CEP295	NM_033395 // RefSeq // Homo sapiens centrosomal protein 295kDa (CEP295), mRNA. // chr11	-1.85271
GEN1	NM_001130009 // RefSeq // Homo sapiens GEN1 Holliday junction 5 flap endonuclease (GEN1	-1.84863
CHAF1A	NM_005483 // RefSeq // Homo sapiens chromatin assembly factor 1, subunit A (p150) (CHAF	-1.84837
ZNF681	NM_138286 // RefSeq // Homo sapiens zinc finger protein 681 (ZNF681), mRNA. // chr19 //	-1.84784
CT47B1	NM_001145718 // RefSeq // Homo sapiens cancer/testis antigen family 47, member B1 (CT47	-1.84425
CEP152	NM_001194998 // RefSeq // Homo sapiens centrosomal protein 152kDa (CEP152), transcript	-1.84363
SGOL1-AS1	NR_132785 // RefSeq // Homo sapiens SGOL1 antisense RNA 1 (SGOL1-AS1), long non-coding	-1.84356
EXOSC1	NM_016046 // RefSeq // Homo sapiens exosome component 1 (EXOSC1), mRNA. // chr10 // 100	-1.84285
COL12A1	NM_004370 // RefSeq // Homo sapiens collagen, type XII, alpha 1 (COL12A1), transcript v	-1.84184
HEG1	NM_020733 // RefSeq // Homo sapiens heart development protein with EGF-like domains 1 (-1.8418
FEN1	NM_004111 // RefSeq // Homo sapiens flap structure-specific endonuclease 1 (FEN1), mRNA	-1.83949
ERCC6L	NM_017669 // RefSeq // Homo sapiens excision repair cross-complementation group 6-like	-1.83925
REEP4	NM_025232 // RefSeq // Homo sapiens receptor accessory protein 4 (REEP4), mRNA. // chr8	-1.83588
ZNF100	NM_173531 // RefSeq // Homo sapiens zinc finger protein 100 (ZNF100), mRNA. // chr19 //	-1.83552
SLC7A1	NM_003045 // RefSeq // Homo sapiens solute carrier family 7 (cationic amino acid transp	-1.83206
PIGP	NM_153681 // RefSeq // Homo sapiens phosphatidylinositol glycan anchor biosynthesis, cl	-1.83136
RASA4B	ENST00000488284 // ENSEMBL // RAS p21 protein activator 4B [gene_biotype:protein_coding	-1.82887
ZNF492	NM_020855 // RefSeq // Homo sapiens zinc finger protein 492 (ZNF492), mRNA. // chr19 //	-1.82851
FOSL1	NM_001300844 // RefSeq // Homo sapiens FOS-like antigen 1 (FOSL1), transcript variant 2	-1.82848
RNASEH2B	NM_001142279 // RefSeq // Homo sapiens ribonuclease H2, subunit B (RNASEH2B), transcrip	-1.82733
KIF4A	NM_012310 // RefSeq // Homo sapiens kinesin family member 4A (KIF4A), mRNA. // chrX //	-1.82716
LOC101929787	XR_917210 // RefSeq // PREDICTED: Homo sapiens uncharacterized LOC101929787 (LOC1019297	-1.82688
SLC16A10	NM_018593 // RefSeq // Homo sapiens solute carrier family 16 (aromatic amino acid trans	-1.82569
RFC5	NM_001130112 // RefSeq // Homo sapiens replication factor C (activator 1) 5, 36.5kDa (R	-1.82462

NEMP1	NM_001130963 // RefSeq // Homo sapiens nuclear envelope integral membrane protein 1 (NE)	-1.82227
RPS6KA3	NM_004586 // RefSeq // Homo sapiens ribosomal protein S6 kinase, 90kDa, polypeptide 3 (-1.82142
C16orf58	NM_022744 // RefSeq // Homo sapiens chromosome 16 open reading frame 58 (C16orf58), mRN	-1.82101
SNORD114-31	NR_003224 // RefSeq // Homo sapiens small nucleolar RNA, C/D box 114-31 (SNORD114-31),	-1.82069
MERTK	NM_006343 // RefSeq // Homo sapiens MER proto-oncogene, tyrosine kinase (MERTK), mRNA.	-1.81997
CDCA3	NM_001297602 // RefSeq // Homo sapiens cell division cycle associated 3 (CDCA3), transc	-1.81946
PABPC4	NM_001135653 // RefSeq // Homo sapiens poly(A) binding protein, cytoplasmic 4 (inducibl	-1.81677
E2F8	NM_001256371 // RefSeq // Homo sapiens E2F transcription factor 8 (E2F8), transcript va	-1.81673
CTGF	NM_001901 // RefSeq // Homo sapiens connective tissue growth factor (CTGF), mRNA. // ch	-1.81624
NCAPD2	NM_014865 // RefSeq // Homo sapiens non-SMC condensin I complex, subunit D2 (NCAPD2), m	-1.8158
FERMT2	NM_001134999 // RefSeq // Homo sapiens fermitin family member 2 (FERMT2), transcript va	-1.81567
ZEB2	NM_001171653 // RefSeq // Homo sapiens zinc finger E-box binding homeobox 2 (ZEB2), tra	-1.81486
LOC105379280	XR_949107 // RefSeq // PREDICTED: Homo sapiens uncharacterized LOC105379280 (LOC1053792	-1.81384
DUSP19	NM_001142314 // RefSeq // Homo sapiens dual specificity phosphatase 19 (DUSP19), transc	-1.81264
LOC105372906	XR_920756 // RefSeq // PREDICTED: Homo sapiens uncharacterized LOC105372906 (LOC1053729	-1.80893
SPC24	NM_182513 // RefSeq // Homo sapiens SPC24, NDC80 kinetochore complex component (SPC24),	-1.80884
ARHGAP11B	NM_001039841 // RefSeq // Homo sapiens Rho GTPase activating protein 11B (ARHGAP11B), m	-1.80219
SMC2	NM_001042550 // RefSeq // Homo sapiens structural maintenance of chromosomes 2 (SMC2),	-1.79989
SMC1B	NM_001291501 // RefSeq // Homo sapiens structural maintenance of chromosomes 1B (SMC1B)	-1.79916
PCNA-AS1	NR_028370 // RefSeq // Homo sapiens PCNA antisense RNA 1 (PCNA-AS1), long non-coding RN	-1.79718
MPV17L2	NM_032683 // RefSeq // Homo sapiens MPV17 mitochondrial membrane protein-like 2 (MPV17L	-1.7964
FBXL7	NM_001278317 // RefSeq // Homo sapiens F-box and leucine-rich repeat protein 7 (FBXL7),	-1.79537
MMS22L	NM_198468 // RefSeq // Homo sapiens MMS22-like, DNA repair protein (MMS22L), mRNA. // c	-1.79497
SGCB	NM_000232 // RefSeq // Homo sapiens sarcoglycan, beta (43kDa dystrophin-associated glyc	-1.79416
TMPO	NM_001032283 // RefSeq // Homo sapiens thymopoietin (TMPO), transcript variant 2, mRNA.	-1.79356
ZNF594	NM_032530 // RefSeq // Homo sapiens zinc finger protein 594 (ZNF594), mRNA. // chr17 //	-1.79018
HM13-AS1	NR_046853 // RefSeq // Homo sapiens HM13 antisense RNA 1 (HM13-AS1), long non-coding RN	-1.7893
PLOD1	NM_000302 // RefSeq // Homo sapiens procollagen-lysine, 2-oxoglutarate 5-dioxygenase 1	-1.78928
EMB	NM_198449 // RefSeq // Homo sapiens embigin (EMB), mRNA. // chr5 // 100 // 53 // 8 // 8	-1.7879
FANCM	NM_001308133 // RefSeq // Homo sapiens Fanconi anemia, complementation group M (FANCM),	-1.78702
PRKAA2	NM_006252 // RefSeq // Homo sapiens protein kinase, AMP-activated, alpha 2 catalytic su	-1.78693
GNPDA1	NM_005471 // RefSeq // Homo sapiens glucosamine-6-phosphate deaminase 1 (GNPDA1), mRNA.	-1.78423
DPYSL5	NM_001253723 // RefSeq // Homo sapiens dihydropyrimidinase-like 5 (DPYSL5), transcript	-1.78283
TACR3	NM_001059 // RefSeq // Homo sapiens tachykinin receptor 3 (TACR3), mRNA. // chr4 // 100	-1.78228

GMNN	NM_001251989 // RefSeq // Homo sapiens geminin, DNA replication inhibitor (GMNN), trans	-1.78099
KIF23	NM_001281301 // RefSeq // Homo sapiens kinesin family member 23 (KIF23), transcript var	-1.77925
LRCH2	NM_001243963 // RefSeq // Homo sapiens leucine-rich repeats and calponin homology (CH)	-1.7786
ATAD2	NM_014109 // RefSeq // Homo sapiens ATPase family, AAA domain containing 2 (ATAD2), mRN	-1.77827
PHF19	NM_001009936 // RefSeq // Homo sapiens PHD finger protein 19 (PHF19), transcript varian	-1.77812
GPLD1	NM_001503 // RefSeq // Homo sapiens glycosylphosphatidylinositol specific phospholipase	-1.77769
HIST2H2AB	NM_175065 // RefSeq // Homo sapiens histone cluster 2, H2ab (HIST2H2AB), mRNA. // chr1	-1.77599
ZP3	NM_001110354 // RefSeq // Homo sapiens zona pellucida glycoprotein 3 (sperm receptor) (-1.7751
SLC25A35	NM_201520 // RefSeq // Homo sapiens solute carrier family 25, member 35 (SLC25A35), mRN	-1.77356
LYRM4-AS1	NR_126016 // RefSeq // Homo sapiens LYRM4 antisense RNA 1 (LYRM4-AS1), transcript varia	-1.77335
ZNF75D	NM_001185063 // RefSeq // Homo sapiens zinc finger protein 75D (ZNF75D), transcript var	-1.77287
STC2	NM_003714 // RefSeq // Homo sapiens stanniocalcin 2 (STC2), mRNA. // chr5 // 100 // 71	-1.77274
TRAJ5	OTTHUMT00000410993 // Havana transcript // T cell receptor alpha joining 5[<i>gene_biotype</i>	-1.77194
KIAA0101	NM_001029989 // RefSeq // Homo sapiens KIAA0101 (KIAA0101), transcript variant 2, mRNA.	-1.76817
C17orf53	NM_001171251 // RefSeq // Homo sapiens chromosome 17 open reading frame 53 (C17orf53),	-1.76815
PROCR	NM_006404 // RefSeq // Homo sapiens protein C receptor, endothelial (PROCR), mRNA. // c	-1.76695
HIST2H2BB	OTTHUMT00000098433 // Havana transcript // histone cluster 2, H2bb (pseudogene)[<i>gene_bi</i>	-1.76424
LOC105375974	XR_929476 // RefSeq // PREDICTED: Homo sapiens uncharacterized LOC105375974 (LOC1053759	-1.76331
POLD2	NM_001127218 // RefSeq // Homo sapiens polymerase (DNA directed), delta 2, accessory su	-1.76292
ESPL1	NM_012291 // RefSeq // Homo sapiens extra spindle pole bodies like 1, separase (ESPL1),	-1.76247
MYPN	NM_001256267 // RefSeq // Homo sapiens myopalladin (MYPN), transcript variant 4, mRNA.	-1.76247
CENPP	NM_001012267 // RefSeq // Homo sapiens centromere protein P (CENPP), transcript variant	-1.76236
SNRPN	AF400486 // GenBank // Homo sapiens clone kid4 SNURF-SNRPN mRNA, downstream untranslate	-1.76199
PMP22	NM_000304 // RefSeq // Homo sapiens peripheral myelin protein 22 (PMP22), transcript va	-1.76135
PPP4R4	NM_020958 // RefSeq // Homo sapiens protein phosphatase 4, regulatory subunit 4 (PPP4R4	-1.76088
SLC35G5	OTTHUMT00000207313 // Havana transcript // solute carrier family 35, member G5[<i>gene_bio</i>	-1.76033
ADAM23	NM_003812 // RefSeq // Homo sapiens ADAM metallopeptidase domain 23 (ADAM23), mRNA. //	-1.75982
ZNF480	NM_001297624 // RefSeq // Homo sapiens zinc finger protein 480 (ZNF480), transcript var	-1.75973
PLEKHH2	NM_172069 // RefSeq // Homo sapiens pleckstrin homology domain containing, family H (wi	-1.7586
SCOC-AS1	NR_033939 // RefSeq // Homo sapiens SCOC antisense RNA 1 (SCOC-AS1), long non-coding RN	-1.75854
VBP1	NM_001303543 // RefSeq // Homo sapiens von Hippel-Lindau binding protein 1 (VBP1), tran	-1.75736
THAP9	NM_024672 // RefSeq // Homo sapiens THAP domain containing 9 (THAP9), mRNA. // chr4 //	-1.7554
ASRGL1	NM_001083926 // RefSeq // Homo sapiens asparaginase like 1 (ASRGL1), transcript variant	-1.75434
MBNL3	NM_001170701 // RefSeq // Homo sapiens muscleblind-like splicing regulator 3 (MBNL3), t	-1.75387

NCAPD3	NM_015261 // RefSeq // Homo sapiens non-SMC condensin II complex, subunit D3 (NCAPD3),	-1.75143
SLC47A1	NM_018242 // RefSeq // Homo sapiens solute carrier family 47 (multidrug and toxin extru	-1.75051
CCNJ	NM_001134375 // RefSeq // Homo sapiens cyclin J (CCNJ), transcript variant 1, mRNA. //	-1.75014

Appendix Table 3 Expression of MMP1 or MMP14 microRNAs in microarray

<u>Gene Symbol</u>	<u>Target</u>	<u>Assignment</u>	<u>Average Fold-Change</u>
MIR9-1	MMP14	NR_029691 // RefSeq // Homo sapiens microRNA 9-1 (MIR9-1), microRNA. // chr1 // 100 //	1.44411
MIR146A	MMP1	NR_029701 // RefSeq // Homo sapiens microRNA 146a (MIR146A), microRNA. // chr5 // 100 //	1.15373
MIR22HG	MMP14	NR_028502 // RefSeq // Homo sapiens MIR22 host gene (MIR22HG), transcript variant 1, lo	1.1216
MIR133A1	MMP14	NR_029675 // RefSeq // Homo sapiens microRNA 133a-1 (MIR133A1), microRNA. // chr18 // 1	-1.04109
MIR34A	MMP1	NR_029610 // RefSeq // Homo sapiens microRNA 34a (MIR34A), microRNA. // chr1 // 100 //	-1.13227
MIR222	MMP1	NR_029636 // RefSeq // Homo sapiens microRNA 222 (MIR222), microRNA. // chrX // 100 //	-1.65699

Appendix Table 4 Expression of MMP activity regulators in microarray

<u>Gene Symbol</u>	<u>Assignment</u>	<u>Average Fold-Change</u>
TIMP2	NM_003255 // RefSeq // Homo sapiens TIMP metalloproteinase inhibitor 2 (TIMP2), mRNA. //	1.25805
TIMP1	NM_003254 // RefSeq // Homo sapiens TIMP metalloproteinase inhibitor 1 (TIMP1), mRNA. //	1.13388
TIMP4	NM_003256 // RefSeq // Homo sapiens TIMP metalloproteinase inhibitor 4 (TIMP4), mRNA. //	1.09581
TIMP3	NM_000362 // RefSeq // Homo sapiens TIMP metalloproteinase inhibitor 3 (TIMP3), mRNA. //	-1.0215333
FURIN	NM_001289823 // RefSeq // Homo sapiens furin (paired basic amino acid cleaving enzyme)	-1.07985
PLG	NM_000301 // RefSeq // Homo sapiens plasminogen (PLG), transcript variant 1, mRNA. // c	-1.10423

Appendix Table 5 Expression of EMT regulating microRNAs microarray

<u>Gene Symbol</u>	<u>Target</u>	<u>Assignment</u>	<u>Average Fold-Change</u>
MIR30A	SNAIL	NR_029504 // RefSeq // Homo sapiens microRNA 30a (MIR30A), microRNA. // chr6 // 100 //	1.6762
MIR101-1	CDH1	NR_029516 // RefSeq // Homo sapiens microRNA 101-1 (MIR101-1), microRNA. // chr1 // 100 //	1.53542
MIR200B	ZEB1/2	NR_029639 // RefSeq // Homo sapiens microRNA 200b (MIR200B), microRNA. // chr1 // 100 //	1.22807
MIR200C	ZEB1/2	NR_029779 // RefSeq // Homo sapiens microRNA 200c (MIR200C), microRNA. // chr12 // 100 //	1.18659
MIR22HG	SNAIL	NR_028502 // RefSeq // Homo sapiens MIR22 host gene (MIR22HG), transcript variant 1, lo	1.1216
MIR200A	ZEB1/2	NR_029834 // RefSeq // Homo sapiens microRNA 200a (MIR200A), microRNA. // chr1 // 100 //	1.07458
MIR429	ZEB1/2	NR_029957 // RefSeq // Homo sapiens microRNA 429 (MIR429), microRNA. // chr1 // 100 //	1.01476
MIR205HG	ZEB1/2	NM_001104548 // RefSeq // Homo sapiens MIR205 host gene (MIR205HG), mRNA. // chr1 // 10	-1.11731
MIR141	ZEB1/2	NR_029682 // RefSeq // Homo sapiens microRNA 141 (MIR141), microRNA. // chr12 // 100 //	-1.25733
MIR9-3	CDH1	NR_029692 // RefSeq // Homo sapiens microRNA 9-3 (MIR9-3), microRNA. // chr15 // 100 //	-1.52468

Curriculum Vitae

ANTHONY ZICCARELLI

EDUCATION

MSc, Physiology and Pharmacology – *The University of Western Ontario* 2016 – 2018
 BMSc, Honors Interdisciplinary Medical Science – *The University of Western Ontario* 2012 – 2016

RESEARCH EXPERIENCE

Master's Student – *The University of Western Ontario* 2016 – 2018
 - Performed cell cultures and treatments, Western blots, DNA transfection, immunofluorescence microscopy, transwell assays, and quantitative polymerase chain reactions.
 - Interpreted data, generated figures, and presented information through poster and oral presentations
 - Analyzed microarray data manually and through Gene Ontology reports

Summer Student Researcher – *Algoma University* 2015 – 2016
 - Performed bacterial transformation, gene cloning, mass spectrometry, DNA/RNA extraction, polymerase chain reactions, gel electrophoresis, and cell culturing.

TEACHING EXPERIENCE

Teaching Assistant – *The University of Western Ontario* 2016 – 2018
 - In-class demonstration of scientific techniques: Cell culture, transfection, ELISA assay, qPCR, Western blotting, immunofluorescence microscopy
 - Organized and conducted review sessions, answered student questions, evaluated quizzes, posters, and exams

AWARDS

Western Graduate Research Scholarship – *The University of Western Ontario* 2016
 NSERC Undergraduate Student Research Award – *Dr. Isabel Molina, Algoma University* 2015
 Dean's Honor List – *The University of Western Ontario* 2014 – 2016
 Western Scholarship of Excellence – *The University of Western Ontario* 2012

POSTER PRESENTATIONS

TGF β type III receptor influences lung cancer cell migration and invasion:
 London Health Research Day – *London, Ontario* 2018
Transforming growth factor-beta type III receptor suppresses lung cancer cell migration:
 Charles W. Gowdey Research Day – *The University of Western Ontario* 2017
Transforming growth factor-beta type III receptor suppresses lung cancer cell migration:
 American Association for Cancer Research Annual Meeting – *Washington, D.C.* 2017
 London Health Research Day – *London, Ontario* 2017
The role of transforming growth factor-beta type III receptor in lung carcinoma cell migration and invasion:
 James A.F. Stevenson Research Day – *The University of Western Ontario* 2016
 Windsor International Cancer Research Conference – *Windsor, Ontario* 2016